TPL-FR-2049

PHASE BEHAVIOR IN TNAZ-BASED AND OTHER EXPLOSIVE FORMULATIONS

Submitted to:

Dr. Sury Iyer/SMCAR-AEE-WW
U.S. Army Armament Research, Development and Engineering Center
Picatinny Arsenal, NJ 07806-5000

Contract Number DAAA21-93-C-0017

Final Report
September, 1994

Submitted by:

Robert D. Chapman, Ph.D.
TPL, Inc. (Albuquerque, NM)

John W. Fronabarger
Exothermics, Inc. (Phoenix, AZ)

William B. Sanborn, Ph.D.
Gary Burr, Ph.D.
Sally Knueppel
Pacific Scientific—Energy Dynamics Division (Chandler, AZ)

TPL, Inc.
An Advanced Materials Technology Company
3768 Hawkins NE
Albuquerque, NM 87109
505/344-6744

REPORT DOCUMENTATION PAGE

Form Approved
OMB No. 0704-0188

1. AGENCY USE ONLY *(Leave blank)*	2. REPORT DATE	3. REPORT TYPE AND DATES COVERED
	30 Sep 94	Final (03/93–08/94)

4. TITLE AND SUBTITLE
Phase Behavior in TNAZ-Based and Other Explosive Formulations

5. FUNDING NUMBERS
DAAA21-93-C-0017

6. AUTHOR(S)
Robert D. Chapman; John W. Fronabarger; William B. Sanborn; Gary Burr; Sally Knueppel

7. PERFORMING ORGANIZATION NAME(S) AND ADDRESS(ES)
TPL, Inc.
3768 Hawkins Street NE
Albuquerque, NM 87109

8. PERFORMING ORGANIZATION REPORT NUMBER
TPL-FR-2049

9. SPONSORING/MONITORING AGENCY NAME(S) AND ADDRESS(ES)
U.S. Army ARDEC
SMCAR-AEE-WW
Picatinny Arsenal, NJ 07806

10. SPONSORING/MONITORING AGENCY REPORT NUMBER

11. SUPPLEMENTARY NOTES

12a. DISTRIBUTION/AVAILABILITY STATEMENT
Approved for public release; distribution unlimited

12b. DISTRIBUTION CODE

13. ABSTRACT *(Maximum 200 words)*

The best predictor of the extent of eutectic formation between explosive ingredients is the difference between their reciprocal melting temperatures ($r^2 > 0.86$ among 61 examples). Though the basis for predicting eutectic behavior from thermodynamic relationships such as van't Hoff's equation has come to be recognized in recent years, the correlation to melting point differences as the major contributor to this behavior seems to have been unrecognized in the energetic materials community. The correlation for binary compositions has the form: $\ln[X(\text{solute})/X(\text{solvent})] = -4314.48\Delta(T_m^{-1}) + 0.0363$, where solvent is defined as the lower-melting component. "Eutectics" between TNAZ and HMX and between TNAZ and 2,4-dinitroimidazole have been measured experimentally as essentially only melting point depressions due to <5% of the higher-melting ingredient as a minor constituent. The observation of this result from the TNAZ–HMX system led to the discovery of the correlation described above, which was confirmed by measurements of the new systems TNAZ–2,4-DNI and TNAZ–tetryl. The binary systems with HMX and with 2,4-DNI are predicted to contain 2.13 mol% and 2.33 mol%, respectively, according to the new correlation. The TNAZ–tetryl system was determined to have a eutectic temperature of 81.05 °C (DSC onset). The predicted composition based on known enthalpies of fusion is 65/35 TNAZ/tetryl.

14. SUBJECT TERMS			15. NUMBER OF PAGES
TNAZ	Phase diagrams	Formulations	67
Eutectics	Explosive	2,4-DNI	16. PRICE CODE

17. SECURITY CLASSIFICATION OF REPORT	18. SECURITY CLASSIFICATION OF THIS PAGE	19. SECURITY CLASSIFICATION OF ABSTRACT	20. LIMITATION OF ABSTRACT
Unclassified	Unclassified	Unclassified	Unlimited

TABLE OF CONTENTS

LIST OF FIGURES

LIST OF TABLES

APPENDICES

INTRODUCTION

One of the advanced energetic materials of special interest to ARDEC's "More Powerful Explosives Program" is the relatively new nitramine 1,3,3-trinitroazetidine (TNAZ), first synthesized at Fluorochem Inc. (Azusa, CA) in 1984.[1] TNAZ exhibits some unusual and potentially valuable properties for explosives applications. The theoretical basis for the utilization of small (≤4-membered) ring molecules as explosives and propellant oxidizers is that the intrinsic strain energy of such molecular systems is released upon combustion along with its chemical energy, thus contributing to the performance of its application as an energetic material. TNAZ has proven to be particularly appealing in this respect. By virtue of its chemical energy plus its strain energy of ~37 kcal/mole, it offers explosive performance exceeding that of the Army's current most powerful explosive, LX-14 (95.5% HMX + Estane binder), according to small-scale testing.[2,3] In addition, BLAKE code calculations estimating TNAZ's performance as a gun propellant ingredient predict it to be better than or equal to the Navy's CL-20, another potential advanced oxidizer.[4] With a melting point of 99 °C, it is a steam-castable explosive like TNT but with significantly greater potential performance. With a higher oxygen balance compared to RDX (+8.3% vs. 0% relative to CO formation), it may be expected that TNAZ will output less carbon on explosion. It is relatively thermally stable, showing no measurable decomposition in the melt at 132 °C and short-term stability to higher temperatures, with an exotherm maximum >240 °C,[2,3] while HMX shows measurable gas evolution at 132 °C. Finally, it shows good compatibility with many materials, including aluminum, steel, brass, and glass. As it lacks any particularly chemically sensitive structural features, it may be expected to show good compatibility with many other stable organic energetic materials, such as TNT, for example.

With prospects in sight for improved synthetic routes and scale-up procedures for TNAZ,[3] the use of TNAZ in formulated explosive compositions deserves development. Such formulations could fill an Army (and DoD) need for improved-performance, insensitive munition for anti-armor,

---

1 Archibald, T.G.; Baum, K. Azusa (CA), 1984, "Research in Energetic Compounds" *Fluorochem Inc. Report ONR-2-6*; AD-A137 484.

2 (a) Iyer, S.; Alster, J.; Sandus, O.; Gelber, N.S.; Slagg, N. *Army Science Conference [Proc.]*, Ft. Monroe, VA, October 1988; Vol. IV, p. 43. (b) Iyer, S.; Velicky, R.; Sandus, O.; Alster, J. Dover (NJ), 1989, "Research Toward More Powerful Explosives" *Report ARAED-TR-89010*; AD-B133 880L.

3 Iyer, S.; Eng, Y.S.; Joyce, M.; Perez, R.; Alster, J.; Stec, D., III "Scaled-Up Preparation of 1,3,3-Trinitroazetidine (TNAZ)" *Joint International Symposium on Compatibility of Plastics and Other Materials with Explosives, Propellants, Pyrotechnics, and Processing of Explosives, Propellants, Pyrotechnics [Proc.]*, San Diego, CA, April 1991, pp. 80-84.

4 BTI Program Project Implementation Plan, "Integrated, High Performance Energetic Materials Program" (April 1988), Dr. David Squire (DARPA), Technical Manager.

mine, and demolition applications. Its likely first use may be in specialty applications such as penetration-augmented munitions (PAMs) or explosively formed penetrators (EFPs). A TNAZ-based improvement upon Composition C-4 (90–91% TNAZ) has also been receiving noteworthy development.[5]

BACKGROUND

A qualitative observation has been reported that TNAZ, unlike HMX, has significant solubility in TNT.[2,3] In addition, TNAZ's chemical similarity to other explosive compounds of possible interest as co-ingredients (especially the nitramines) suggested that the potential for *their* solubility in TNAZ should also be considered. This is an important determination to make before undertaking extensive computational efforts to predict performance of new formulations. Important physical properties of such mixtures (i.e., *solid solutions*) are susceptible to potentially significant change depending on apparently minor effects like crystal lattice differences, even among chemically similar species. Solubility properties have been determined for the components of some well established formulations, such as Composition B: RDX's solubility in liquid TNT ranges from 4.5 g/100 g TNT at 81 °C to 8.2 g/100 g at 110 °C.[6] Thus, an understanding of the principles of *phase equilibria* is important here. A possible condition existing for some of the ingredients and formulations to be considered within a program for development of new TNAZ formulations is that a solid ingredient may be partially soluble in another solid just as liquids may be partially miscible with other liquids.

Furthermore, even in the absence of appreciable solubility as solid solutions, many mutually similar covalent organics may interact to produce appreciable physical effects in the mixture. A common example of such a phenomenon is freezing-point depression to a low-melting *eutectic*. Such interactions and effects have previously been noted in several binary explosive mixtures, as tabulated in the Picatinny Arsenal "Encyclopedia of Explosives and Related Items."[7] The existence of lower-melting eutectics in binary formulations could offer an advantage of easier processing of melt casts. On the other hand, possible disadvantages are that a formulation's properties may be adversely affected by certain types of interactions. Specific examples could be different densities of solid-state solutions (than expected for heterogeneous mixes); different thermal expansion/contraction effects as a result of phase changes partially or entirely throughout a sample; or different hazard sensitivities than those of the separate ingredients. For these reasons,

5 Iyer, S. *et al.* "TNAZ Based Composition C-4 Development" *Eleventh Annual Working Group Institute on Synthesis of High Energy Density Materials [Proc.]*, Kiamesha Lake, NY, June 1992, pp. 495-504.

6 Fedoroff, B.T.; Sheffield, O.E. "Encyclopedia of Explosives and Related Items"; Picatinny Arsenal: Dover, NJ, 1966; Vol. 3, p. C 615.

7 Fedoroff, B.T.; Sheffield, O.E. "Encyclopedia of Explosives and Related Items"; Picatinny Arsenal: Dover, NJ, 1974; Vol. 6, pp. E 343-E 346.

ARDEC has been interested in characterizing binary formulations involving TNAZ with certain other explosive ingredients of interest. In discussions between the current Principal Investigator and ARDEC technical personnel, the binary systems of interest were tentatively chosen to be those of TNAZ with HMX, 2,4-dinitroimidazole (2,4-DNI), and nitrotriazolone (NTO).

The experimental method that was chosen to study the phase behavior of these systems is differential scanning calorimetry (DSC). Although there are other good methods for making such measurements, DSC offers certain advantages, such as sensitivity toward very small thermal transitions. The technique is also well established for making such measurements, as described, for example, in standard textbooks on thermal analysis.[8] In the classical benzoic acid–naphthalene system shown in Figure 1, there is seen upon addition of benzoic acid to pure naphthalene an initial lowering of the naphthalene melting point to a low-melting *eutectic mixture* of the two. Upon addition of excess benzoic acid, there is a separate endotherm for melting of the benzoic acid component, which approaches the melting point of pure benzoic acid as its relative concentration is increased.

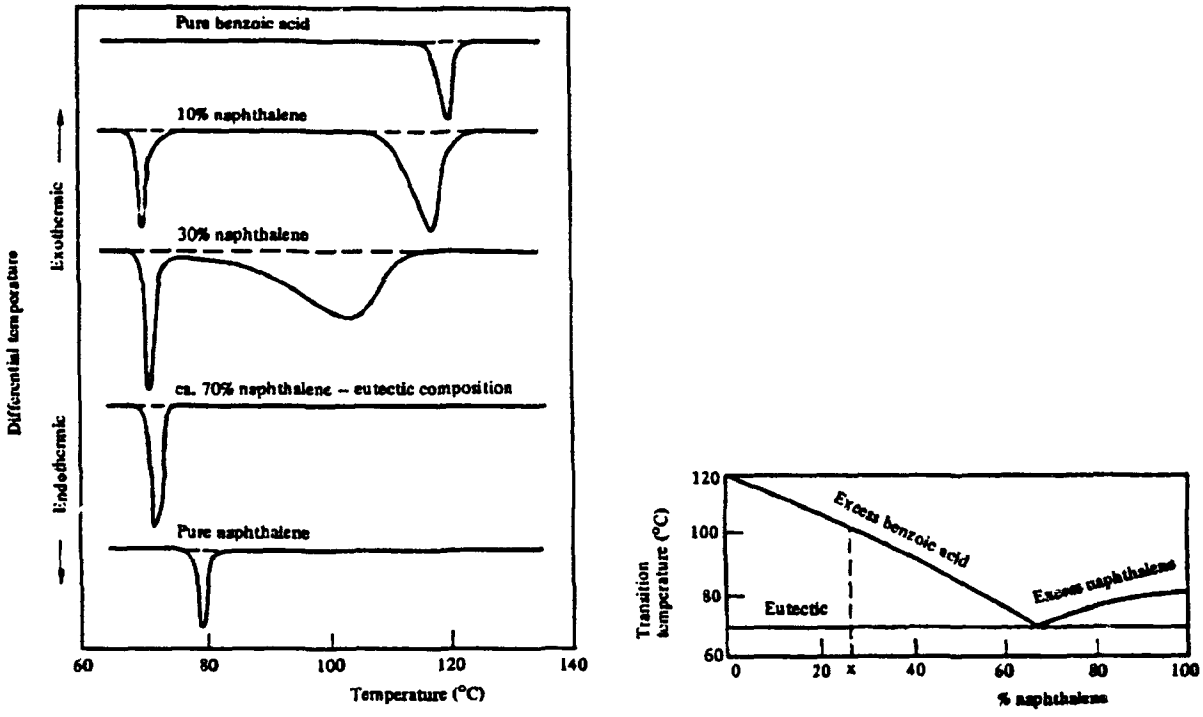

Figure 1. Differential scanning calorimetry for phase diagram elucidation of the benzoic acid–naphthalene system (from reference 8)

8 Daniels, T.C. "Thermal Analysis"; Halsted Press: New York, 1973.

Experimental measurements like these allow construction of eutectic phase diagrams—such as the simple eutectic system for naphthalene–benzene shown in Figure 2 below—by determination of the solidus line, the temperature at which first liquefaction occurs (a low-melting eutectic in this case), and the liquidus line (curve *CED*), the temperature and composition at which complete liquefaction occurs.[9]

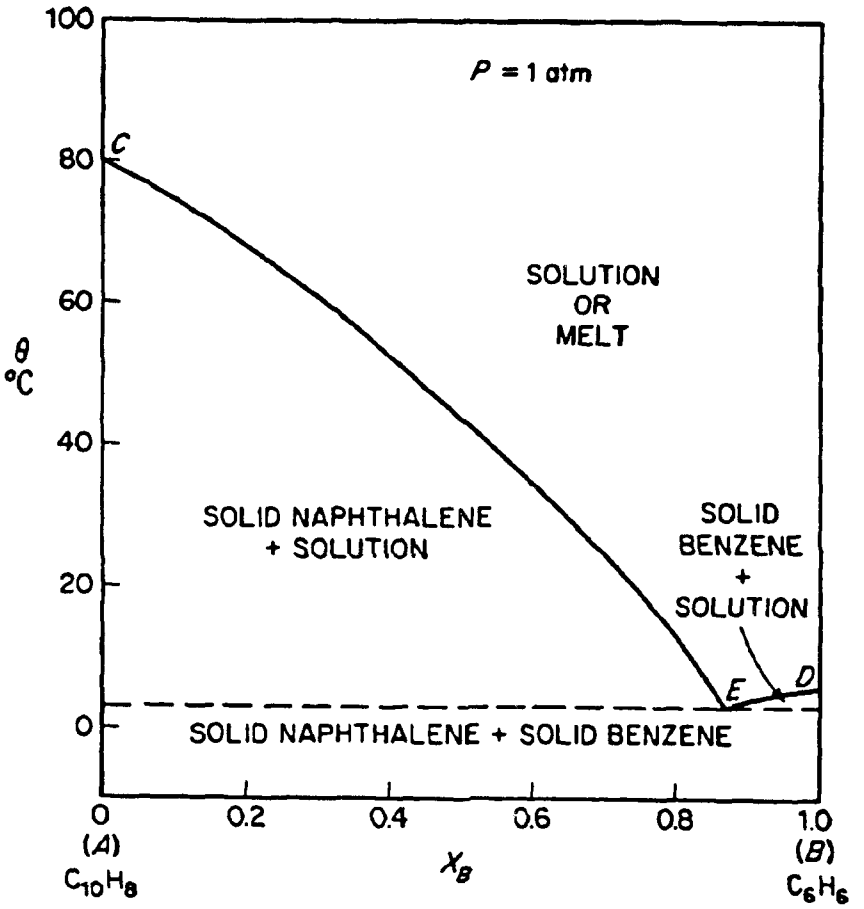

Figure 2. Temperature–composition diagram for the system naphthalene (*A*) and benzene (*B*) (from reference 9). The solids are mutually insoluble and the liquid solution is practically ideal.

9 Moore, W.J. "Physical Chemistry", 4th ed.; Prentice-Hall, 1972; p. 248.

RESULTS AND DISCUSSION

TNAZ–HMX SYSTEM

The sample of TNAZ used in these studies was provided by ARDEC. The HMX sample was pure production-grade material on hand at Pacific Scientific. Most mixtures were prepared by blending precisely weighed quantities in a dry state. Static problems required that the mix of 5% TNAZ/95% HMX be blended as a paste (with water plus 2-propanol) and then thoroughly dried.

Figure 3 shows a typical DSC thermogram of pure TNAZ subjected to a repetitive heating/cooling regimen, cycling between 30 °C and 175 °C at a typical heating rate of 5 °C/min. The repetitive cycling was expected to allow establishment of compositional equilibrium in the mixtures with co-ingredients, and this analysis of the pure TNAZ confirmed its stability (as detectable by DSC) in this temperature range. The conspicuous features in this thermogram are the melting endotherm around 100 °C, and upon cooling, a sharp exotherm at a lower temperature. Figure 4 shows seven repetitive cycles overlaid. In all cases, the exothermic crystallization transitions for TNAZ occur at peak temperatures in the range of 44–54 °C and therefore represent examples of unavoidable *supercooling* of the liquid TNAZ under these physical conditions; the supercooling temperature is not precisely reproducible. The same phenomenon can be seen in later analyses of the mixtures.

In the TNAZ–HMX system, samples of the following TNAZ/HMX mole ratios were prepared and analyzed: 95/5, 75/25, 50/50, 25/75, 5/95.

Figure 5 is a typical DSC thermogram of one of the TNAZ/HMX mixtures studied, this one comprised of 95 mol% TNAZ with 5 mol% HMX. We have concentrated on the TNAZ melting endotherm as a diagnostic for phase modification effects (e.g., eutectic formation) in most of our analyses. A sequence of four cycles of the 95/5 mixture is overlaid in Figure 6. A qualitative trend was distinctly apparent, because the transition temperatures decreased monotonically through the set of cycles. In fact, the trend quantitatively follows a clean decaying exponential, as determined by statistical analysis of all of the data sets, leading to constant equilibrium values. Figure 7 shows a typical example of the statistical analysis, using this same experiment. The observed trend can be attributed to the relatively slow establishment of compositional equilibrium because of the static condition of the sample with respect to motion; equilibrium is therefore achieved by diffusion of the ingredients throughout the thermal cycling. In this case, HMX—which turns out to be only slightly soluble in TNAZ at the melting point, as concluded from results below—only gradually dissolves to establish equilibrium.

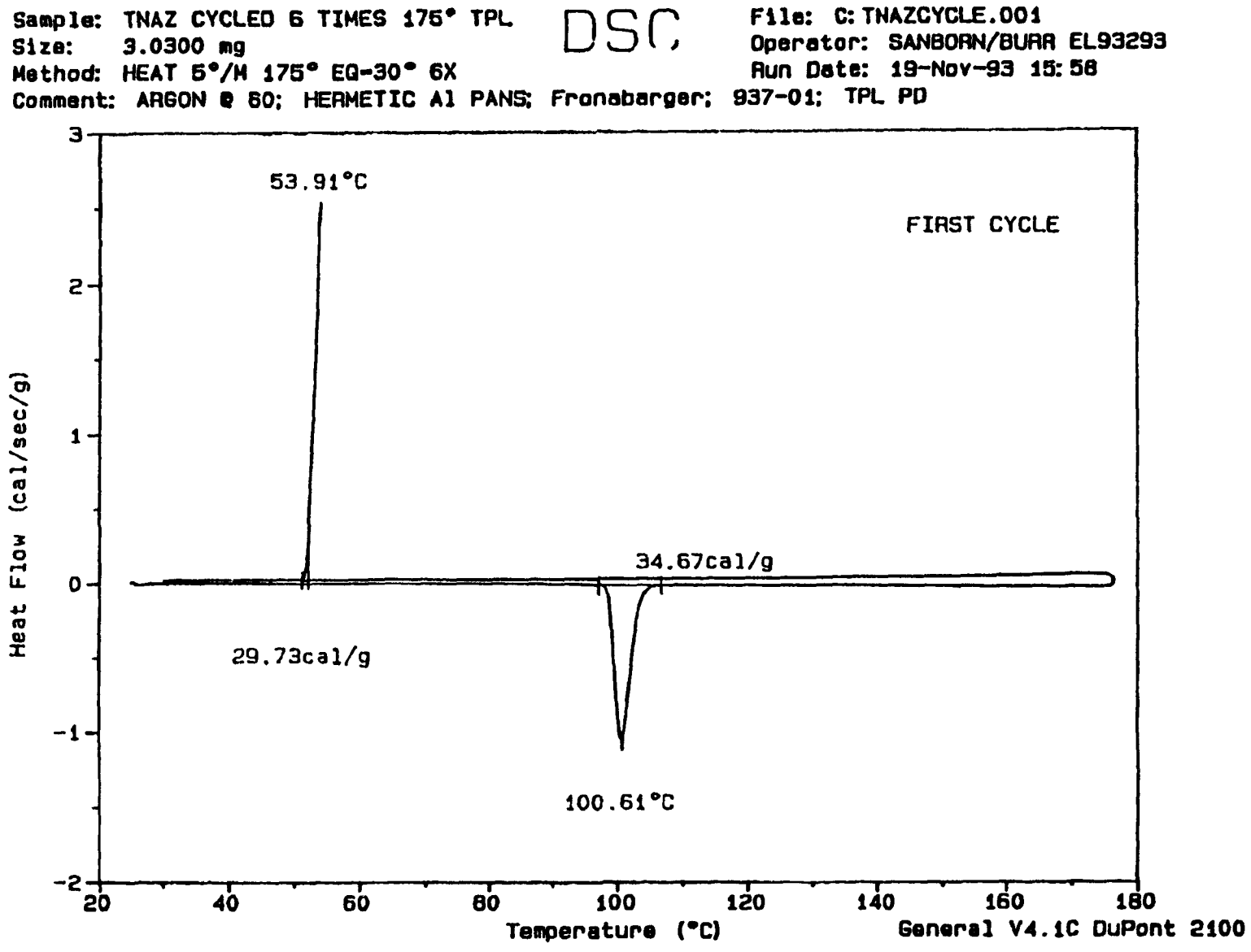

Figure 3. DSC thermogram of pure TNAZ, first cycle through 30–175 °C (5 °C/min)

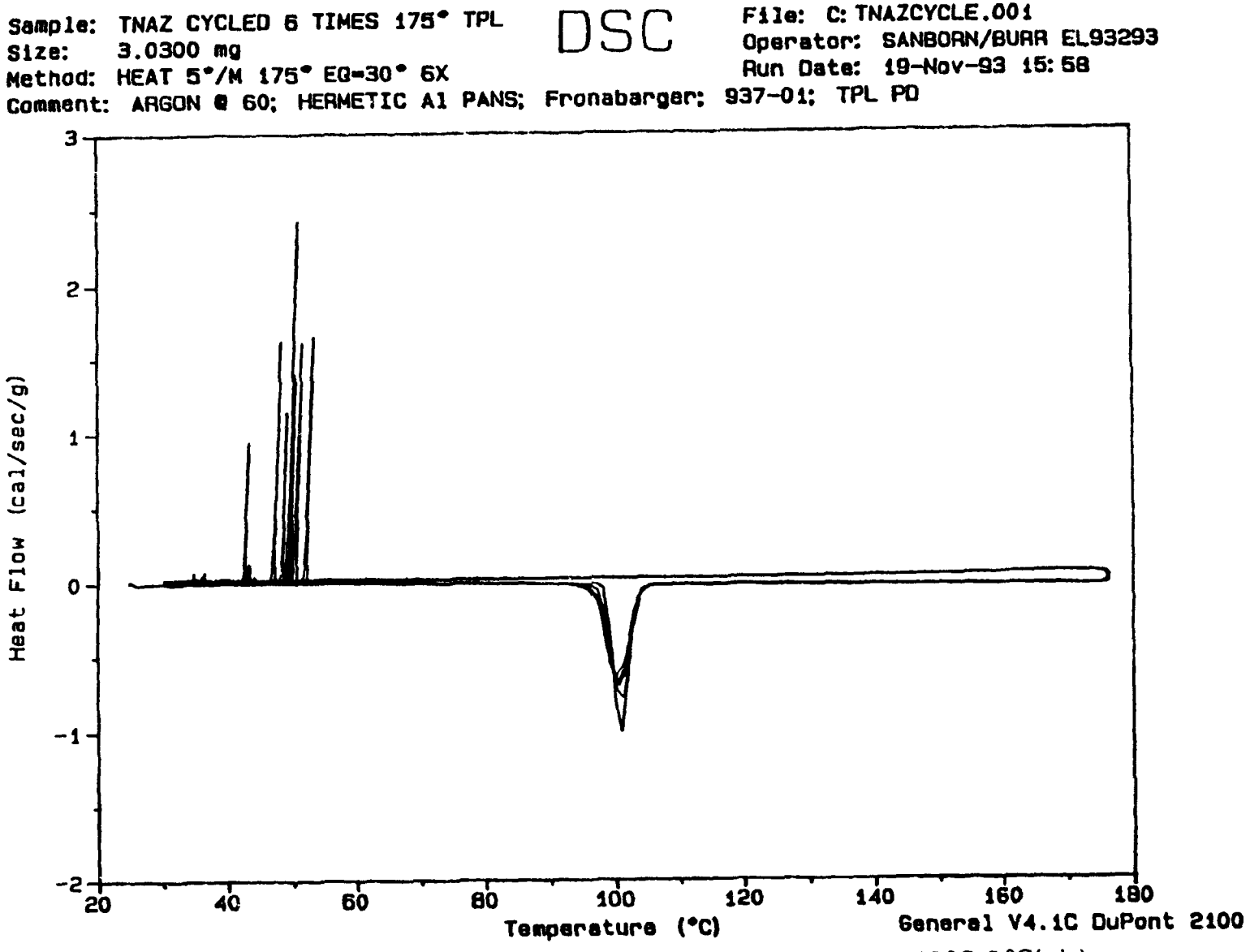

Figure 4. Overlay of seven repetitive thermograms of pure TNAZ (30–175 °C, 5 °C/min)

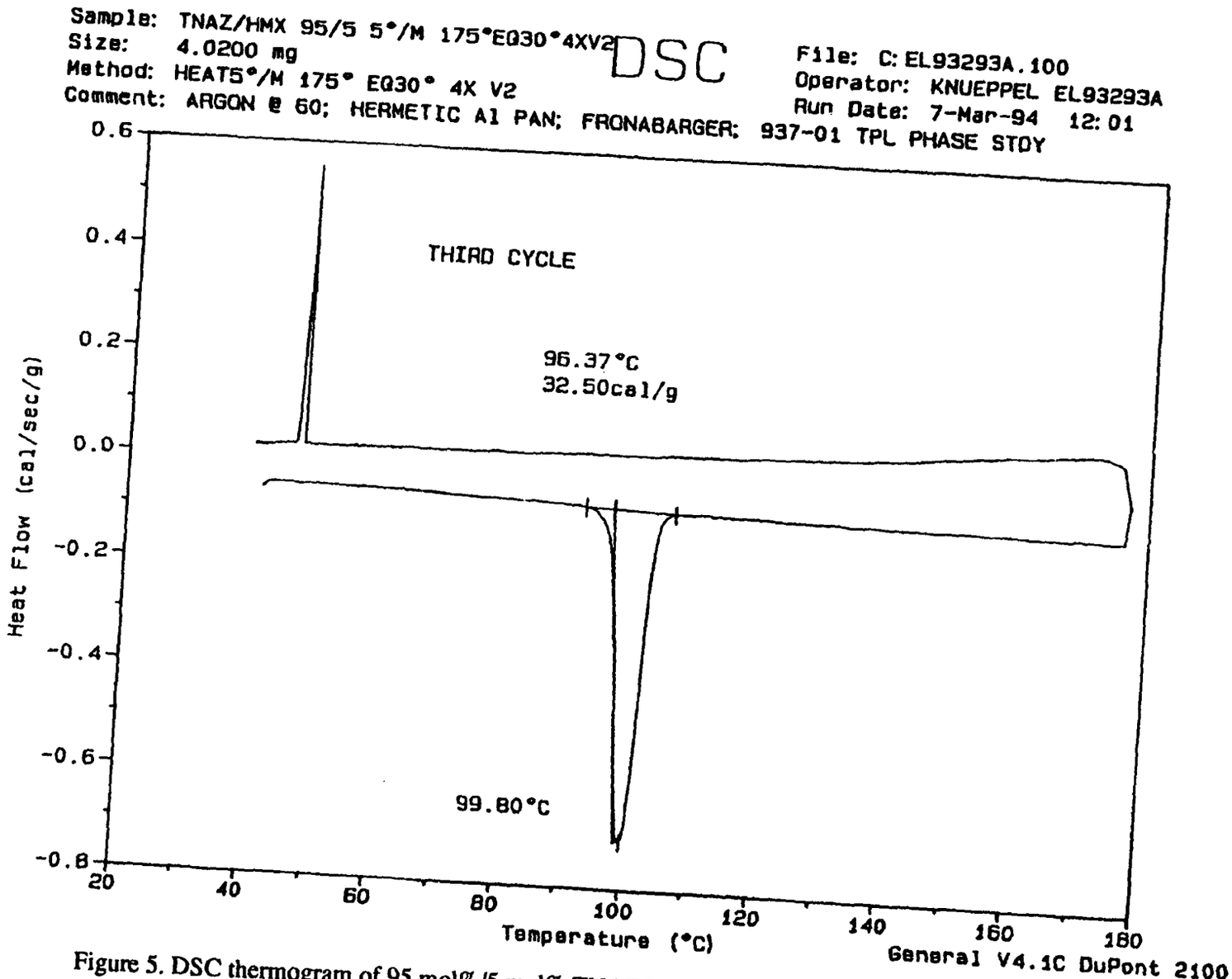

Figure 5. DSC thermogram of 95 mol%/5 mol% TNAZ/HMX, third cycle through 30–175 °C (5 °C/min)

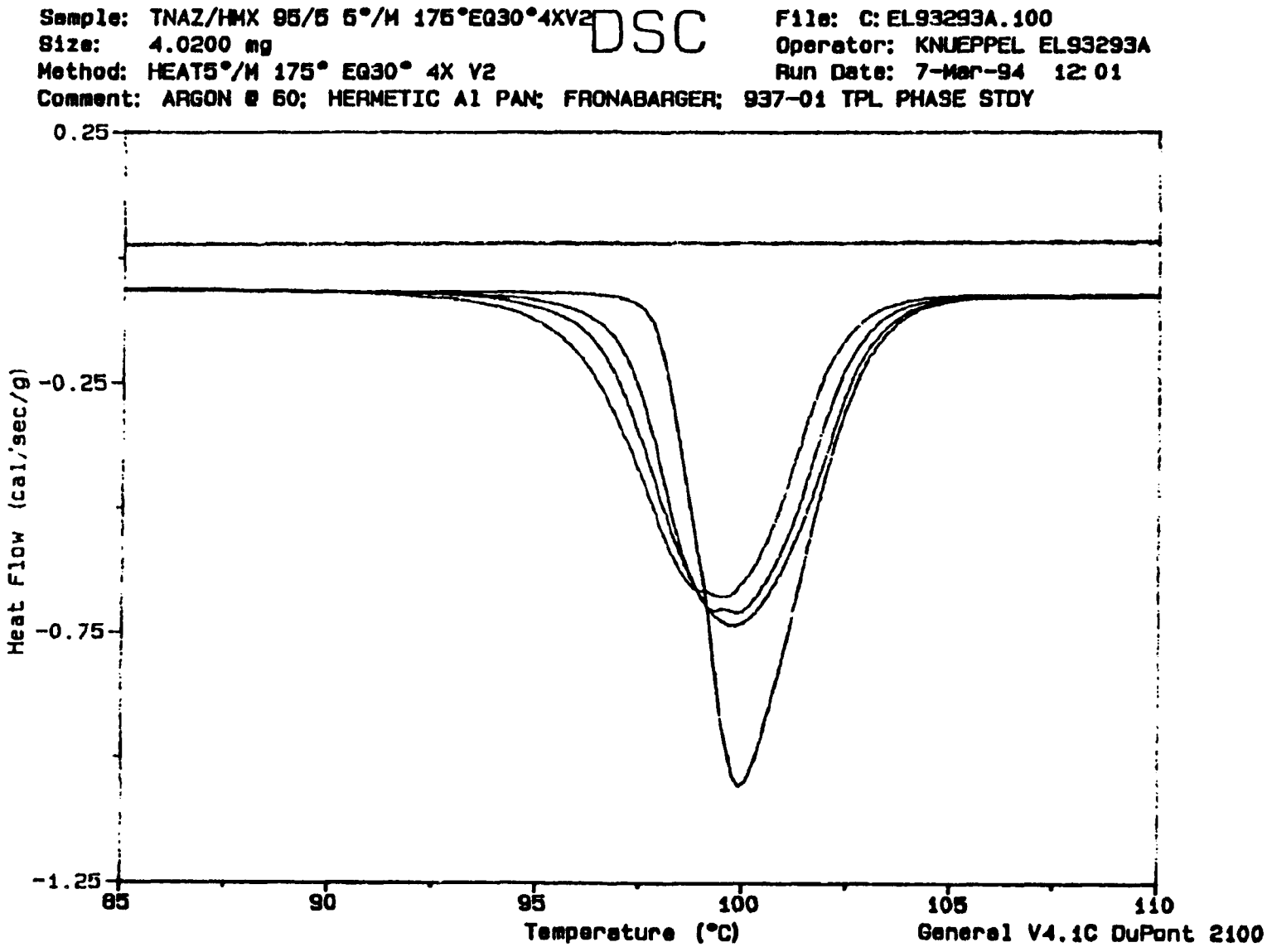

Figure 6. Overlay of four repetitive thermograms of 95/5 TNAZ/HMX (30–175 °C, 5 °C/min)

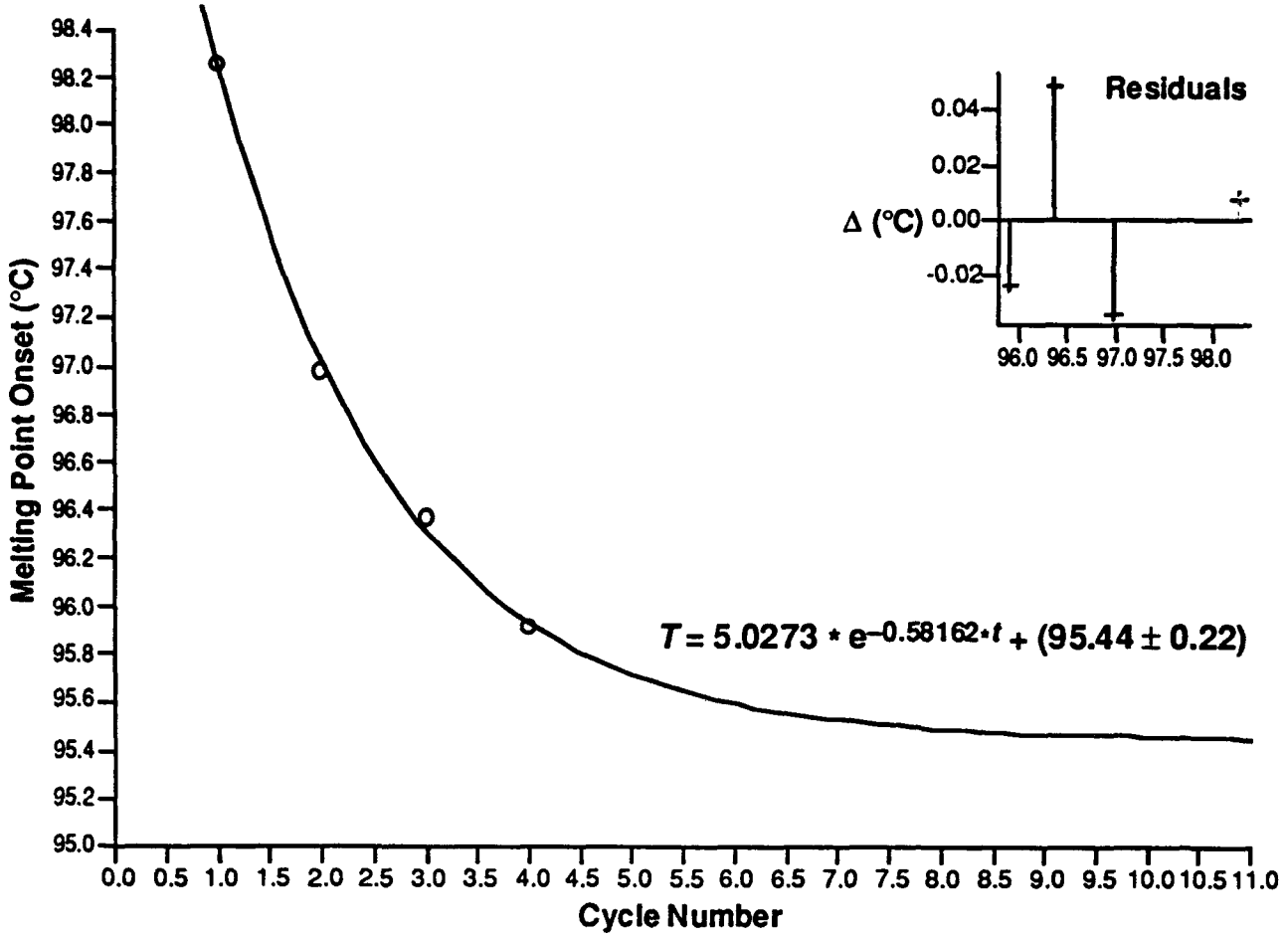

Figure 7. TNAZ/HMX 95%/5% (cycled 30–175 °C): analysis of melting onset temperatures as a function of thermal cycling

Thermal analysis of the 75/25 TNAZ/HMX composition looks qualitatively typical (Figure 8): an endotherm around 100 °C, and supercooling in this case to 60–70 °C. This system was allowed to go through the longest equilibration of the mixtures studied, going through 20 cycles up to 175 °C and recooling to 30 °C. Statistical analysis of this equilibration is shown in Figure 9. In a fast heating run to decomposition after the cycling (Figure 10), there is seen the major decomposition of TNAZ peaking at about 260 °C, with a slight shoulder due to the minor HMX present.

A 50/50 mixture looks qualitatively still the same (Figure 11): there are no significant phase effects (manifested in the TNAZ melting endotherm) of having these ingredients in a mixture. A similar exponential decay of the transition temperatures exists (Figure 12), though it is not as well defined as in some of the other experiments. The statistics can reflect this uncertainty. In a heating run of the equilibrated mixture (Figure 13), distinct decomposition exotherms for the equimolar ingredients, TNAZ and HMX, are apparent. There is a small but distinct feature at about 181 °C.

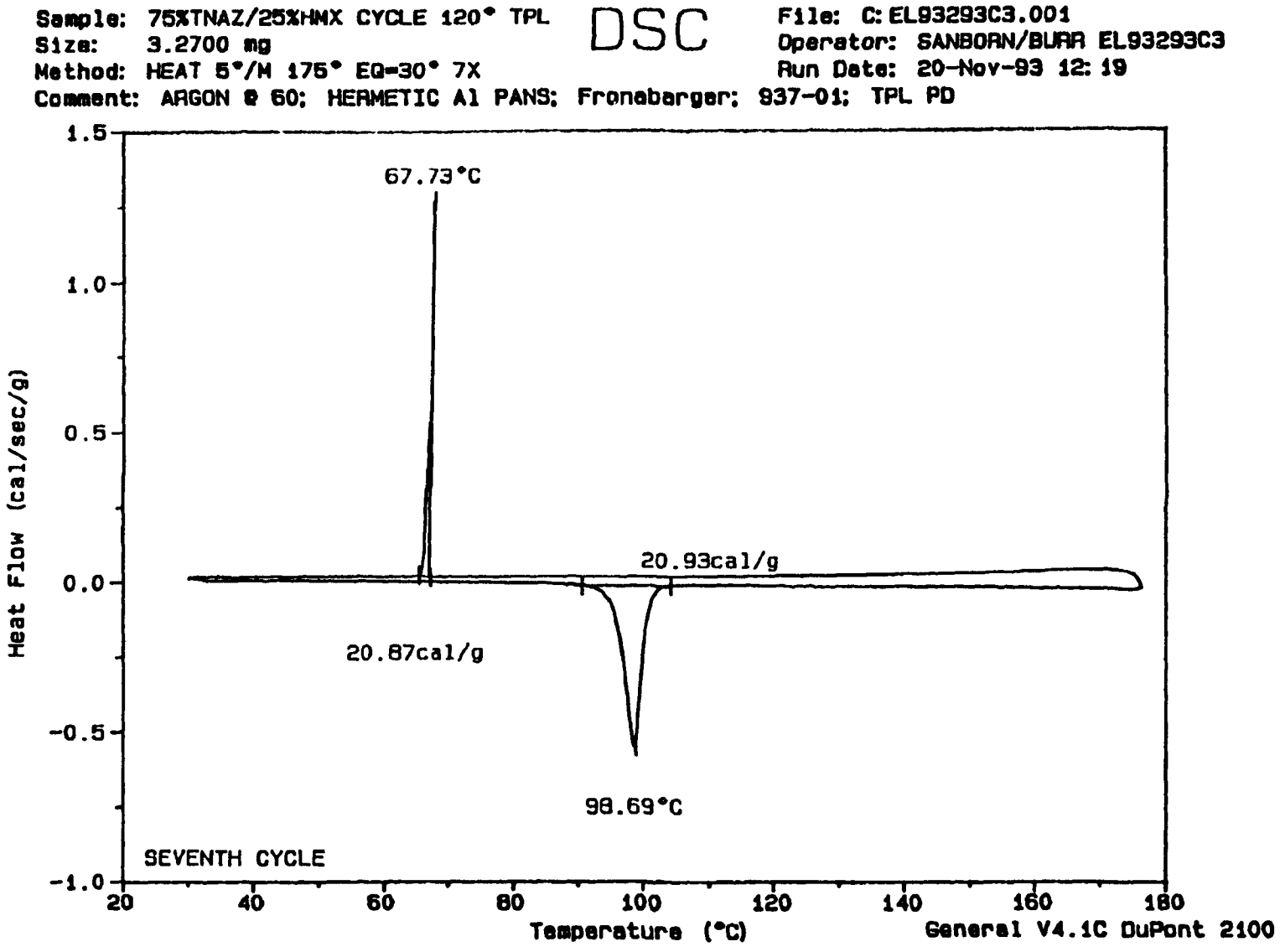

Figure 8. DSC thermogram of 75 mol%/25 mol% TNAZ/HMX, seventh cycle through 30–175 °C (5 °C/min)

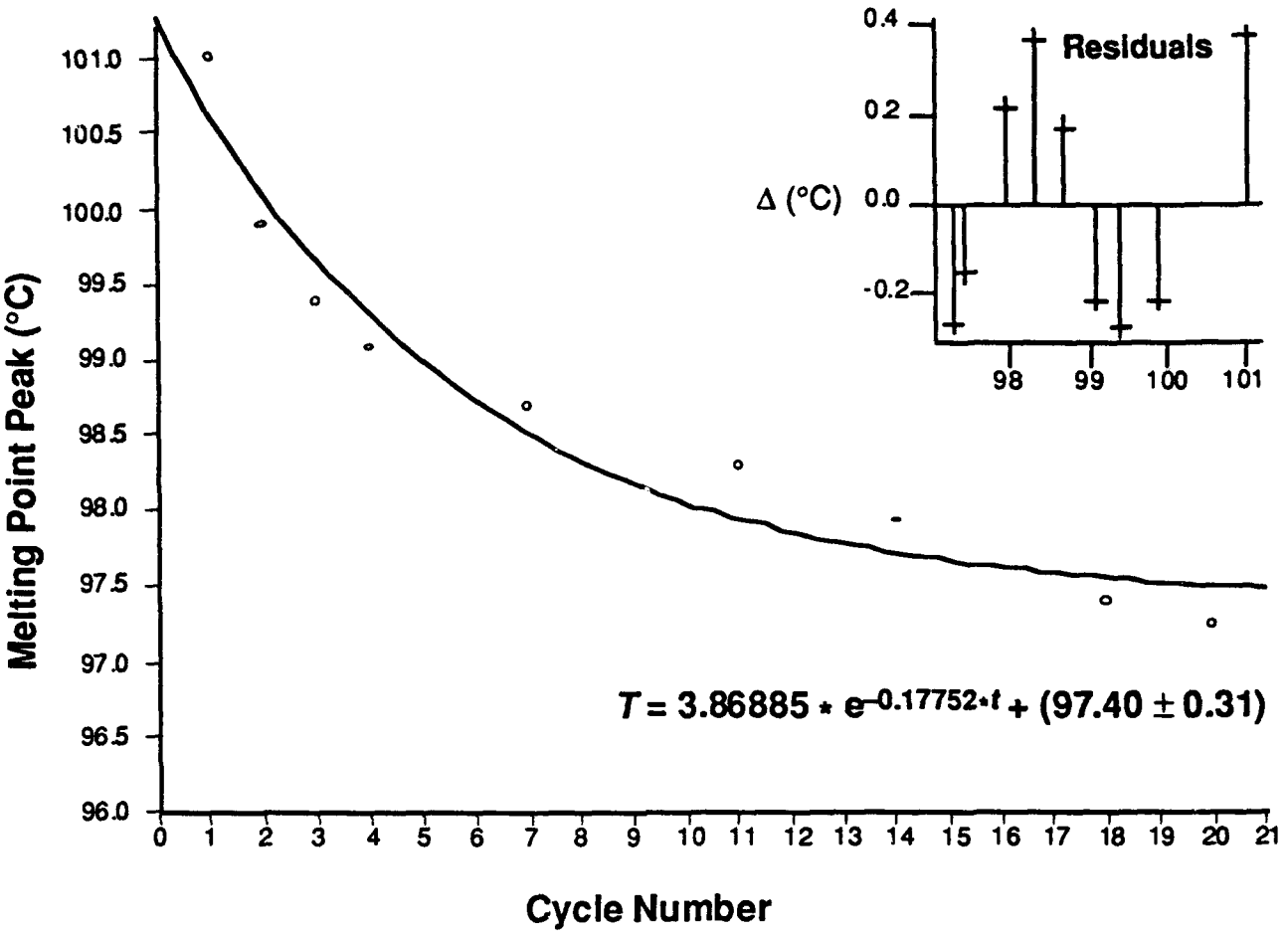

Figure 9. TNAZ/HMX 75%/25% (cycled 30–175 °C):
analysis of melting peak temperatures as a function of thermal cycling

This feature is an endotherm for the β-to-δ polymorph transition of HMX,[10] which is not seen upon cycling only to 175 °C.

The 25/75 TNAZ/HMX mixture *still* exhibits similar behavior of the TNAZ endotherm, as shown in the statistical analysis of Figure 14.

In a 5/95 TNAZ/HMX mixture, the TNAZ melting transition is much smaller, indicated by the noise in the thermogram (Figure 15). This is a situation in which DSC may have advantages over other methods of analysis, such as optical methods in which melting of a small

[10] (a) Hall, P.G. *Trans. Faraday Soc.* **1971**, *67*, 556-562. (b) Goetz, F.; Brill, T.B. *J. Phys. Chem.* **1979**, *83*, 340-346. (c) Brill, T.B.; Karpowicz, R.J. *J. Phys. Chem.* **1982**, *86*, 4260-4265. (d) Achuthan, C.P.; Jose, C.I. *Propellants Explos. Pyrotech.* **1990**, *15*, 271-275. (e) Quintana, J.R.; Ciller, J.A.; Serna, F.J. *Propellants Explos. Pyrotech.* **1992**, *17*, 106-109.

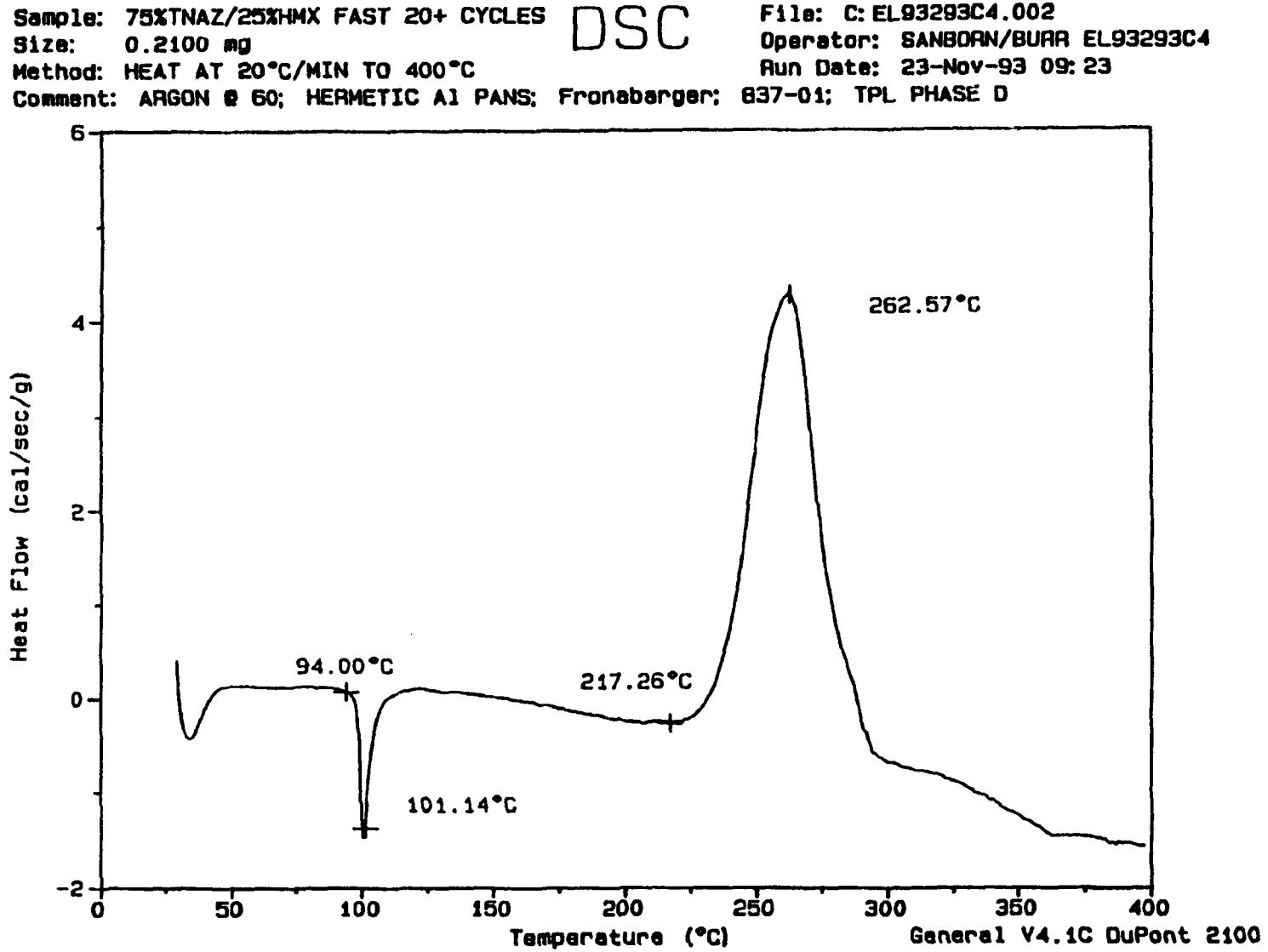

Figure 10. DSC thermogram of 75 mol%/25 mol% TNAZ/HMX, heating run to decomposition (20 °C/min)

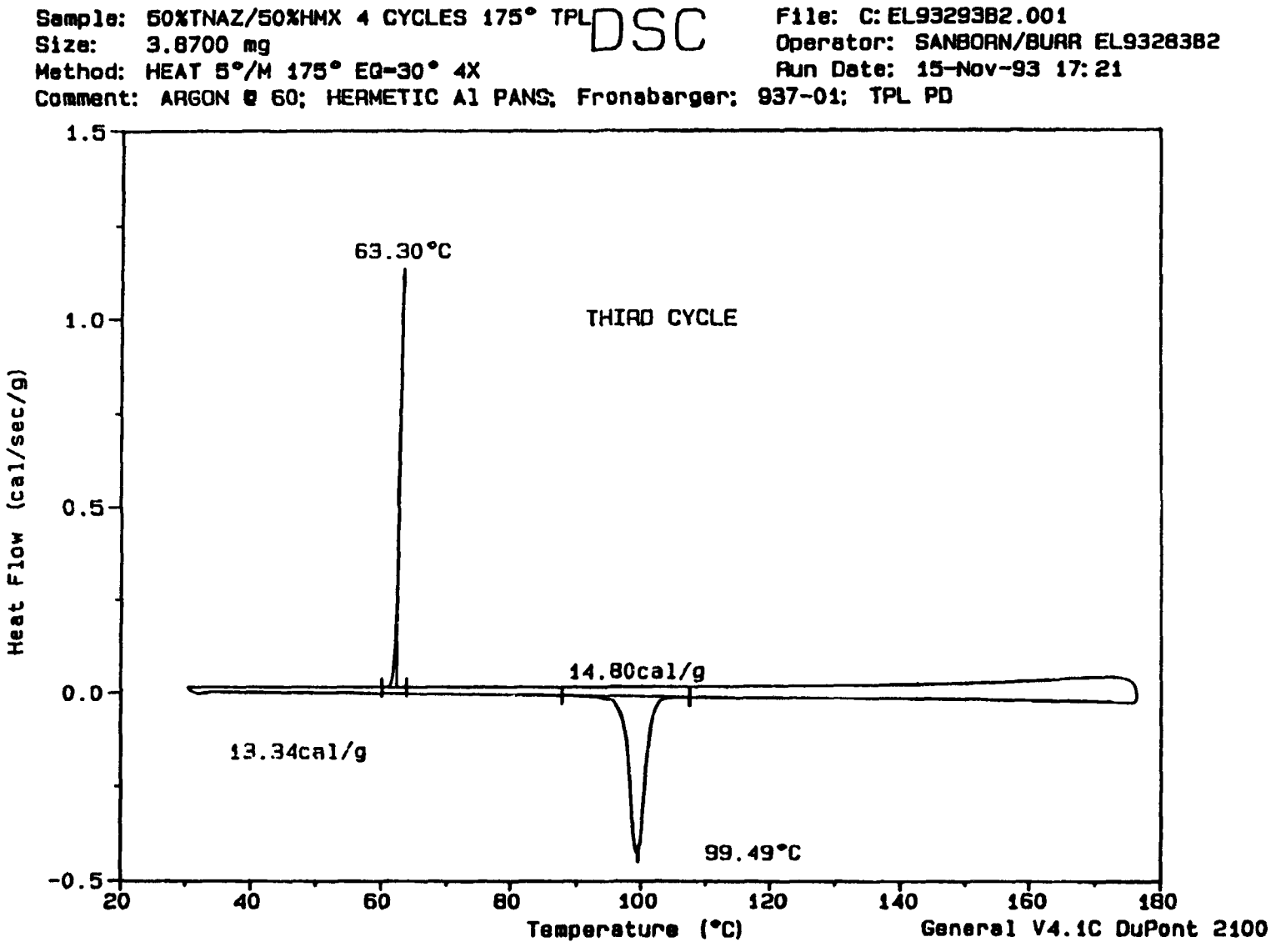

Figure 11. DSC thermogram of 50 mol%/50 mol% TNAZ/HMX, third cycle through 30–175 °C (5 °C/min)

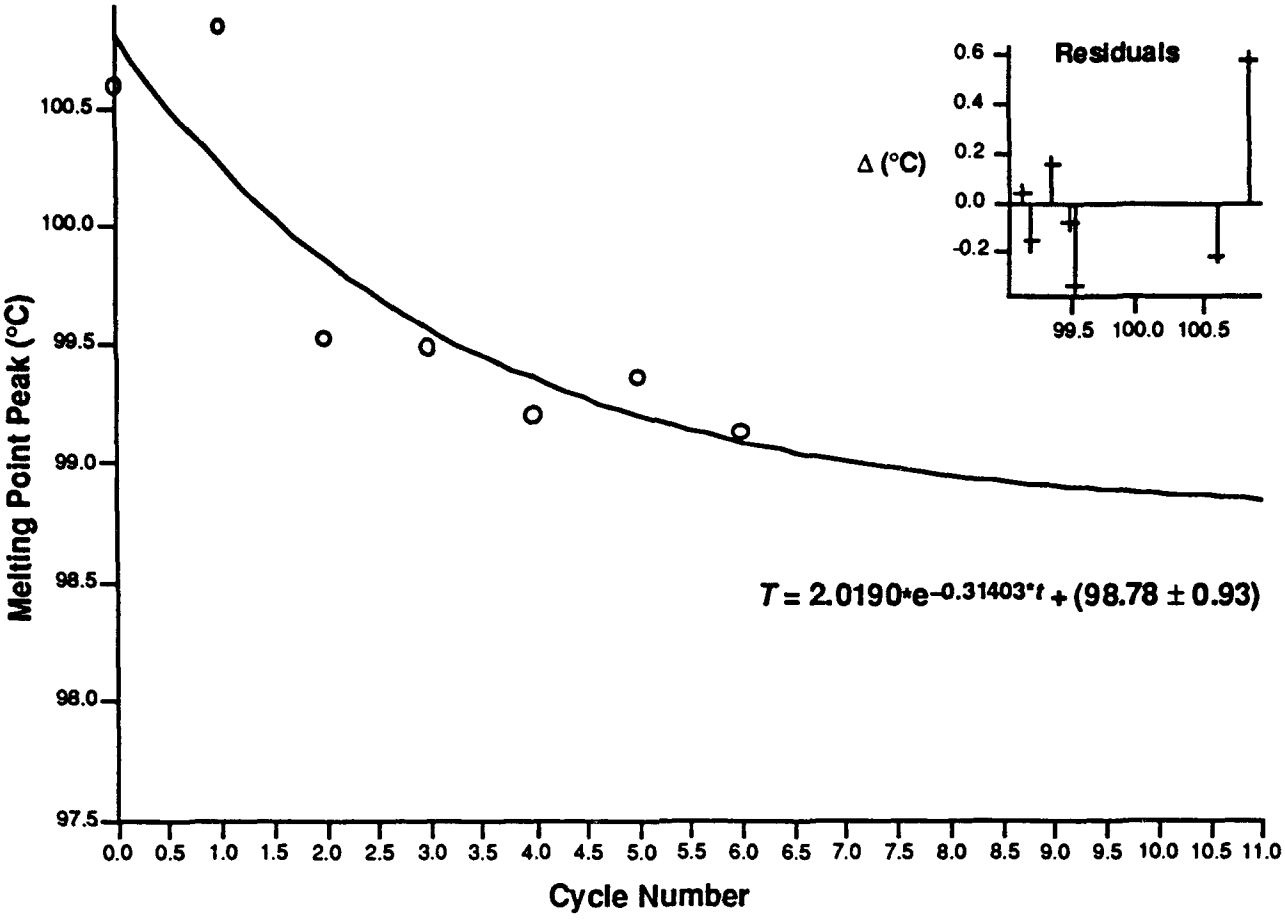

Figure 12. TNAZ/HMX 50%/50% (cycled 30–175 °C):
analysis of melting peak temperatures as a function of thermal cycling

homogeneously mixed component occurs in the presence of a large excess of solid. The decaying temperature trend is still well behaved, nevertheless (Figure 16).

Overlaid thermograms of pure TNAZ were shown previously (Figure 4). A similar analysis of the endotherm temperatures as a function of cycling is also informative (Figure 17). In particular, a distinct decreasing trend is not seen as in all of the mixtures. The whole span of temperatures is also smaller than the changes undergone by the mixtures. The seven points show a standard deviation of 0.26 °C, which is reasonably within the reproducibility of DSC as a technique. Even taking a forced regression line through these points includes *a line of constant temperature* within its 95% confidence limits, so the average temperature, 100.59 °C, was taken as the melting transition peak of this TNAZ. On the other hand, the DSC feature generally accepted as corresponding to a pure organic's melting point is the melting transition onset. In the pure TNAZ used in this study, the melting onset occurred at 98.68 °C in the first thermogram of the sequence of seven thermal cycles. Subsequent melting onsets appeared at an average temperature of 97.27 °C.

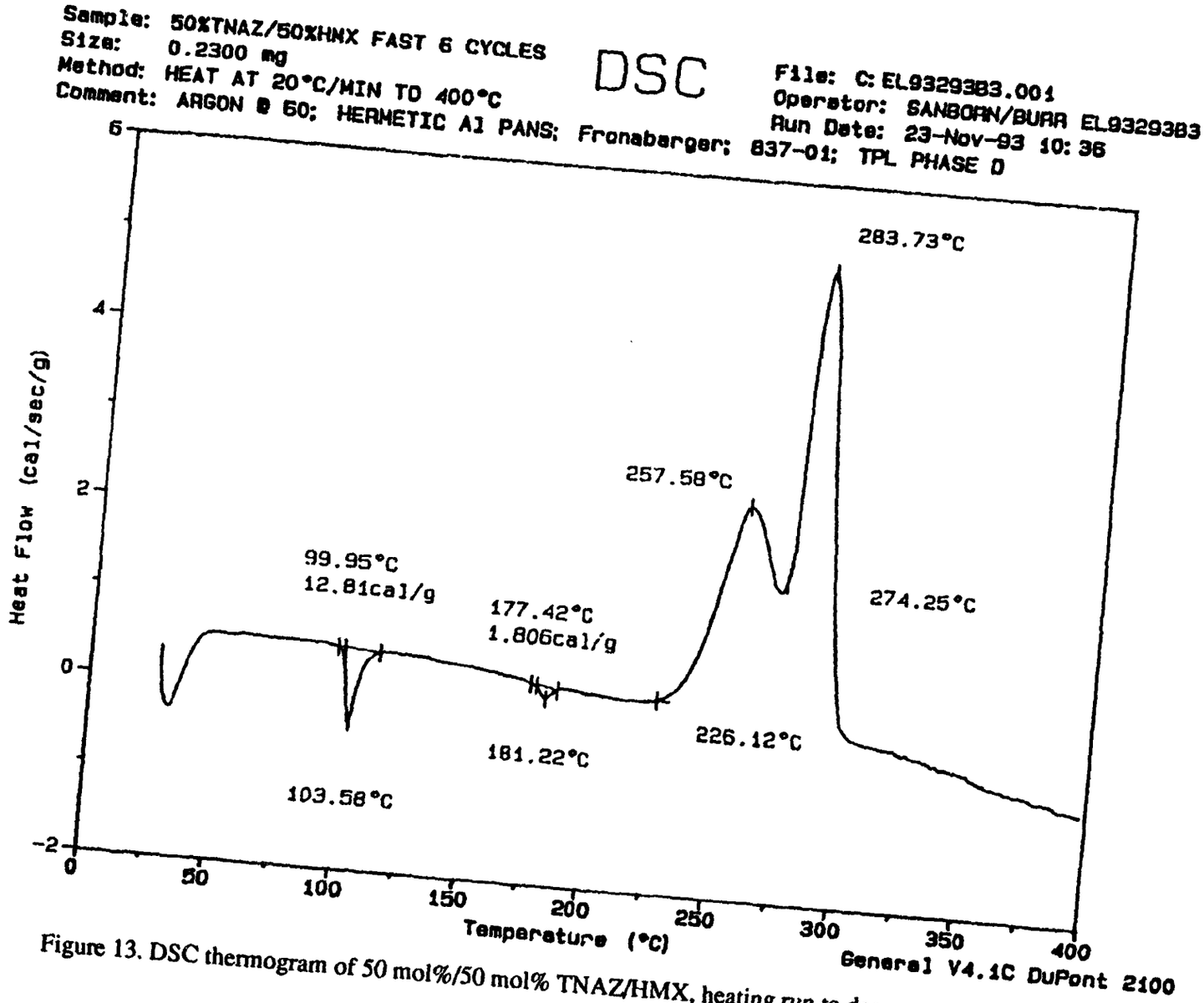

Figure 13. DSC thermogram of 50 mol%/50 mol% TNAZ/HMX, heating run to decomposition (20 °C/min)

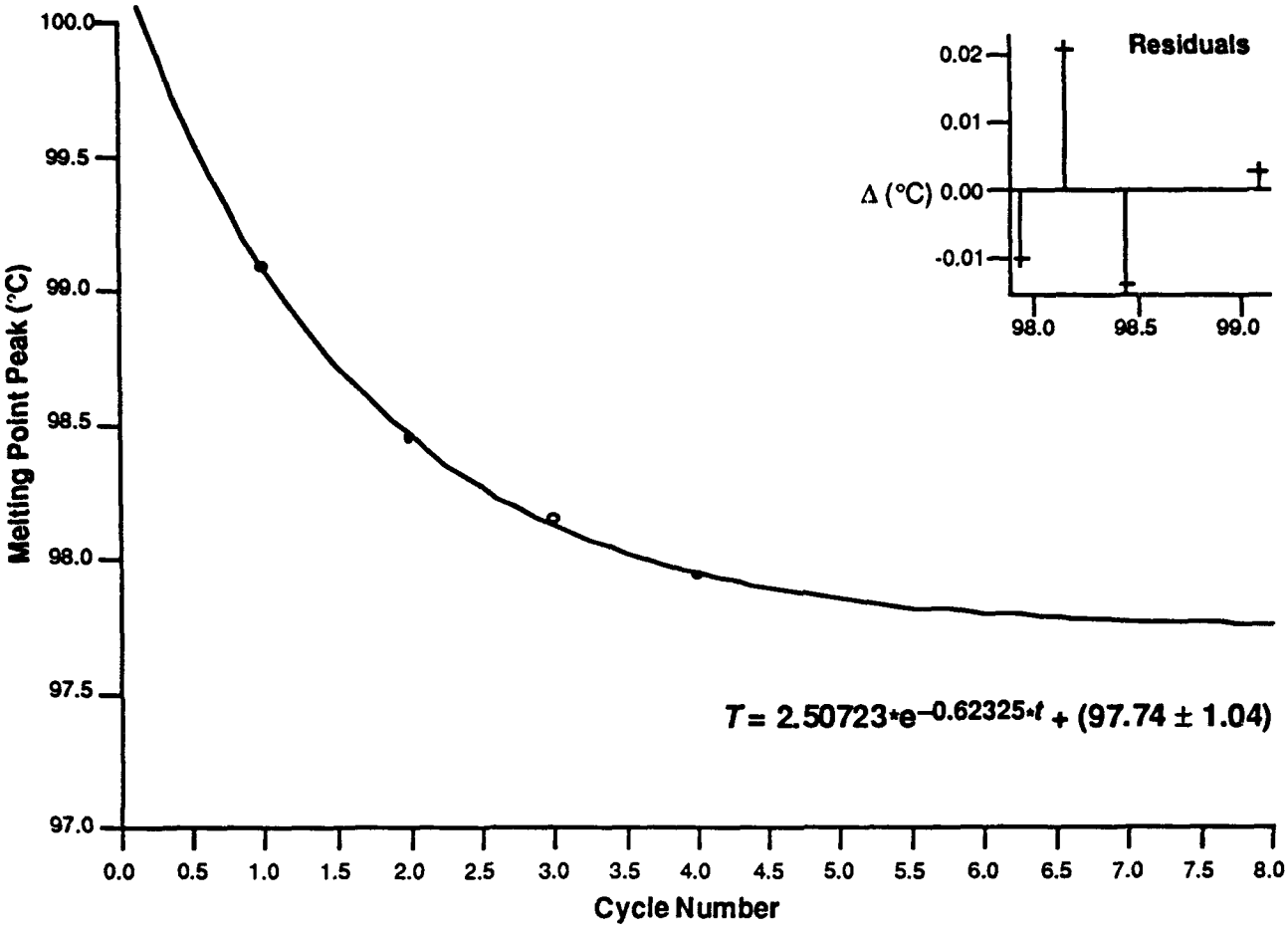

Figure 14. TNAZ/HMX 25%/75% (cycled 30–175 °C):
analysis of melting peak temperatures as a function of thermal cycling

The first melting onset corresponds to the melting point of TNAZ (99 °C) previously reported by ARDEC.[2b]

Another analysis may have a bearing on interpretations of DSC temperatures. Radomski and Radomska[11] showed that equation (1)—which describes the *temperature interval*, ΔT_{iso}, of an isothermal transition (the temperature difference between the onset of the transition and its peak)—also applies to the *absolute temperature of the transition peak* with respect to a dependence on the square root of the heating rate:

$$\Delta T_{iso} = \left[\dot{T}_p \Delta H \left(2R_0 + \frac{rm}{A^2 \rho}\right)\right]^{1/2} \qquad (1)$$

[11] Radomski, R.; Radomska, M. *J. Thermal Anal.* **1982**, *24*, 101-109.

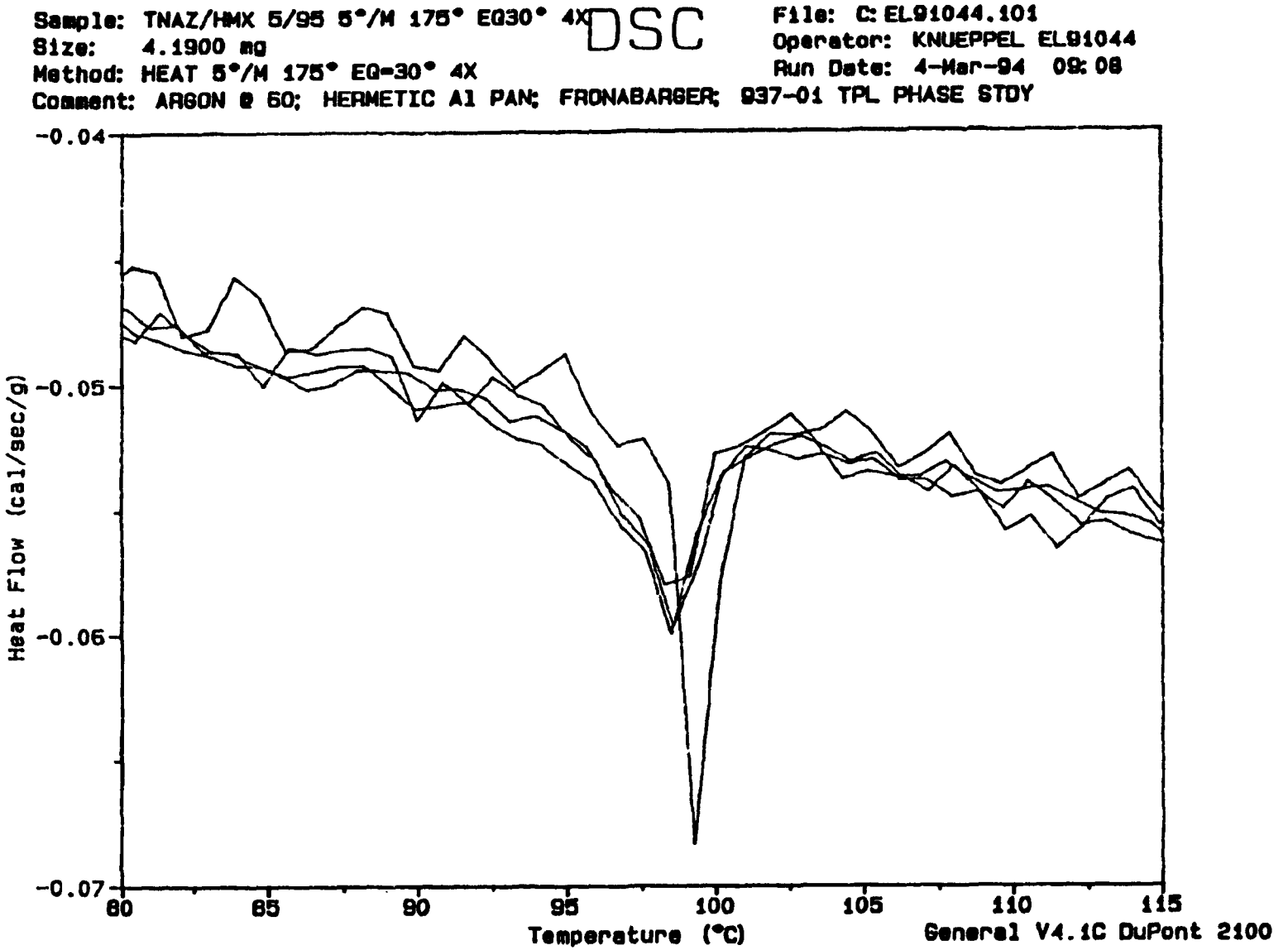

Figure 15. Overlay of four repetitive thermograms of 5/95 TNAZ/HMX (30–175 °C, 5 °C/min)

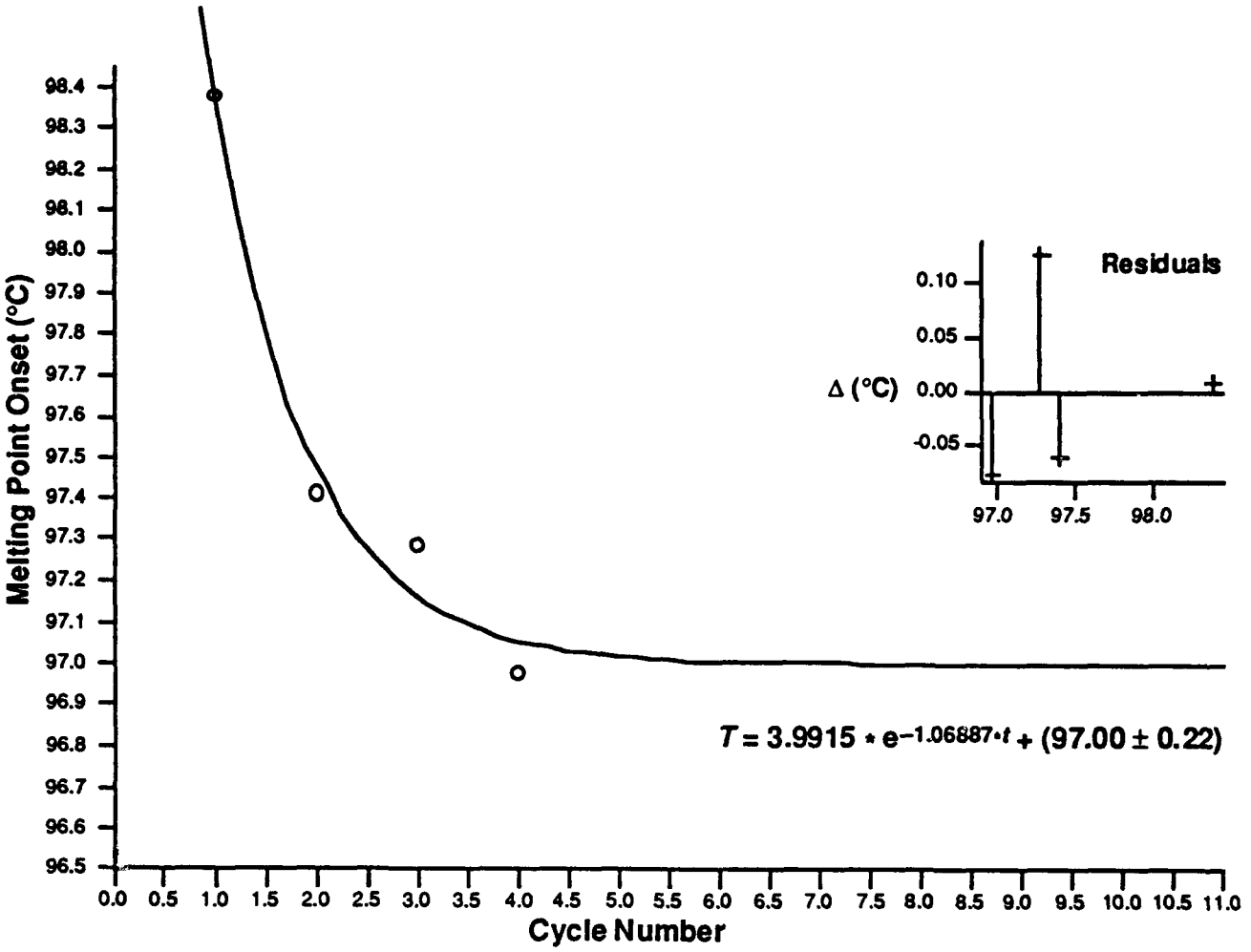

Figure 16. TNAZ/HMX 5%/95% (cycled 30–175 °C):
analysis of melting onset temperatures as a function of thermal cycling

Data points for TNAZ with three different heating rates are plotted in Figure 18. This indicates that a variation of up to 4 °C can be easily obtained in a melting endotherm depending on the DSC heating rate used. While the transition peak is above 102 °C at 20°/min, it extrapolates to 98.64 °C at infinitely slow heating. All of our thermal cycling analyses were run at 5°/min. The extrapolated melting *peak* temperature coincides with the melting *onset* seen in the first thermogram of pure TNAZ.

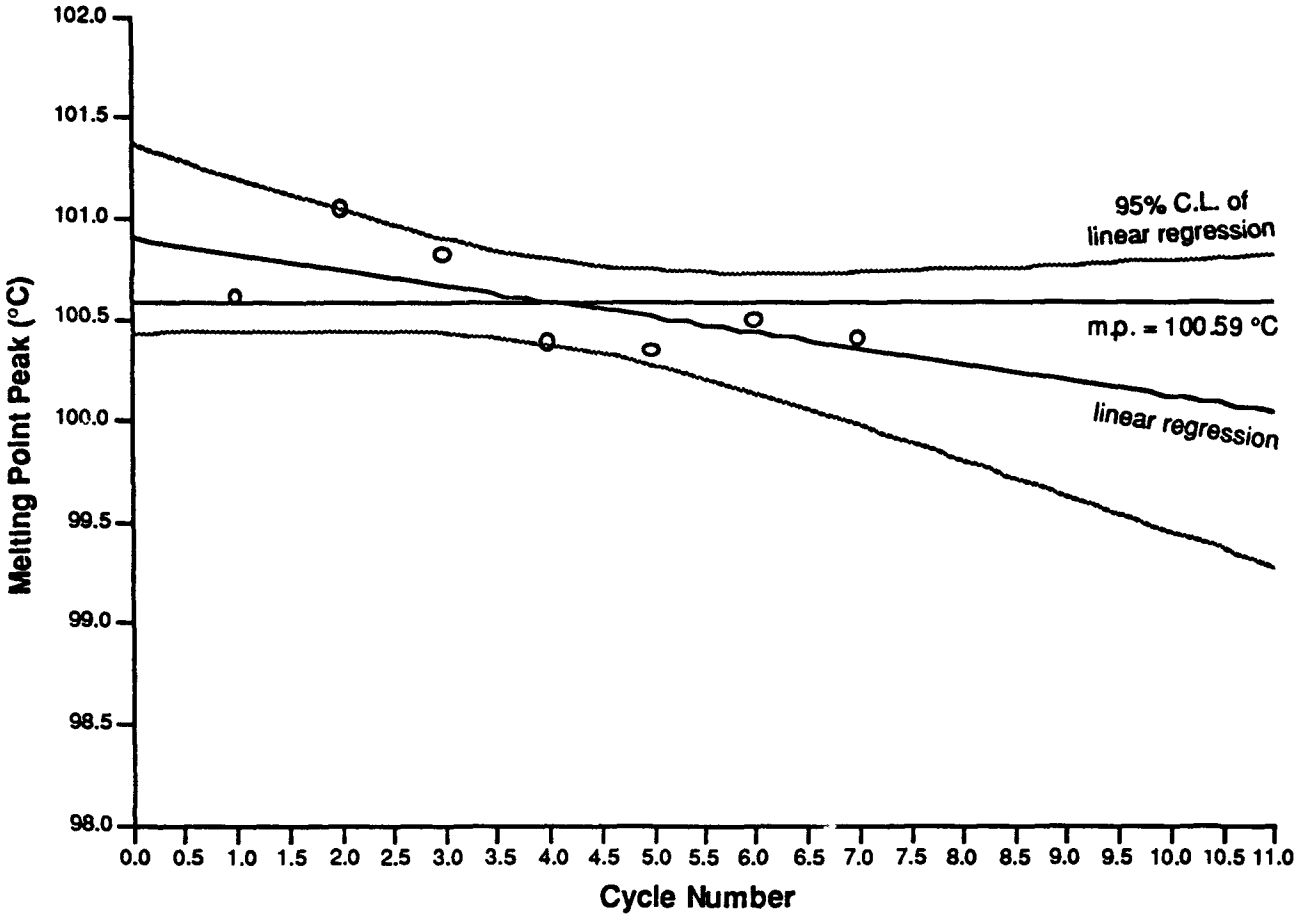

Figure 17. 100% TNAZ (cycled 30–175 °C):
analysis of melting peak temperatures as a function of thermal cycling

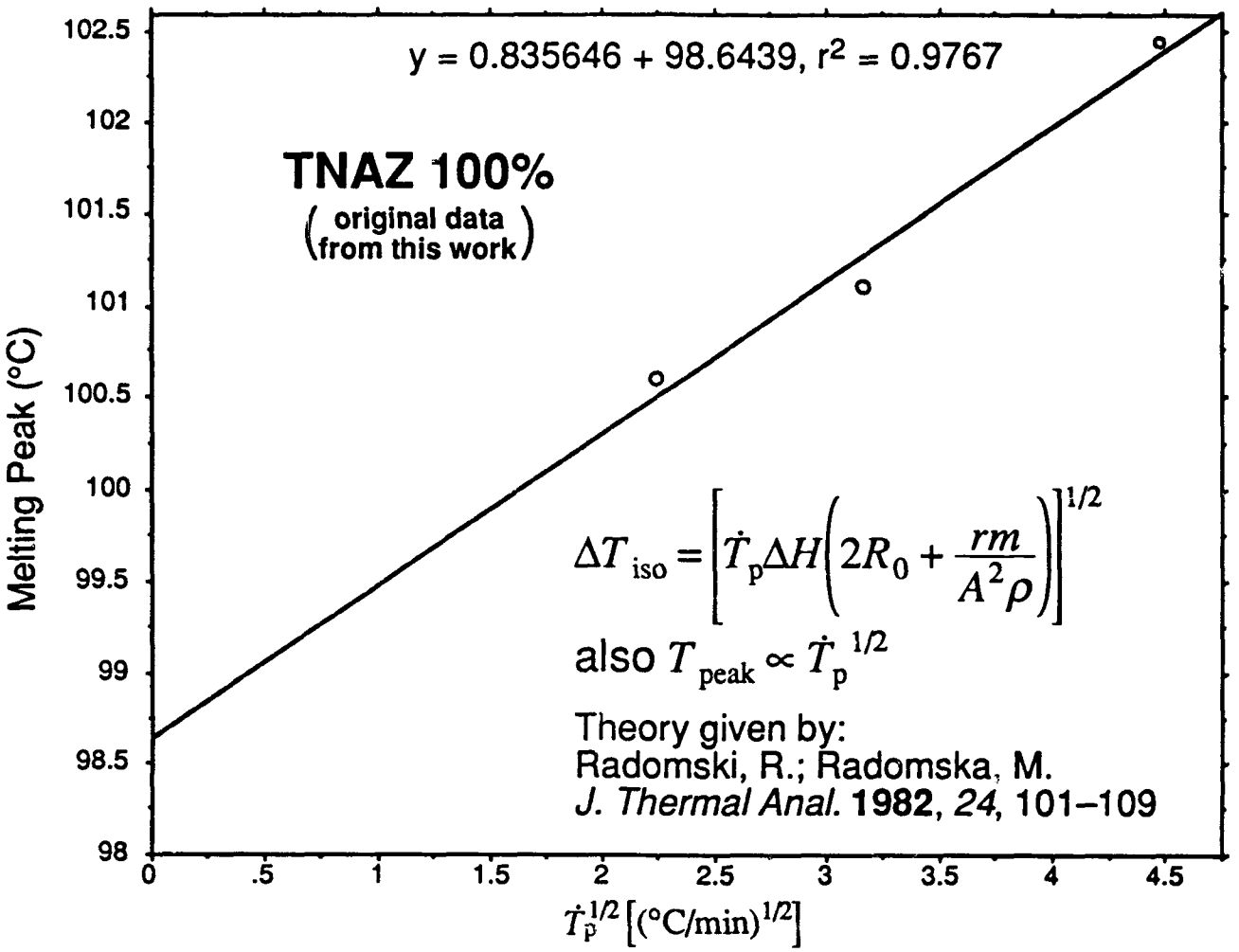

Figure 18. Effect of heating rate on DSC transition temperatures

There was concern about possible thermal degradation of the ingredients (especially TNAZ) at temperatures higher than 175 °C. After seeing HMX's polymorphic transition in the final heating run of the 50/50 mix (Figure 13), we also ran a series of tests cycling to at least 200 °C. Figure 19 is a thermogram of 75/25 TNAZ/HMX cycled up to 205 °C. In this, the first cycle, the HMX polymorph transition can be seen, which is small because of the low HMX content but definitely present. However, distinct—perhaps obvious—indications of the first stages of exothermic decomposition are also apparent. By the third cycle, no polymorph transition is apparent at all (Figure 20). These transitions are known *not* to be rapidly reversible.[10,12] (In the case of our 50/50 mix in which the transition was first observed, the sample sat for four days before the final heating run.) While faster equilibration by going through higher temperature ranges might be

[12] Reich, L. *Thermochim. Acta* **1973**, *7*, 57-67.

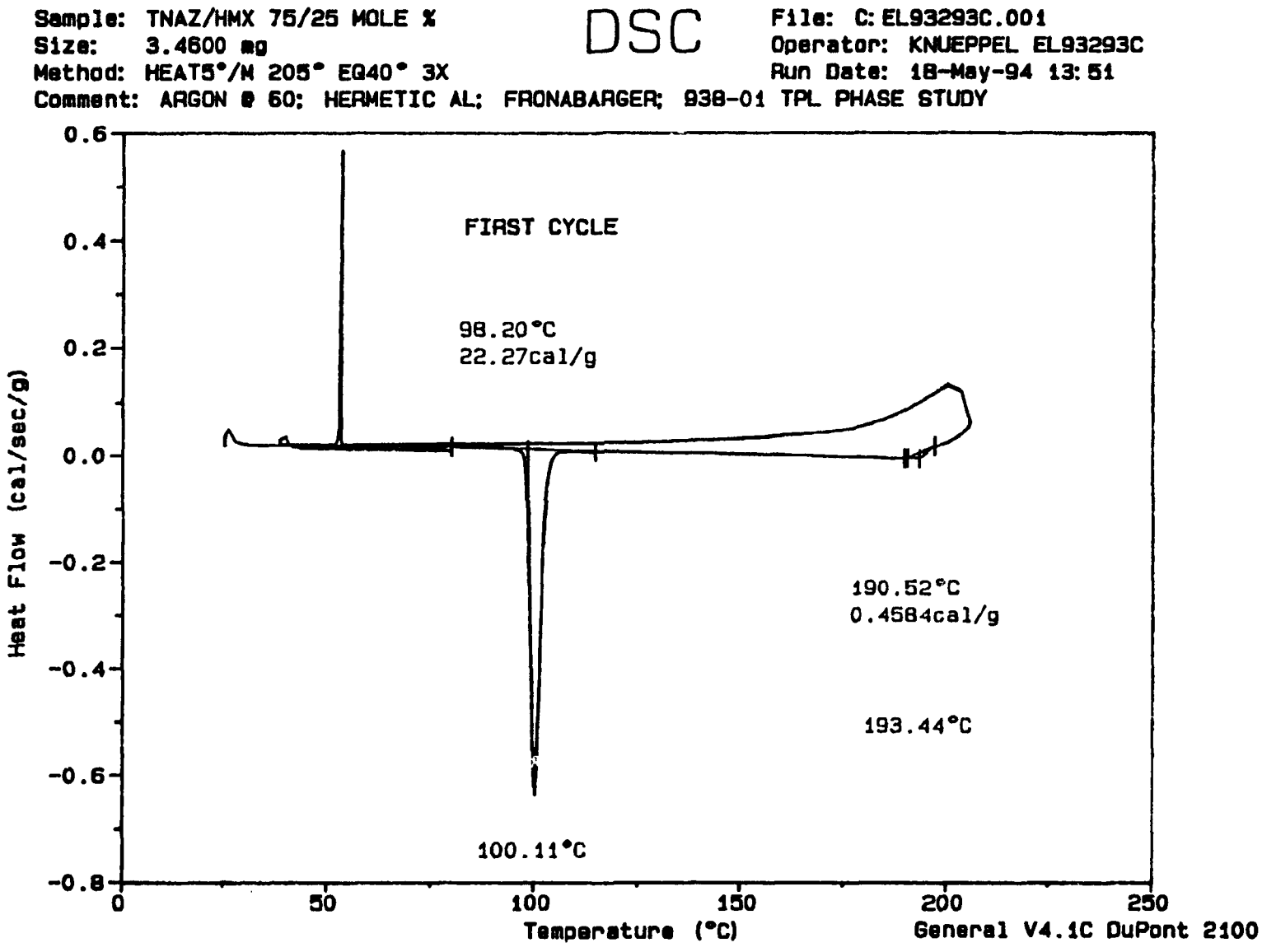

Figure 19. DSC thermogram of 75 mol%/25 mol% TNAZ/HMX, first cycle through 40–205 °C (5 °C/min)

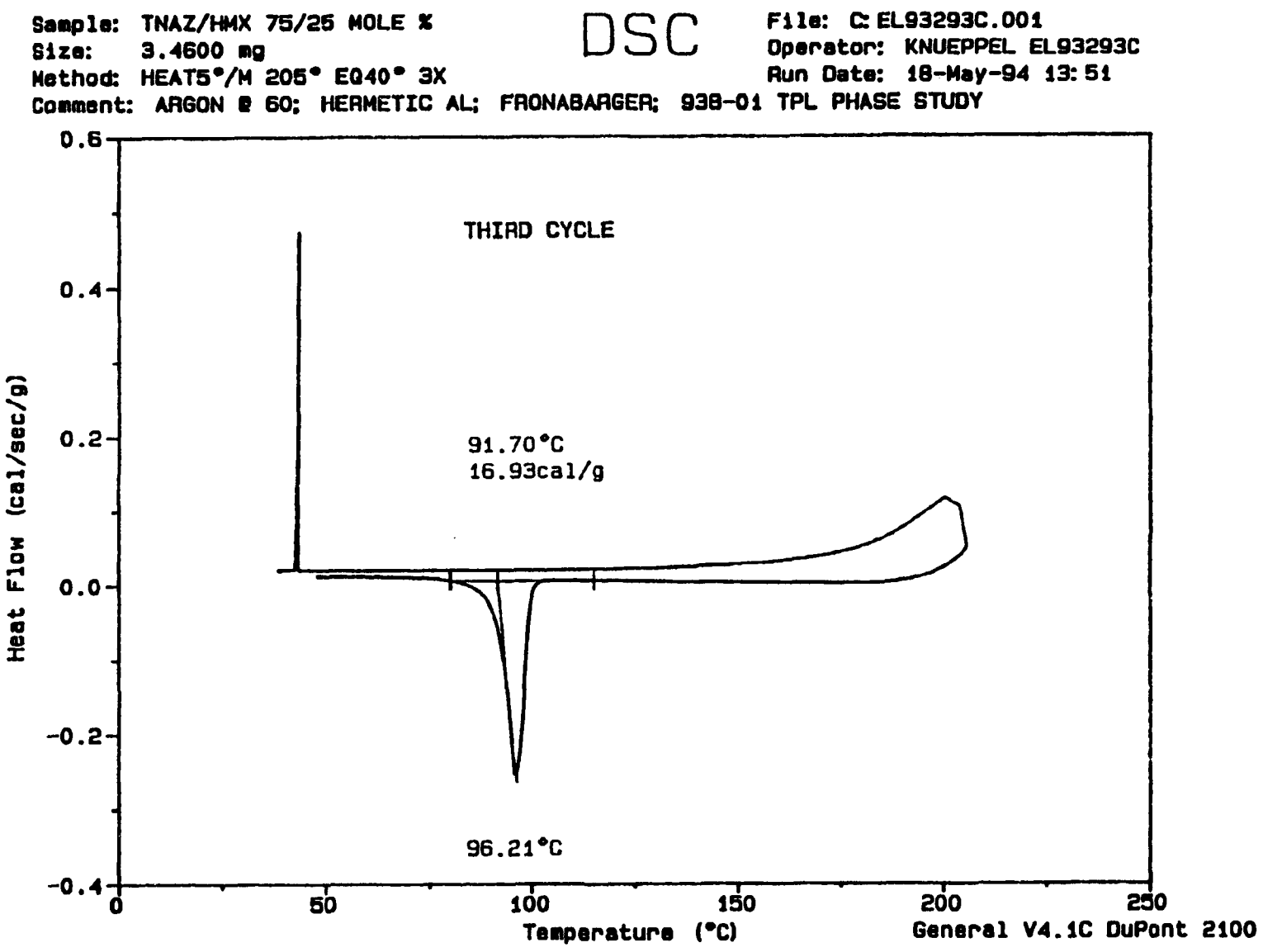

Figure 20. DSC thermogram of 75 mol%/25 mol% TNAZ/HMX, third cycle through 40–205 °C (5 °C/min)

reasonably expected, the apparent ultimate equilibration temperature appears much lower under these conditions (Figure 21) than in the runs cycled only to 175 °C: melting onsets for 75/25 TNAZ/HMX are about 91 °C vs. about 97 °C for the previous experiments. In 50/50 TNAZ/HMX cycled to 200 °C, the temperature trend is similar, decreasing more rapidly to about 92 °C (Figure 22).

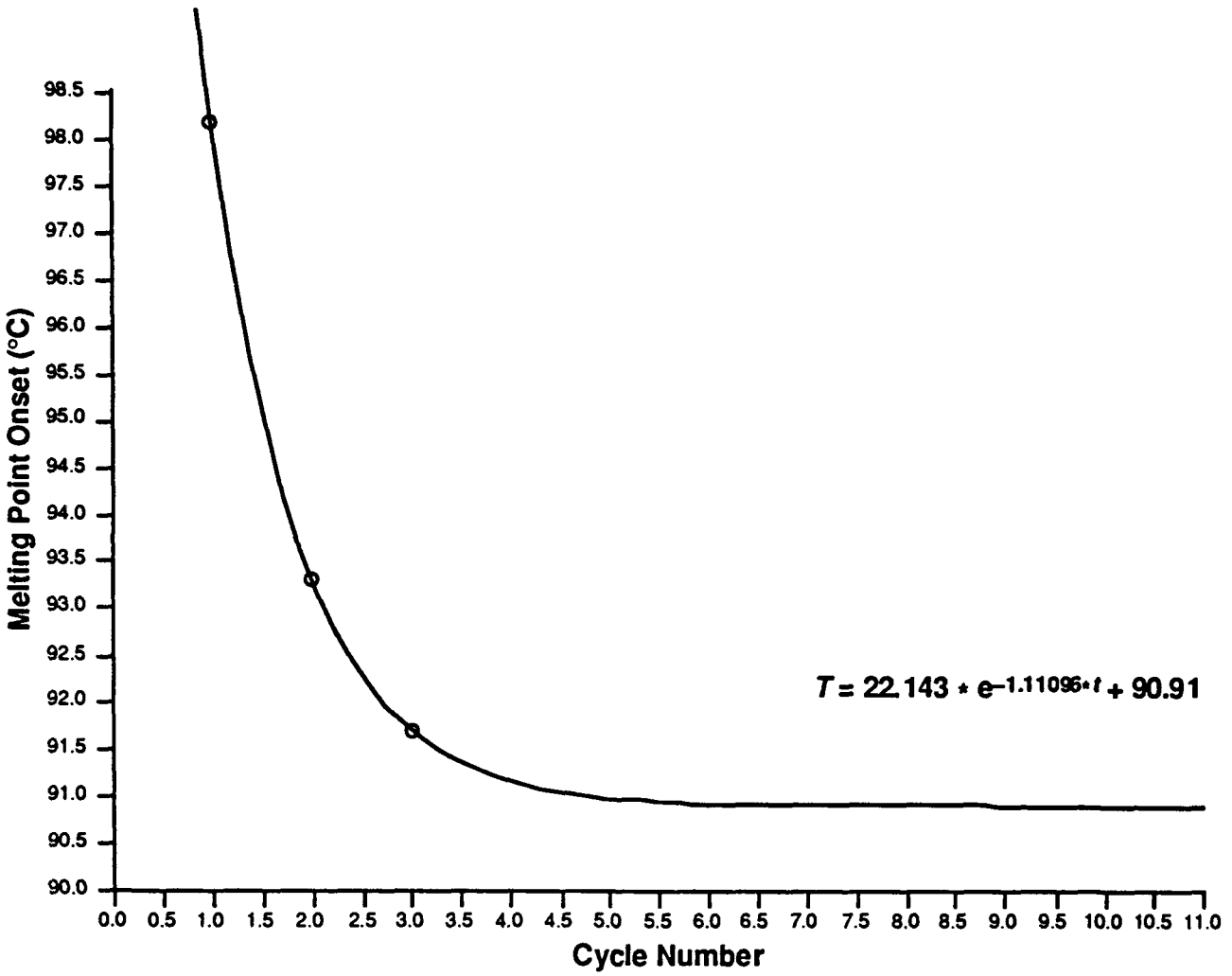

Figure 21. TNAZ/HMX 75%/25% (cycled 40–205 °C):
analysis of melting onset temperatures as a function of thermal cycling

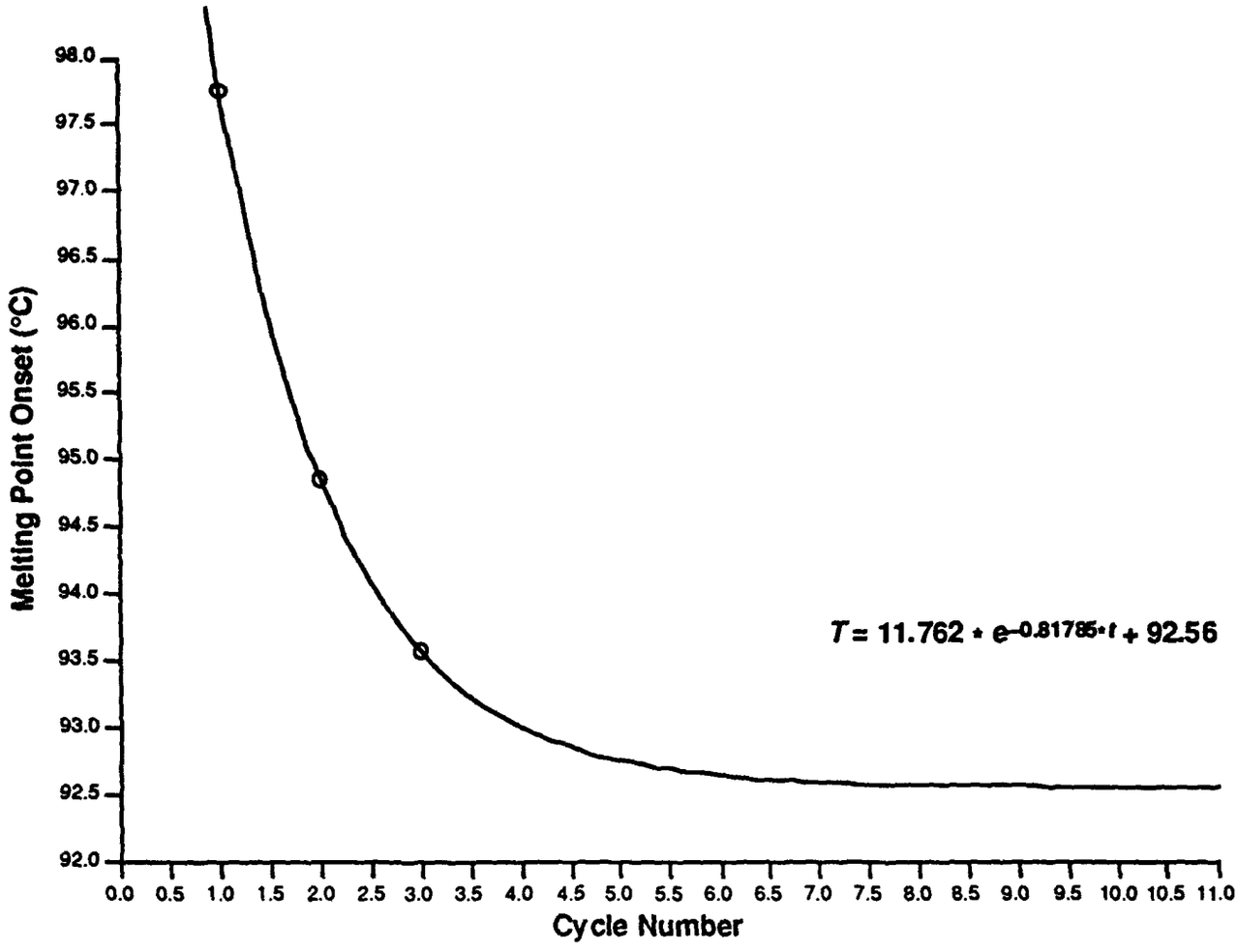

Figure 22. TNAZ/HMX 50%/50% (cycled 40–200 °C):
analysis of melting onset temperatures as a function of thermal cycling

In the 25/75 TNAZ/HMX mix, the polymorph transition is even more conspicuous in the first cycle of the thermograms (Figure 23). The temperature trend is still similar (Figure 24), decaying quicker to about 89 °C.

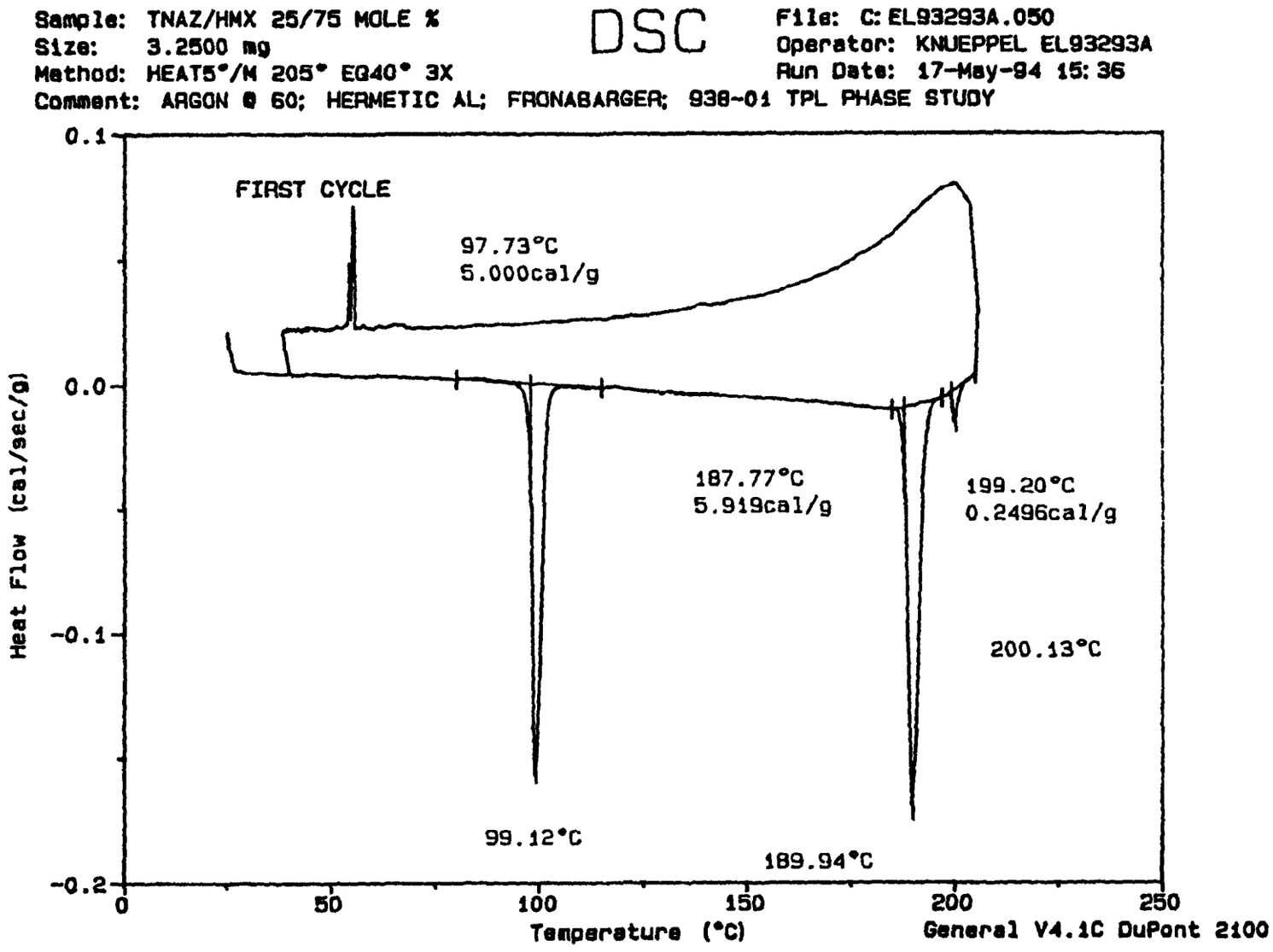

Figure 23. DSC thermogram of 25 mol%/75 mol% TNAZ/HMX, first cycle through 40–205 °C (5 °C/min)

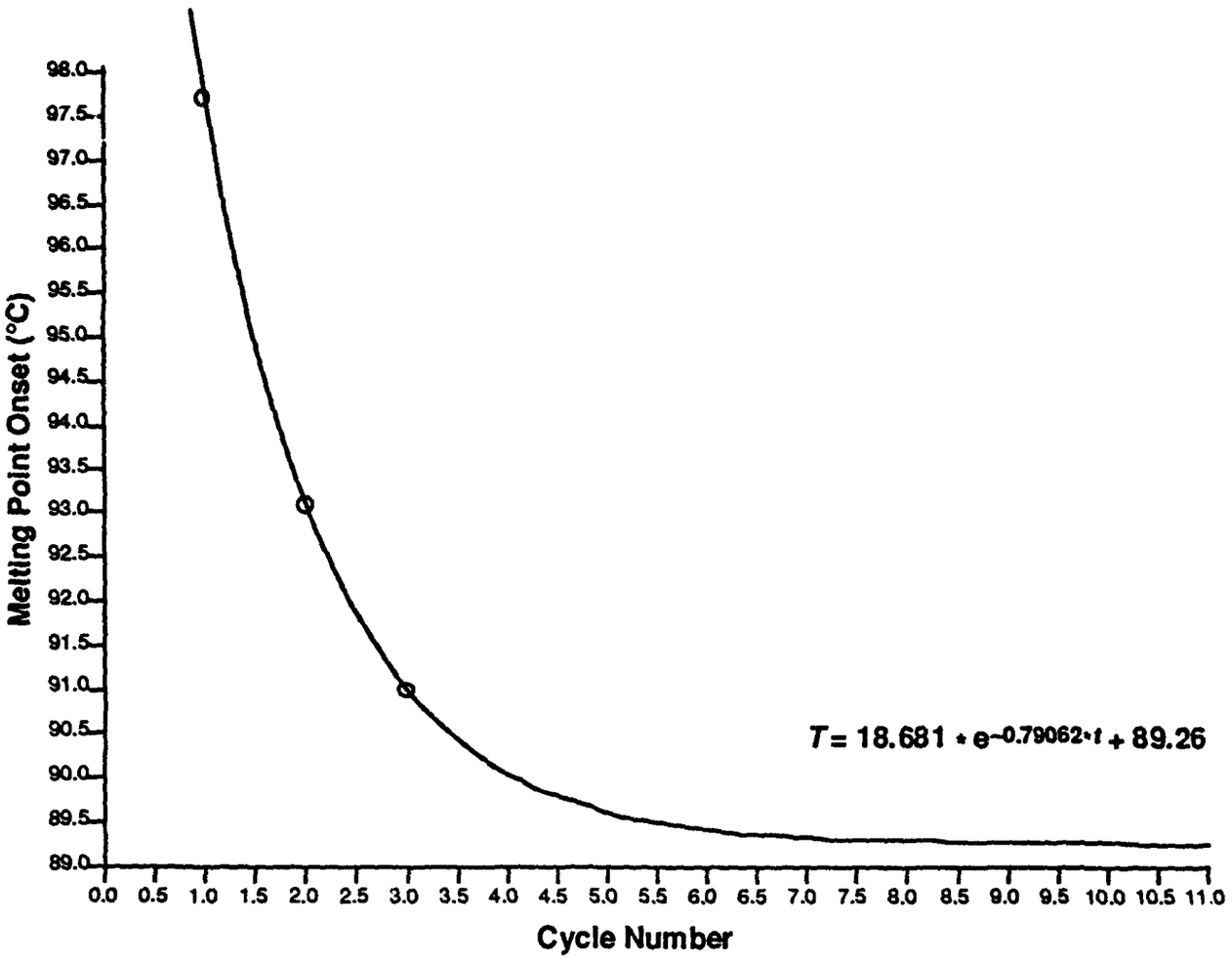

Figure 24. TNAZ/HMX 25%/75% (cycled 40–205 °C):
analysis of melting onset temperatures as a function of thermal cycling

As proof that these lower equilibrated transition temperatures are a result of real thermal degradation, the temperature trend for pure TNAZ cycled through 205 °C was also measured (Figure 25). The onset and peak temperatures are no longer constant or levelling off to an equilibrium temperature, but rather they appear to be accelerating their melting point depression. This may be due to autocatalytic decomposition. Whatever the mechanistic explanation, this evidence should evoke a concern about TNAZ's long-term stability up to 205 °C.

In Table I are summarized the results of analyses of the TNAZ melting phenomenon in the TNAZ–HMX system. Taking into account experimental uncertainties (indicated by the standard deviations of asymptotes of the decaying exponential data), it appears that throughout essentially the whole composition range studied, there is only a small depression from the normal melting

point of pure TNAZ. The melting *peak* temperatures of 95/5 and 5/95 appear statistically different from the means, but there may be systematic reasons for those differences other than differences in chemical phase behavior. The slight melting point depressions suggest a quite small HMX content in the melting TNAZ throughout the composition range studied.

Table I. TNAZ–HMX Eutectic Data (Summary)

TNAZ/HMX (mol%)	Onset $T_\infty \pm s_{T_\infty}$(95%) (°C)	Peak $T_\infty \pm s_{T_\infty}$(95%) (°C)
100/0	97.27 ± 0.08(0.20)	100.59 ± 0.10(0.24)
95/5	95.44 ± 0.22(2.79)	99.55 ± 0.21(0.92)
75/25	93.36 ± 0.51(1.10)	97.40 ± 0.31(0.75)
50/50	95.93 ± 0.63(7.96)	98.78 ± 0.93(2.58)
25/75	95.74 ± 0.24(3.01)	97.74 ± 0.08(1.04)
5/95	97.00 ± 0.22(2.84)	98.62 ± 0.13(0.58)
$\overline{T_\infty}$ (weighted)[a] = 95.91 ± 0.12(0.33)		$\overline{T_\infty}$ = 97.73 ± 0.08(0.34)

[a] $\overline{T_\infty}\text{(weighted)} = \dfrac{1/n\sum_i \dfrac{(T_\infty)_i}{\sigma_i^2}}{1/n\sum_i \dfrac{1}{\sigma_i^2}}$, $\sigma^2_{\overline{T_\infty}} = \dfrac{1}{\sum_i \dfrac{1}{\sigma_i^2}}$

Reference: Bevington, P.R. "Data Reduction and Error Analysis for the Physical Sciences"; McGraw-Hill: New York, 1969.

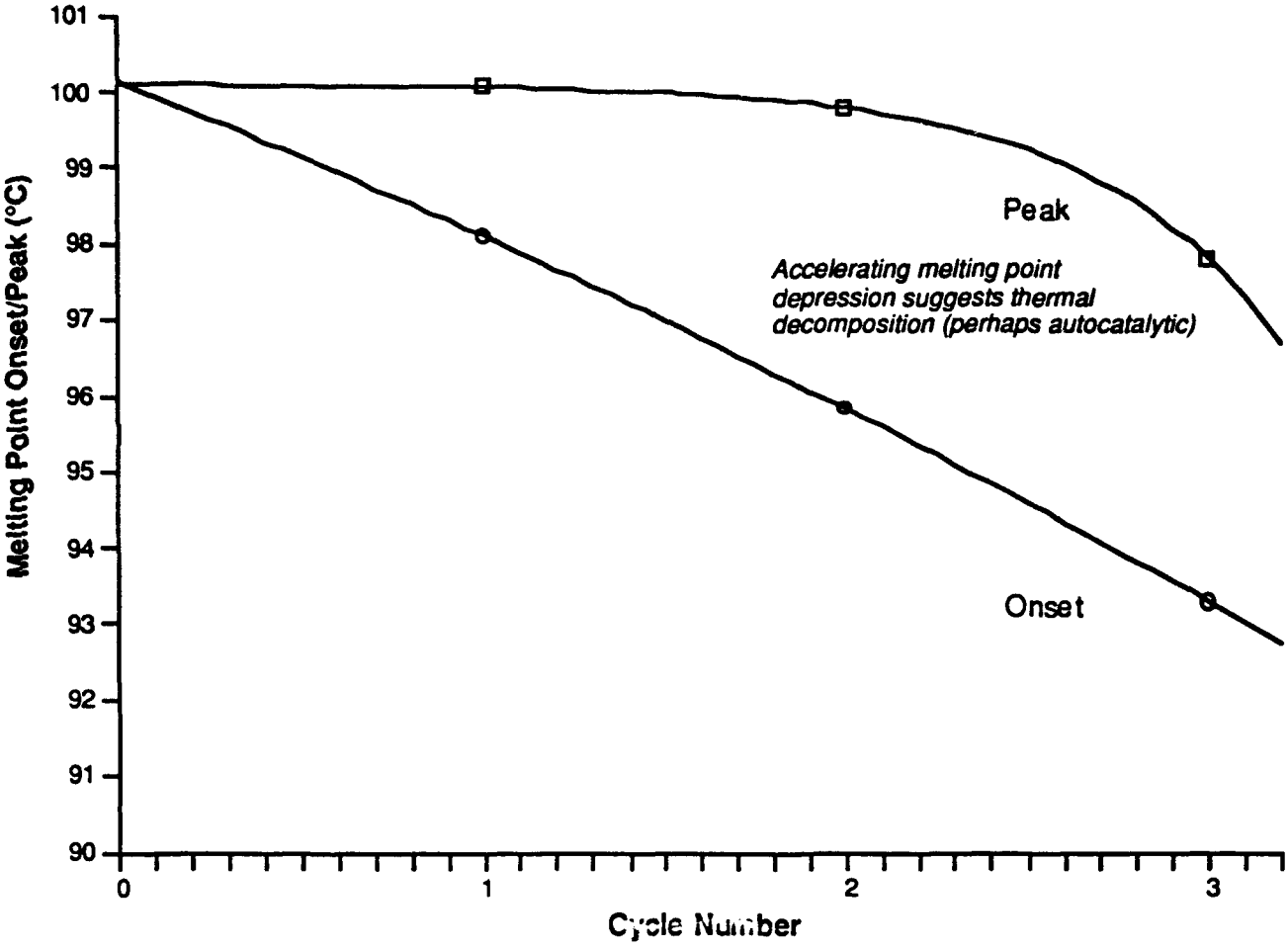

Figure 25. 100% TNAZ (cycled 40–205 °C):
analysis of melting onset temperatures as a function of thermal cycling

From these data, one can construct an approximate phase diagram of the TNAZ–HMX system, which is shown in Figure 26. Both the melting onset and peak are indicated, depending on which is preferred to indicate the solidus. The composition and behavior below 5% TNAZ comprise a gray area because that composition range was not actually studied, but it is likely that this is a typical system of low eutectic content and no significant solid-state solubility. As HMX was in excess (relative to the exact eutectic composition) in the composition range studied here, the solidus line should appear at an effectively constant eutectic temperature continuously throughout this range down to zero TNAZ content. The average melting peak temperature is about 97.73 °C, which is a depression of only 2.86 °C.

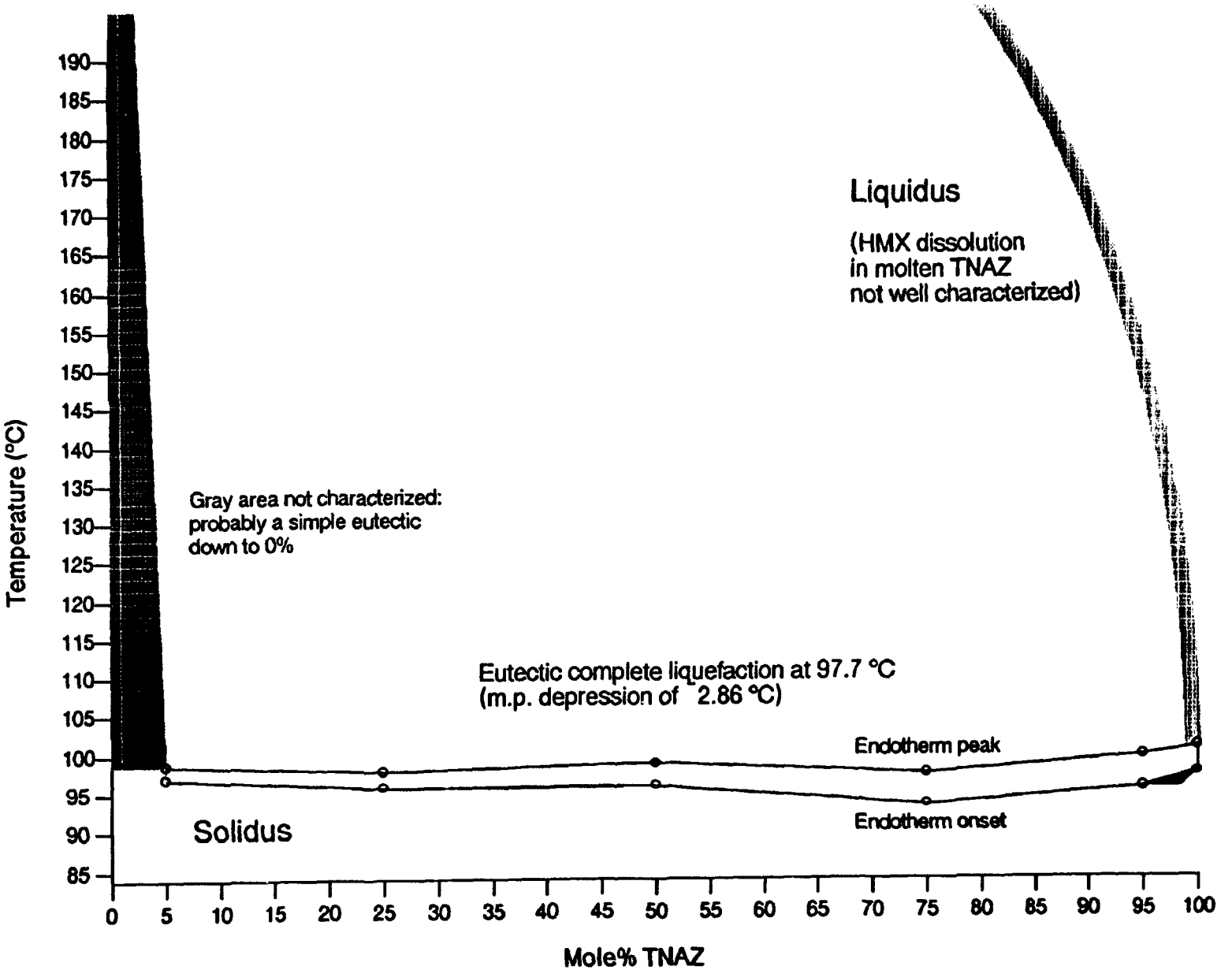

Figure 26. Partial TNAZ–HMX phase diagram

OTHER EXPLOSIVE EUTECTICS

This result of an insignificant eutectic composition in the TNAZ–HMX system evoked consideration of other known explosive eutectic systems, especially those involving nitramines. Urbański has tabulated RDX's eutectics with several other ingredients, as reproduced in Figure 27.[13] In these data, a qualitative correlation was apparent between the melting point of the major component of the eutectic system and the content of RDX in that system.

TABLE 18

EUTECTIC MIXTURES WITH CYCLONITE

Second component	Content of cyclonite in eutectic mixture %	Freezing point of eutectic °C
p-Nitrotoluene	about 0.5	50.4
p-Nitroanisole	about 0.5	50.9
α-Nitronaphthalene	about 1.5	55.4
m-Dinitrobenzene	8	85.5
α-Trinitrotoluene	2.5	78.6
1,3,5-Trinitrobenzene	about 3	113.8
Picric acid	12	112.9
Tetryl	10	118.1
sym-Dimethyldiphenylurea	17	112.4
sym-Diethyldiphenylurea	3	70.4
Camphor	22	137.5

This Content value is a typographical error. See original literature data.

Figure 27. Table of RDX binary eutectics from Urbański (reference 13)

On further consideration of the theoretical basis for temperature dependences of solid-liquid equilibria, the expression for the solubility of covalent organics in ideal solutions, equation (2), comes to mind.

$$\ln X_A = -\frac{\Delta H^A_{fus}}{R}\left[\frac{1}{T} - \frac{1}{(T_m)^0_A}\right] \qquad (2)$$

[13] Urbański, T. "Chemistry and Technology of Explosives"; Pergamon Press: New York, 1964; Vol. III, page 80.

Equation (2) has been referred to variously as the "van't Hoff equation"[12,14] or the "Schröder equation."[15] This explicit form is indeed first attributable to Schröder[16] but is directly derivable from van't Hoff's precedent equations, and it will be called the van't Hoff equation here. This is also the quantitative expression for the phenomenon of *freezing point depression* and is the basis for the cryoscopic determination of molecular weights. Equation (3) and Figure 28 depict a textbook example of its application.[9] In an ideal solution, naphthalene should be soluble to the extent of 29.8% at 25 °C based on its heat of fusion, its normal melting point, and the system temperature. Table II shows some experimental solubilities, which indicate the deviations from ideality of the various solutions; e.g., benzene is very good (ideal), but hexane is not.

$$\ln X_{\text{naphthalene}} = -\frac{19{,}290\ \text{J}\cdot\text{mol}^{-1}}{8.314\ \text{J}\cdot\text{K}^{-1}\text{mol}^{-1}}\left(\frac{1}{298.2\ \text{K}} - \frac{1}{353.2\ \text{K}}\right) \qquad (3)$$

$$X_{\text{naphthalene}} = 0.298$$

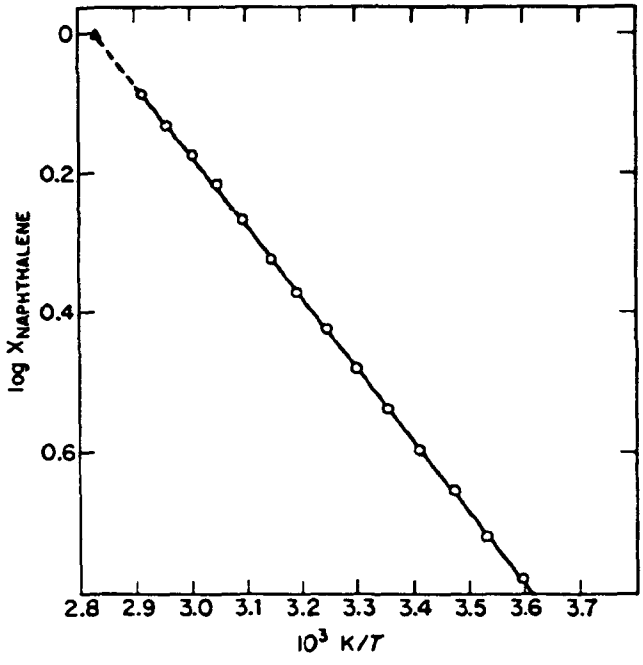

Figure 28. Solubility of naphthalene in benzene (from reference 9).
Data of Figure 2 plotted in the form of equation (2).

14 Reisman, A. "Phase Equilibria"; Academic Press: New York, 1970; p. 130.

15 (a) Vozdvizhenskii, V.M. *Russ. J. Phys. Chem.* **1964**, *38*, 1550-1555. (b) Szulc, J.; Witkiewicz, Z. *Wiad. Chem.* **1982**, *36*, 315-333.

16 Schröder, I. *Z. physik. Chem.* **1893**, *11*, 449-465.

Table II. Experimental Solubilities of Naphthalene in Solvents	
Solvent	Mole fraction, $X_{naphthalene}$
Benzene	0.296
Chlorobenzene	0.317
Toluene	0.286
Acetone	0.224
Hexane	0.125
Source: Moore, W.J. "Physical Chemistry", 4th ed.; Prentice-Hall, 1972; p. 249.	

A convenient analysis of this apparent correlation involved a plot of Urbański's tabulated RDX contents of the eutectics and of the normal melting points of the major components (which may be called the solvents of the RDX), both as forms consistent with the van't Hoff equation (2). This plot, shown in Figure 29, quickly confirmed a clear-cut trend. (Also included in the plot are two data points for RDX with the stable and labile forms of nitroglycerine, originally reported by Hackel,[17] as given by Urbański in reference 13.)

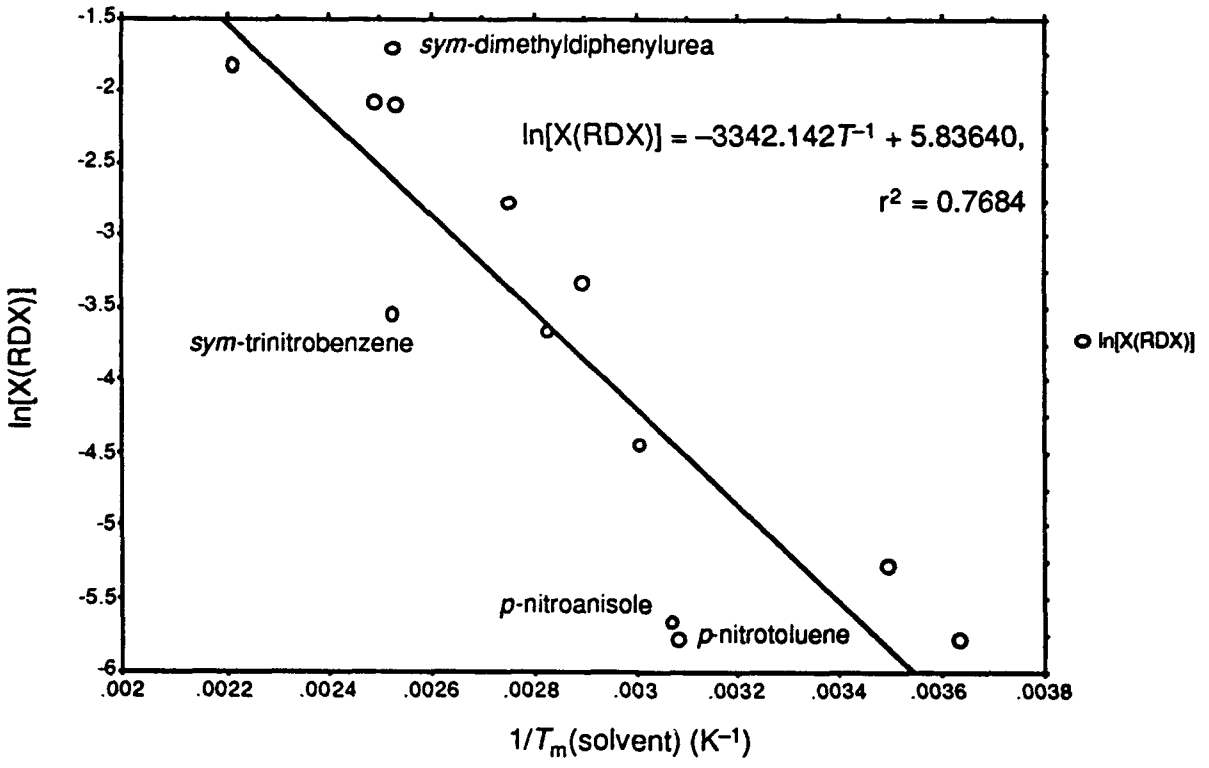

Figure 29. RDX binary eutectic compositions (Figure 27 data plus RDX–nitroglycerine)

[17] Hackel, J. *Rocz. Chem.* **1936**, *16*, 323-333.

There are apparent outliers from the linear trend, however. These are most conveniently assessed by comparison of the *statistical residuals*, the differences between observed data and those predicted by a linear regression fit to the van't Hoff equation, as shown in Table III. The most deviant data points belong to the systems of RDX with *p*-nitrotoluene (m.p. 51.2 °C), *p*-nitroanisole (m.p. 52.7 °C), 1,3,5-trinitrobenzene (m.p. 123.4 °C), and dimethyldiphenylurea (m.p. 122.7 °C). A comparison to Urbański's original article reporting these data[18] revealed that the RDX–trinitrobenzene system clearly has a eutectic temperature (melting point minimum) at *~13%* (Figure 30). So the value for trinitrobenzene in the table (Figure 27) is a *typographical error*. The correct value is "about 13"%. Furthermore, a careful statistical analysis of the other original data reported by Urbański and Rabek-Gawrońska revealed that the RDX–*p*-nitroanisole system has a eutectic composition of approximately *1.13%* RDX, rather than "about 0.5"%. The values tabulated for *p*-nitrotoluene and dimethyldiphenylurea appear consistent with the original data.

Table III. RDX Eutectic Data and van't Hoff Equation Regression Analysis Residuals

T_m, solvent (°C)	*X*(RDX)	T_m (K)	T_m^{-1} (K^{-1})	ln[*X*(RDX)]	*Residual*
2.0	.00307	275.15	.00363438	–5.787055394	.523199
51.2	.00309	324.35	.00308309	–5.779584188	–1.311831
52.7	.00345	325.85	.00306890	–5.669381048	–1.249062
12.9	.00511	286.05	.00349589	–5.276360199	.571043
59.3	.01173	332.45	.00300797	–4.445605616	–.228909
80.5	.02555	353.65	.00282765	–3.667117962	–.053067
123.4	.02882	396.55	.00252175	–3.546789788	–.955118
71.8	.03602	344.95	.00289897	–3.323680939	.528720
89.9	.06175	363.05	.00275444	–2.784661303	.584701
121.8	.12331	394.95	.00253197	–2.093053769	.532762
128.5	.12559	401.65	.00248973	–2.074732646	.409923
178.2	.16199	451.35	.00221558	–1.820220674	–.251831
122.7	.18139	395.85	.00252621	–1.707105870	.899470

Source: Urbański, T. "Chemistry and Technology of Explosives"; Pergamon Press: New York, 1964.

[18] Urbański, T.; Rabek-Gawrońska, I. *Rocz. Chem.* **1934**, *14*, 239-245.

p-Trójnitrobenzen — heksogen. (rys. 5).

Nr.	% trójnitro-benzenu	% heksogenu	P. K.	K. E.
1	100	0	123,4	—
2	90	10	116,6	113,8
3	87	13	114,1	113,8
4	85	15	117,3	113,8
5	80	20	125,7	113,8
6	70	30	144,0	113,8
7	60	40	155,6	113,7
8	50	50	165,2	113,7
9	40	60	173,8	(110,7)
10	30	70	181,0	(110,0)
11	20	80	188,2	(109,0)
12	10	90	Rozkład	
13	0	100	205,5	—

minimum at 13.475%

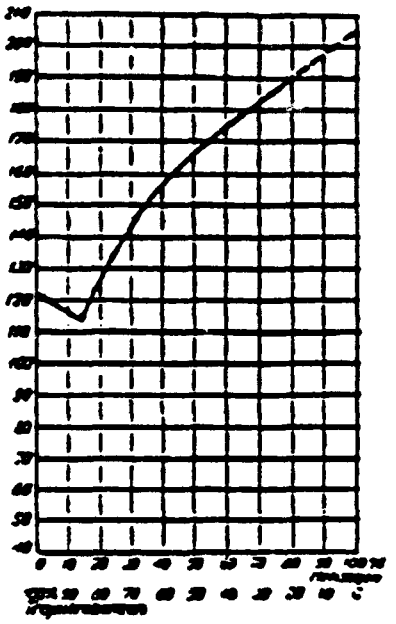

Key, left to right:
No.; % Trinitrobenzene; % Hexogen;
Solidification point; Solidification of eutectic;
Decomposition

Figure 5.
Trinitrobenzene; Hexogen

Figure 30. Original data of Urbański and Rabek-Gawrońska on RDX–TNB system (from reference 18)

After correction of the two erroneous data points, Urbański's RDX eutectic data may be replotted as shown in Figure 31, yielding a squared linear correlation coefficient of $r^2 \approx 0.88$. Under these conditions, only the point for *p*-nitrotoluene still appears deviant. If this one outlier were rejected, the correlation would go to $r^2 \approx 0.94$. The physical significance of this statistic is that ~94% of the variation in ln[*X*(RDX)] for binary eutectics with one constituent constant is accounted for solely by the reciprocal melting point of the other component.

A qualitative observation of this nature has been offered in the literature; the following quote by Rossell[19] is enlightening: "...it is the melting point difference which exerts the greatest effect, and the view that 'like dissolves like' is of little value within the limited context of triglyceride systems. When the melting point difference is small, however, it is then that specific structural forces come into play, governing the formation of eutectic or peritectic mixtures, or continuous solid solutions."

19 Rossell, J.B. *Adv. Lipid Res.* **1967**, *5*, 353–408.

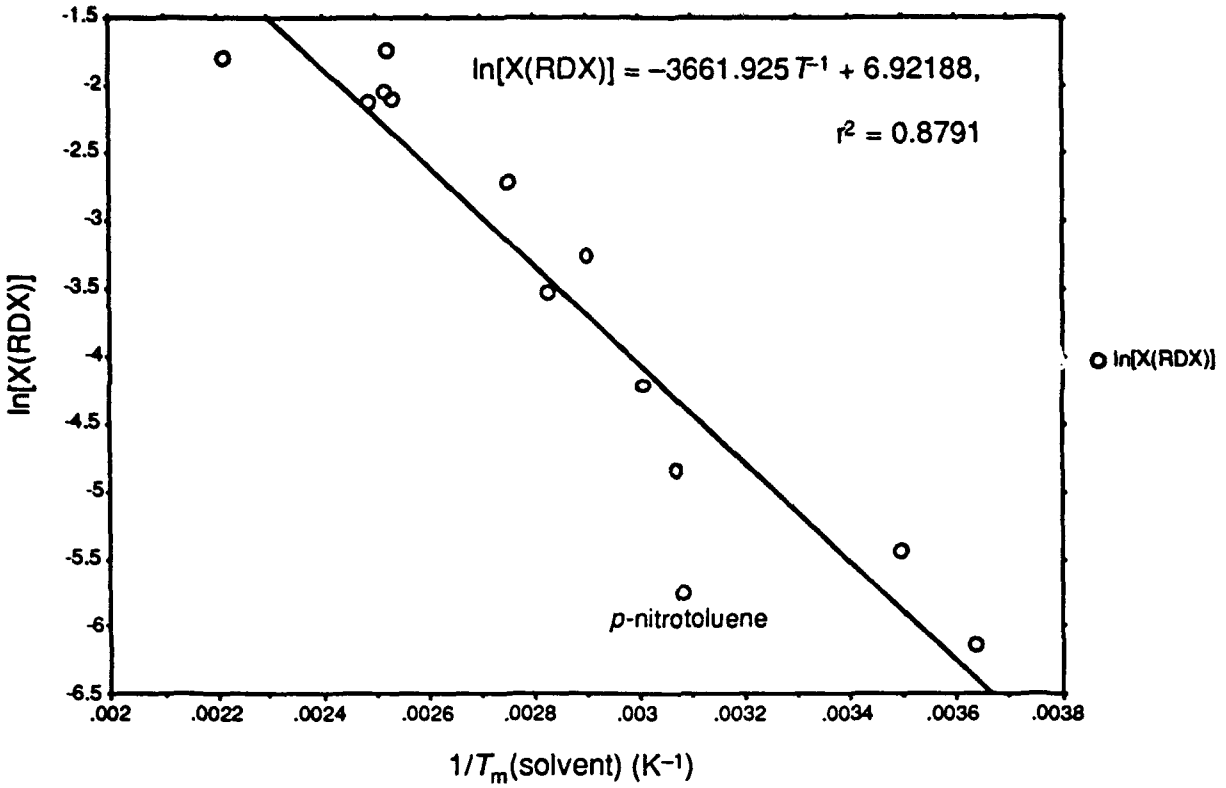

Figure 31. RDX binary eutectic data (trinitrobenzene and *p*-nitroanisole corrected)

Indeed, several *empirical* relationships have been claimed over the years for predicting eutectic compositions from other available data, such as measured eutectic temperature. These include a popular relation expressed by Kordes in equation (4):[20]

$$\frac{X_A^{eut}}{X_B^{eut}} = \frac{\left(\frac{T_B^0 - T^{eut}}{T_B^0}\right)}{\left(\frac{T_A^0 - T^{eut}}{T_A^0}\right)} \qquad (4)$$

Variations were later used by Vozdvizhinskii[21] and Vasil'ev,[22] as expressed in equations (5) and (6), respectively.

---

20 Kordes, E. *Z. anorg. allgem. Chem.* **1927**, *167*, 97–112.

21 Vozdvizhinskii, V.M. *Russ. J. Phys. Chem.* **1963**, *37*, 1326–1330.

22 Vasil'ev, M.V. *Russ. J. Phys. Chem.* **1970**, *44*, 1231–1233.

$$X_A^{eut} = \frac{T_B^0 - T_A^0}{T_B^0 - T^{eut}} \tag{5}$$

$$\frac{X_A^{eut}}{X_B^{eut}} = \frac{\int_{T^{eut}}^{T_B^0} (C_P)_B \, dT}{\int_{T^{eut}}^{T_A^0} (C_P)_A \, dT} = \frac{\int_{T^{eut}}^{T_B^0} (a_B + b_B T) \, dT}{\int_{T^{eut}}^{T_A^0} (a_A + b_A T) \, dT} \tag{6}$$

Although these empirical equations adequately describe certain eutectic systems under certain conditions, it may be recognized that the van't Hoff equation (2) theoretically applies to either constituent of a binary eutectic. Thus, if normal melting points, T_A and T_B, and enthalpies of fusion, ΔH_{fus}^A and ΔH_{fus}^B, are known for both ingredients, the eutectic point may be seen as the intersection of the two liquidus curves for freezing-point depression of the constituents (cf. Figure 2). Then estimation of the eutectic point (composition and temperature) entails only a simultaneous solution of the separate van't Hoff equations:

$$\ln X_A = -\frac{\Delta H_{fus}^A}{R}\left(\frac{1}{T_{eut}} - \frac{1}{T_A}\right) \tag{7}$$

$$\ln X_B = -\frac{\Delta H_{fus}^B}{R}\left(\frac{1}{T_{eut}} - \frac{1}{T_B}\right) = \ln (1 - X_A) \tag{8}$$

$$X_A = 1 - \exp\left[-\frac{\Delta H_{fus}^B}{R}\left(\frac{1}{T_{eut}} - \frac{1}{T_B}\right)\right] = \exp\left[-\frac{\Delta H_{fus}^A}{R}\left(\frac{1}{T_{eut}} - \frac{1}{T_A}\right)\right] \tag{9}$$

Rearrangement of the right equality yields an equation with only T_{eut} as an unknown:

$$1 - \exp\left[-\frac{\Delta H_{fus}^B}{R}\left(\frac{1}{T_{eut}} - \frac{1}{T_B}\right)\right] - \exp\left[-\frac{\Delta H_{fus}^A}{R}\left(\frac{1}{T_{eut}} - \frac{1}{T_A}\right)\right] = 0 \tag{10}$$

Although this approach follows straightforwardly from the van't Hoff equations, this method for eutectic estimation seems not to have been reported in the literature until the early 1980's,[23,24] perhaps a result of the difficulty of solution of the transcendental equation (10) by

[23] Karunakaran, K. *J. Solution Chem.* **1981**, *10*, 431–435.

[24] Du, Y.-J.; Yen, T.-T.; Chen, L.-R. *Phys. Stat. Solidi B* **1985**, *130*, K5-K10.

conventional mathematical methods. Nevertheless, when the four thermodynamic parameters involved in this equation are available, this is a straightforward method for estimating eutectic properties, including those of explosive formulations. For example, of the >60 binary eutectics that have been reported in convenient compilations,[7,13] thirty pairs have both the normal melting points and enthalpies of fusion known for both partners. These values are given in Table IV. This allows estimation of the eutectic temperature by solution of equation (10) for each binary system as well as its composition by application of the eutectic temperature to the van't Hoff equations (8–9).

A comparison of observed eutectic *temperatures* in these systems to those predicted by solution of equation (10) is shown in Figure 32. Although the observed eutectic temperature of the tetryl–trinitroanisole system seems far out of line from an otherwise quite clear trend, the original literature on this system[25] confirms the tabulated result,[7] as shown. Allowing this outlier leaves a root-mean-square residual of 7.1 °C between observed eutectic temperatures and those predicted for the observed systems (30 data points), with a squared correlation coefficient $r^2 > 0.96$.

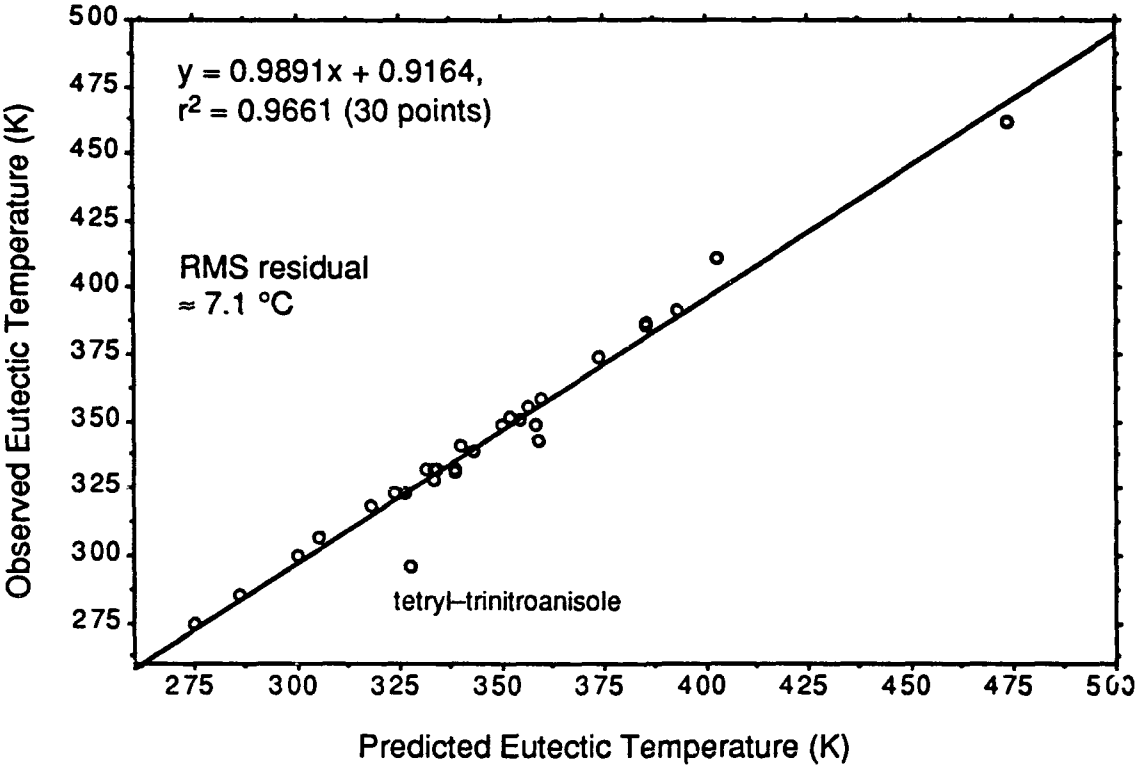

Figure 32. Correlation of observed to predicted melting temperatures for binary eutectics containing explosives, according to equation (10)

25 Efremov, N.N.; Tikhomirova, A.M. *Ann. Inst. Anal. Phys.-Chim. (Leningrad)* **1928**, *4*, 92-117; *Chem. Abstr.* **1929**, *23*, 3214.

Table IV. Enthalpies of Fusion for Binary Eutectics with Explosives			
Ingredient	Melting point (°C)	ΔH_{fus}, cal/mol (ref.)	Recommended ΔH_{fus}, cal/mol
HMX	280	16,711 (a) 17,000 (b)	16,856
PETN	140	11,508 (c) 11,820 (b)	11,666
RDX	205.5	7890 (b) 8530 (c)	8208
Nitroglycerine (stable)	12.9	6364 (a) 7544 (a)	6954
TNAZ	98.68	6254 (d)	6254
Trinitrocresol	101.2	6200 (c)	6200
Tetryl	126.8–128.72	5485 (c) 5900 (e) 6375 (b) 6099 (d)	5965
TNT	80.27–80.6	5247 (c) 5345 (b)	5296
2,4-Dinitrotoluene	69.4–69.54	4754 (c)	4754
Trinitroanisole	63.8	4692 (c)	4692
Picryl chloride	81.2	4332 (c)	4332
Picric acid	121.8–122.4	4170 (c)	4170
1,3-Dinitrobenzene	89.5–89.9	4153 (a)	4153
4-Nitrotoluene	51.2–54.5	3692 (a)	3692
1,3,5-Trinitrobenzene	121.5–123.4	3410 (c)	3410
Camphor	178.2	1541 (a) 1636 (a)	1589
Nitroglycerine (labile)	2.0	1181.7 (a)	1181.7

References:

(a) BEILSTEIN database file on STN International, © 1994 Beilstein Informationssysteme GmbH.

(b) Gibbs, T.R.; Popolato, A., Eds. "LASL Explosive Property Data"; University of California Press: Berkeley, 1980.

(c) Köhler, J.; Meyer, R. "Explosives", 4th ed.; VCH Publishers: New York, 1993.

(d) This work.

(e) "Military Explosives" *Department of the Army Technical Manual* 1984, TM 9-1300-214.

Likewise, the corresponding eutectic *compositions* can be predicted at the eutectic temperatures, using the van't Hoff equations as described above. This comparison of observed to predicted compositions, ln[*X*(A)/*X*(B)], is shown in Figure 33 for the same thirty systems. Here the root-mean-square residual is 0.499 in ln[*X*(A)/*X*(B)] (factor of 1.65), with a squared correlation coefficient r^2 = 0.91. It is recognized that deviations from the compositions predicted by application of van 't Hoff's relationship to the components of a binary eutectic are due to non-ideality in the eutectic mixture, i.e., $\gamma_A^{eut} \neq \gamma_B^{eu} \neq 1$.[26]

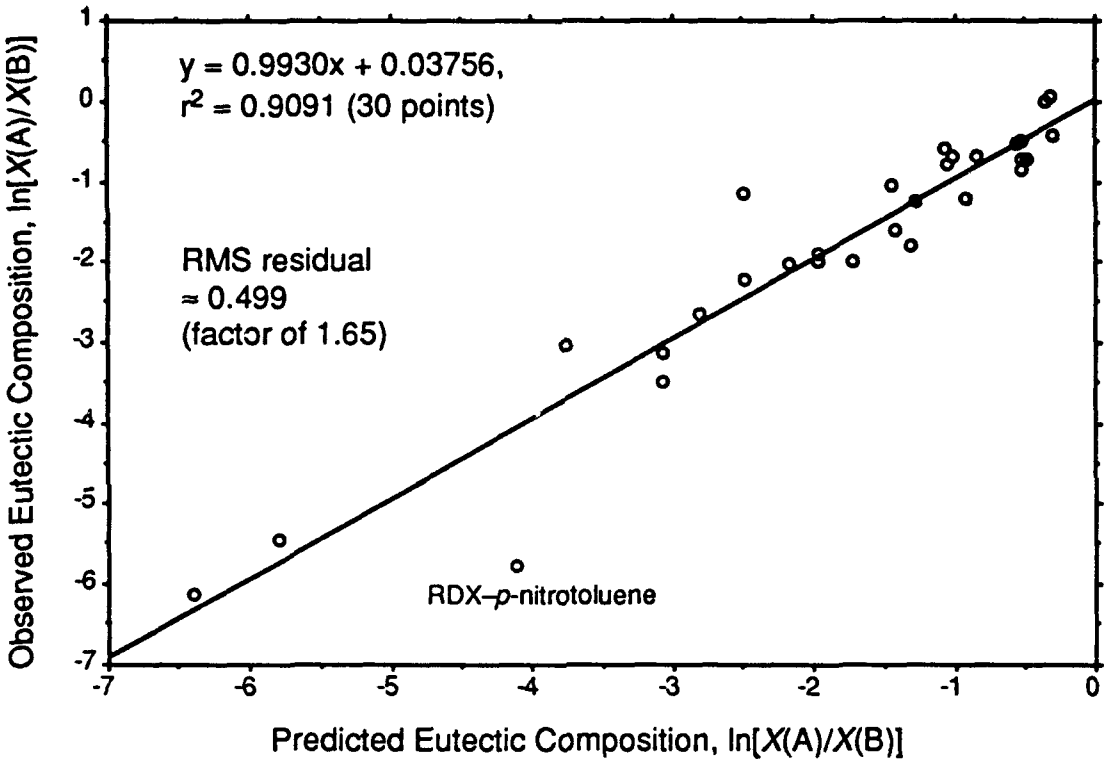

Figure 33. Correlation of observed to predicted compositions of binary eutectics containing explosives, according to equation (10)

Next, we derive and propose a predictive correlation for eutectic compositions that we demonstrate to be much more convenient than and comparable in accuracy (and therefore applicability) to the method requiring simultaneous solution of the van't Hoff equations with knowledge of the melting points and enthalpies of fusion of the eutectic ingredients. This derivation still begins with the assumption that the van't Hoff relationship applies to each ingredient to define that component's liquidus contour in the phase diagram; at the intersection of the liquidus contours, therefore:

[26] Rai, U.S.; Singh, O.P.; Singh, N.P.; Singh, N.B. *Thermochim. Acta* **1983**, *71*, 373–375.

$$\ln\left(\frac{a_A^{eut}}{a_B^{eut}}\right) = -\frac{1}{R}\left[\Delta H_A^{eut}\left(\frac{1}{T^{eut}} - \frac{1}{T_A^m}\right) - \Delta H_B^{eut}\left(\frac{1}{T^{eut}} - \frac{1}{T_B^m}\right)\right] \tag{11}$$

Equation (11) may be recognized as a simple difference of equations (7) and (8), with the concentration ratio expressed as a ratio of absolute activities a, related to formal mole fractions simply by the activity coefficients γ:

$$\ln\left(\frac{a_A^{eut}}{a_B^{eut}}\right) = \ln\left(\frac{X_A^{eut}}{X_B^{eut}}\right) + \ln\left(\frac{\gamma_A^{eut}}{\gamma_B^{eut}}\right) \tag{12}$$

Next, we make an assumption that $\Delta H_A^{eu} \approx \Delta H_B^{eu} \approx \Delta H^{eut}$ *at the eutectic point* for chemically similar species (e.g., covalent organics) without drastic non-ideal interactions. In this case, the dependence on absolute temperature (T^{eut}) cancels out, so ΔH_{fus}^A and ΔH_{fus}^B are not required:

$$\ln\left(\frac{a_A^{eut}}{a_B^{eut}}\right) = -\frac{1}{R}\left[\frac{\Delta H_B^{eut}}{T_B^m} - \frac{\Delta H_A^{eut}}{T_A^m}\right] \approx -\frac{\Delta H^{eut}}{R}\left[\frac{1}{T_B^m} - \frac{1}{T_A^m}\right] \tag{13}$$

An approximation that

$$\ln\left(\frac{a_A^{eut}}{a_B^{eut}}\right) \approx \ln\left(\frac{X_A^{eut}}{X_B^{eut}}\right) \tag{14}$$

allows a convenient correlation based solely on the measured melting points of the components of a binary eutectic:

$$\ln\left(\frac{X_A^{eut}}{X_B^{eut}}\right) = -\frac{1}{R}\left[\frac{\Delta H_B^{eut}}{T_B^m} - \frac{\Delta H_A^{eut}}{T_A^m}\right] \approx -\frac{\Delta H^{eut}}{R}\left[\frac{1}{T_B^m} - \frac{1}{T_A^m}\right] \tag{15}$$

Deviations from linearity in a plot of $\ln\left(\frac{X_A^{eut}}{X_B^{eut}}\right)$ vs. $\left(\frac{1}{T_B^m} - \frac{1}{T_A^m}\right)$ should be due to $\Delta H_A^{eu} \neq \Delta H_B^{eu}$ and/or $\gamma_A^{eut} \neq \gamma_B^{eu}$.

Figure 31 may now be recognized as a special case of the application of equation (15), in which the reciprocal melting point of RDX appears as a constant subtracted from the dependent variable. As a demonstration of the generality of equation (15) to explosive systems in particular, the collective eutectic data cited above[6,7,10e,13,17] have been plotted as Figure 34 . In this plot, the lower-melting component was defined as the solvent B regardless of the observed content in the eutectic. The resulting correlation ($r^2 > 0.86$) is so good that several outlying values in the first plot of the tabulated data from the Picatinny Arsenal "Encyclopedia of Explosives and Related Items"[7] could be diagnosed as typographical errors, confirmed by comparisons to the original literature. Errors could most easily be seen in a tabulation of $\ln[X(A)/X(B)]$ vs. mp(A)/mp(B)—even though the latter quantity has no physical significance—because it was expected that

$\ln[X(A)/X(B)] < 1$ for A defined as the higher-melting solute, i.e., mp(A)/mp(B) > 1. With the corrected data, only 3 of the 61 points violated this expectation. For reference, the "Encyclopedia" table is reproduced in Appendix A with corrections. The collective eutectic data used for the correlation shown in Figure 34 are tabulated in Appendix B.

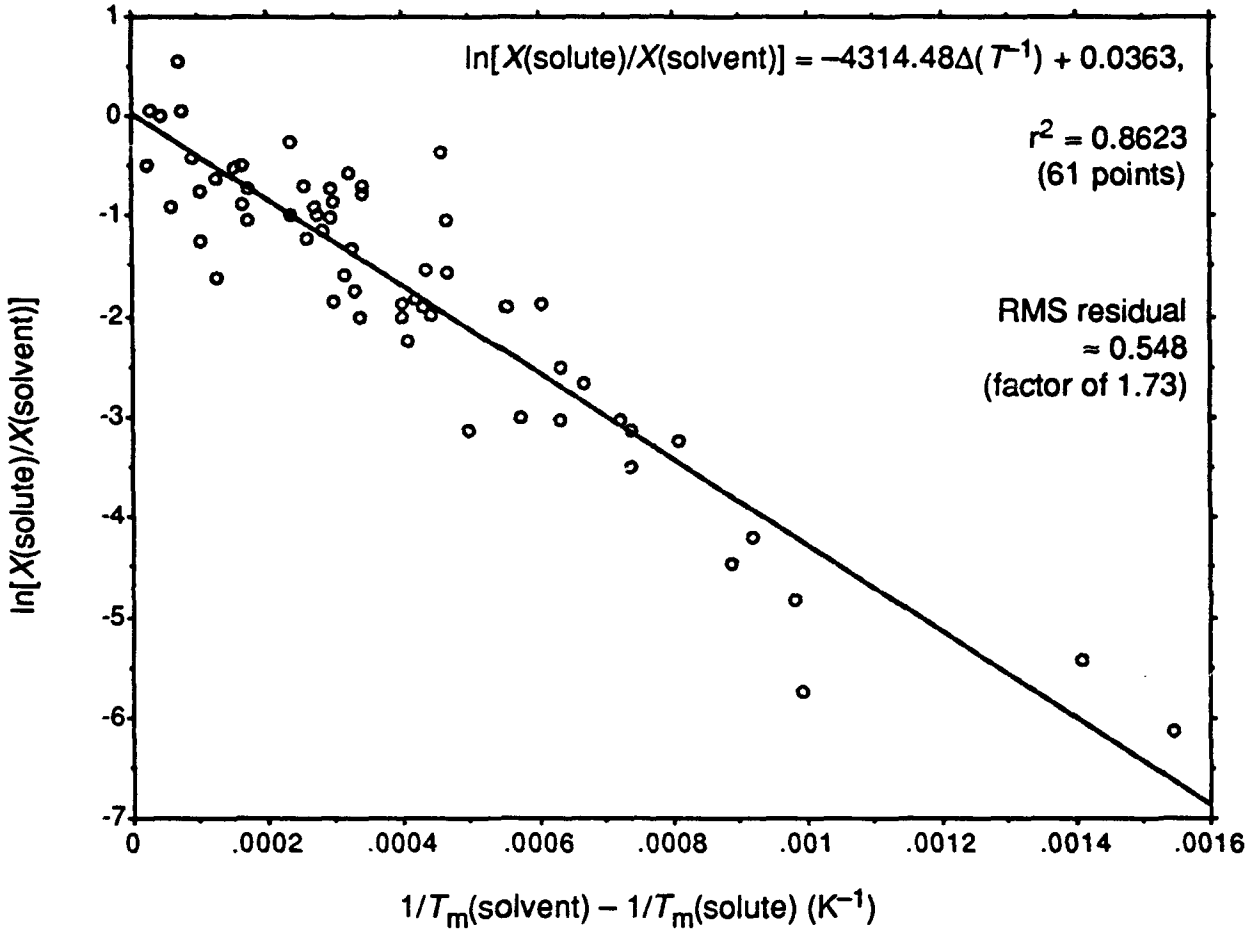

Figure 34. Plot of explosive eutectic compositions according to equation (15)

As shown in Figure 34, the regression line fitting equation (15) to 61 binary eutectics involving at least one explosive ingredient corresponds to:

$$\ln[X(\text{solute})/X(\text{soivent})] = -4314.48\Delta(T_m^{-1}) + 0.0363 \qquad (16)$$

The standard error of the slope in this regression is 224.44.

This new correlation therefore allows us to predict with reliability and greater convenience than previously the likely extent of any eutectic formation between explosive ingredients. This prediction requires only melting points of the pure ingredients (generally obtained upon the first synthesis of a new compound) and can be made without knowledge of precise enthalpies of

fusion. Predictions can therefore be made using old literature data on compounds of interest as well as on exotic compounds for which thermophysical properties have not yet been reported. The correlation obtained with the assumptions inherent in equation (15) is almost as good as that obtained with measured enthalpies of fusion, shown in Figure 33: $r^2 = 0.8623$ vs. 0.9091. Another consequence of this correlation is that the enthalpy of fusion for a "typical" explosive eutectic is estimated to be $4314.48R \pm 224.44R \approx (8574 \pm 446)$ cal/mol. Therefore, eutectic temperatures of hypothetical compositions may also be estimated by solution of van't Hoff equation (7) or (8), using the predicted eutectic composition from equation (15) and either this approximation of an enthalpy of fusion or an otherwise available value.

Also, predictions may be made about extents of eutectic formation among the binary compositions proposed for initial study in this program. Melting points were measured or have been reported as: TNAZ 98.68 °C, HMX 284.15 °C (melting peak and onset of decomposition), 2,4-dinitroimidazole 277.91 °C (*vide infra*), and NTO 273 °C (onset of decomposition). Another advantage of the correlation of equations (15)–(16) is that eutectic properties may be estimated involving ingredients that significantly decompose upon melting as neat ingredients, preventing accurate measurements of enthalpies of fusion of the pure ingredients. The binary eutectic compositions of each of the co-ingredients with TNAZ are then calculated to be: HMX 2.13 mol%; 2,4-DNI 2.33 mol%; NTO 2.49 mol%. The predicted eutectic composition estimated for the TNAZ–HMX system by equation (16) is consistent with the minor HMX content (<5%) measured above (Figure 26).

TNAZ–2,4-DNI SYSTEM

For comparison to the eutectic behavior predicted from thermodynamic theory, the TNAZ–2,4-DNI system was measured experimentally analogously to the TNAZ–HMX system. A sample of 2,4-DNI provided by ARDEC was oven-dried before thermal analysis, which removed 0.12–0.13% moisture & volatiles. A thermogram of neat 2,4-DNI heated up through thermal decomposition is shown in Figure 35. The endotherm (melting) peak and onset of exothermic decomposition occurs at 277.91 °C. TNAZ–2,4-DNI mixtures were made in mole ratios of 75/25, 50/50, and 25/75. Samples were cycled between 40 °C and 175 °C to establish compositional equilibrium. Results from the 75/25 system were qualitatively typical of all of the mixtures. A sample thermogram is shown in Figure 36. The melting transition of TNAZ still occurs in the range of 96–100 °C, and the TNAZ component supercools during the cooling stages of the thermal cycling. Figure 37 shows a typical statistical analysis of the equilibration of the melting temperatures. The melting temperature data are summarized in Table V.

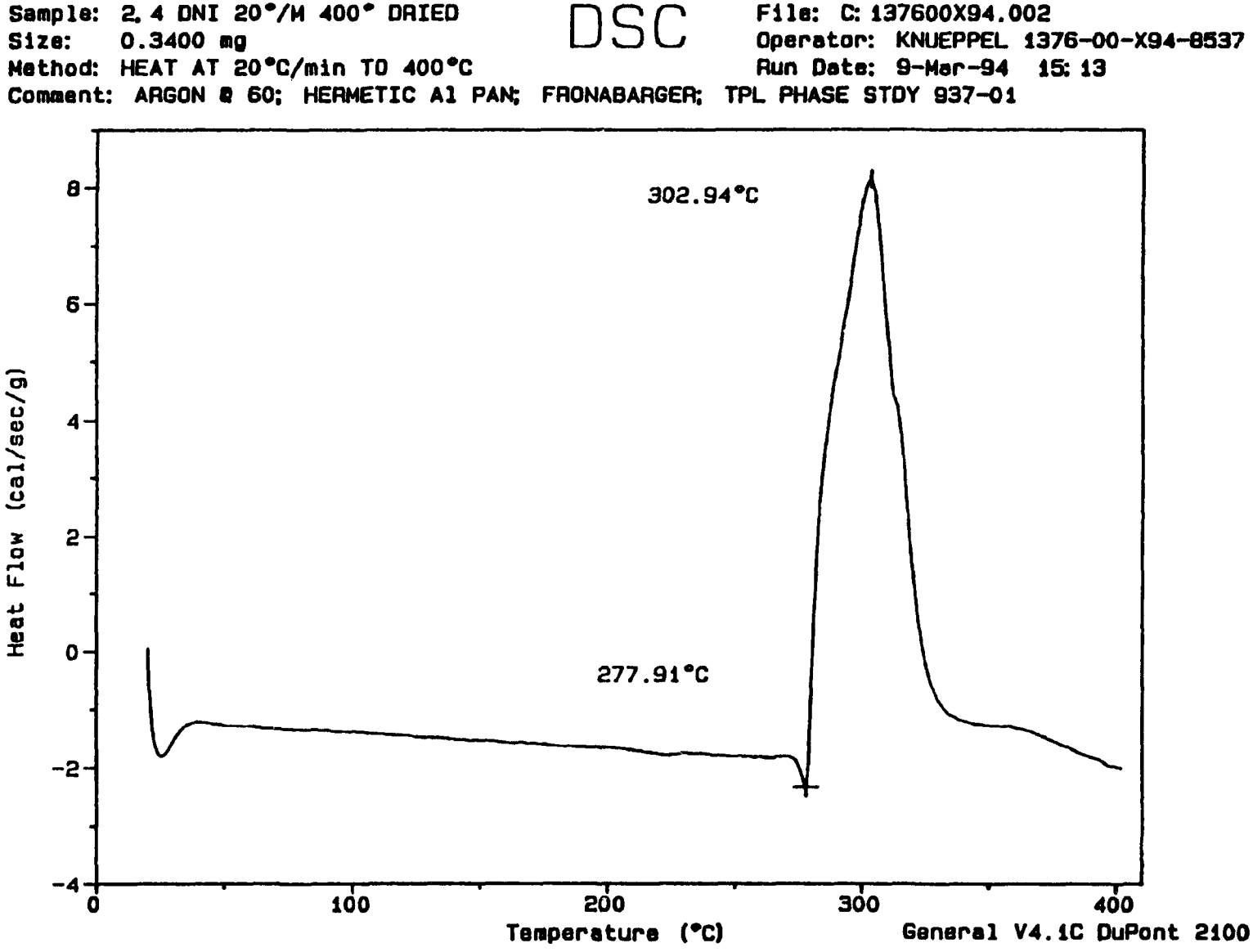

Figure 35. DSC thermogram of pure 2,4-DNI, heating run to decomposition (20 °C/min)

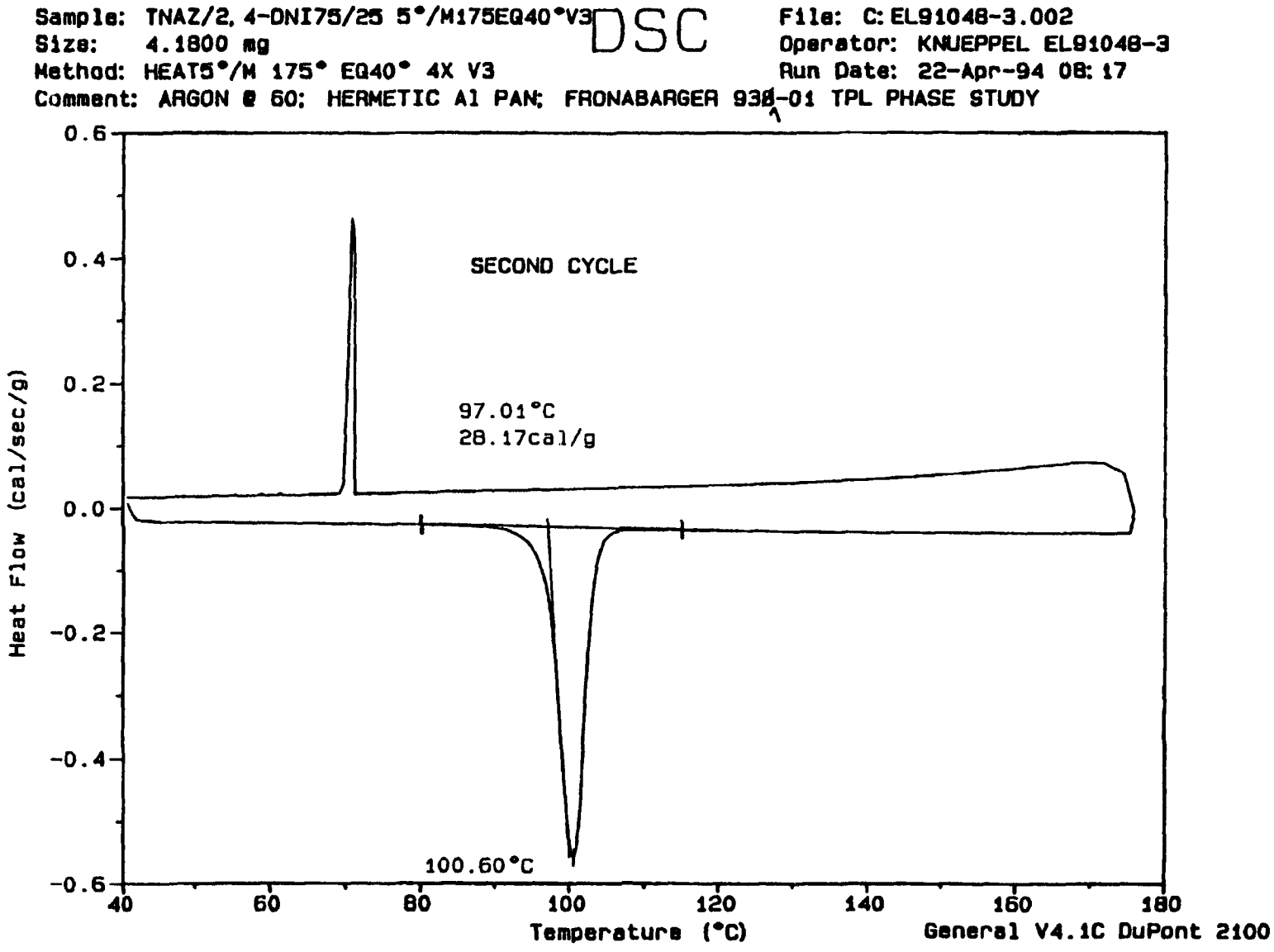

Figure 36. DSC thermogram of 75 mol%/25 mol% TNAZ/2,4-DNI, second cycle through 40–175 °C (5 °C/min)

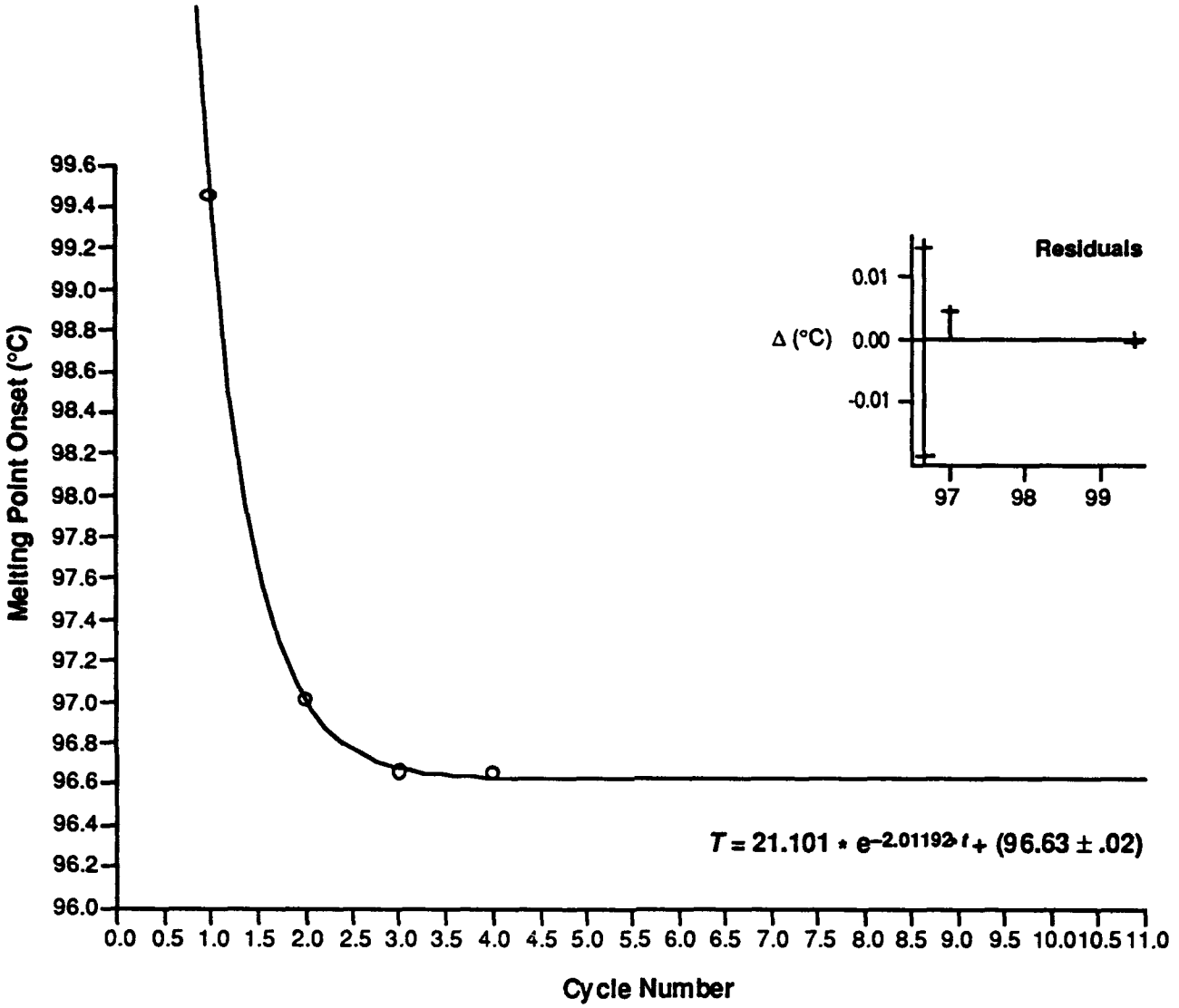

Figure 37. TNAZ/2,4-DNI 75%/25% (cycled 40–175 °C):
analysis of melting onset temperatures as a function of thermal cycling

Table V. TNAZ–2,4-DNI Eutectic Data (Summary)

TNAZ/2,4-DNI (mol%)	Onset $T_\infty \pm s_{T_\infty}$(95%) (°C)	Peak $T_\infty \pm s_{T_\infty}$(95%) (°C)
100/0	97.27 ± 0.08(0.20)	100.59 ± 0.10(0.24)
75/25	96.63 ± 0.02(0.26)	100.30 ± 0.11(1.38)
50/50	96.32 ± 0.01(0.13)	99.61 ± 0.005(0.06)
25/75	94.77 ± 0.06(0.78)	98.37 ± 0.06(0.77)
$\overline{T_\infty}$ (weighted) = 96.28 ± 0.01(0.04)		$\overline{T_\infty}$ = 99.60 ± 0.005(0.02)

The observations of melting points given in Table V allow partial construction of the TNAZ–2,4-DNI phase diagram; the solidus portion of the diagram is shown in Figure 38. Throughout the range of 25–75% 2,4-DNI that was studied, the melting point depression is only on the order of 1.0 °C. This slight effect of 2,4-DNI on the melting of TNAZ is consistent with the small extent of eutectic formation predicted above.

A careful study of the composition range below 5% of the higher-melting component would be required in order to elucidate the phase diagrams more precisely for either the TNAZ–HMX or TNAZ–2,4-DNI system.

TNAZ–TETRYL SYSTEM

As a result of the observations of insignificant eutectics formed between TNAZ and high-melting ingredients like HMX and 2,4-DNI, a third system was chosen—in preference to NTO—in which a significant eutectic effect was predicted to be seen. Thus, the system of TNAZ–tetryl was preliminarily studied in the remainder of this Phase I program. Having a melting point (129.51 °C) closer to that of TNAZ, tetryl is predicted by the correlation of equation (16) to form a eutectic with TNAZ to the extent of ~30 mol% tetryl. In comparison, solution of equation (10) (with knowledge of the enthalpies of fusion of both ingredients) yields a prediction of ~35% tetryl in the binary eutectic. Likewise, the eutectic temperature is estimated as 88.0 °C using the approximation of $\Delta H^{eut} \approx 8574$ cal/mol (*vide supra*) in equation (8); the prediction via equation (10) using known enthalpies of fusion is 80.4 °C.

The only composition of the TNAZ–tetryl system studied in this Phase I program was 50/50 mol%. The initial thermogram of this system is shown in Figure 39. The observed melting onset is labelled at 81.05 °C. The asymmetry apparent in the endotherm is most likely due to dissolution of the excess tetryl (in this 50/50 TNAZ/tetryl mix vs. the predicted 65/35 eutectic) at the higher-temperature end of liquefaction. Upon repeated cycling between 40 °C and 125 °C, the mixture remained supercooled and never recrystallized. The eutectic behavior of the TNAZ–tetryl system is also in semi-quantitative agreement with predictions made from thermodynamic theories described above.

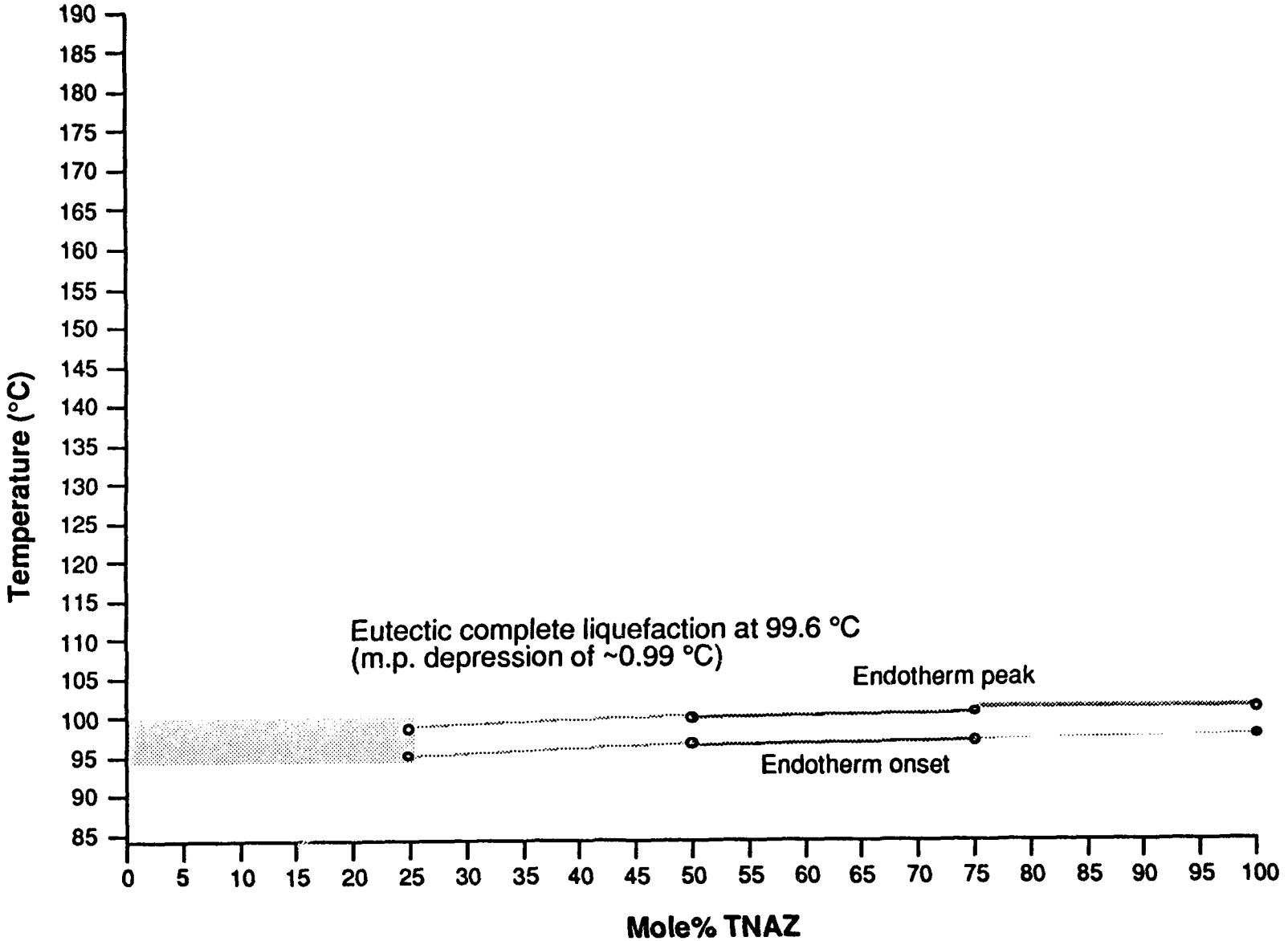

Figure 38. Partial TNAZ–2,4-DNI phase diagram (solidus)

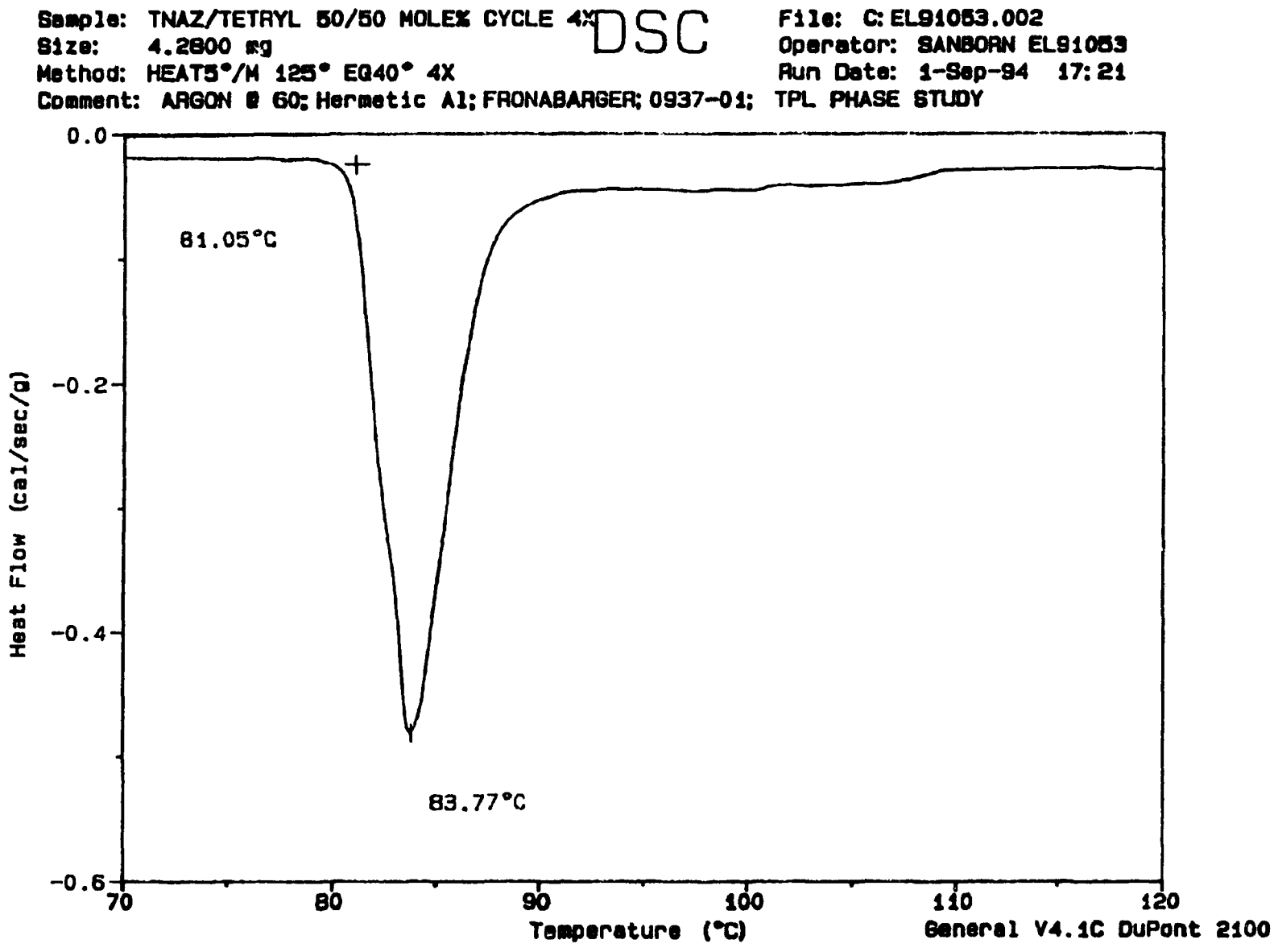

Figure 39. DSC thermogram of 50 mol%/50 mol% TNAZ/tetryl, first cycle through 40–125 °C (5 °C/min)

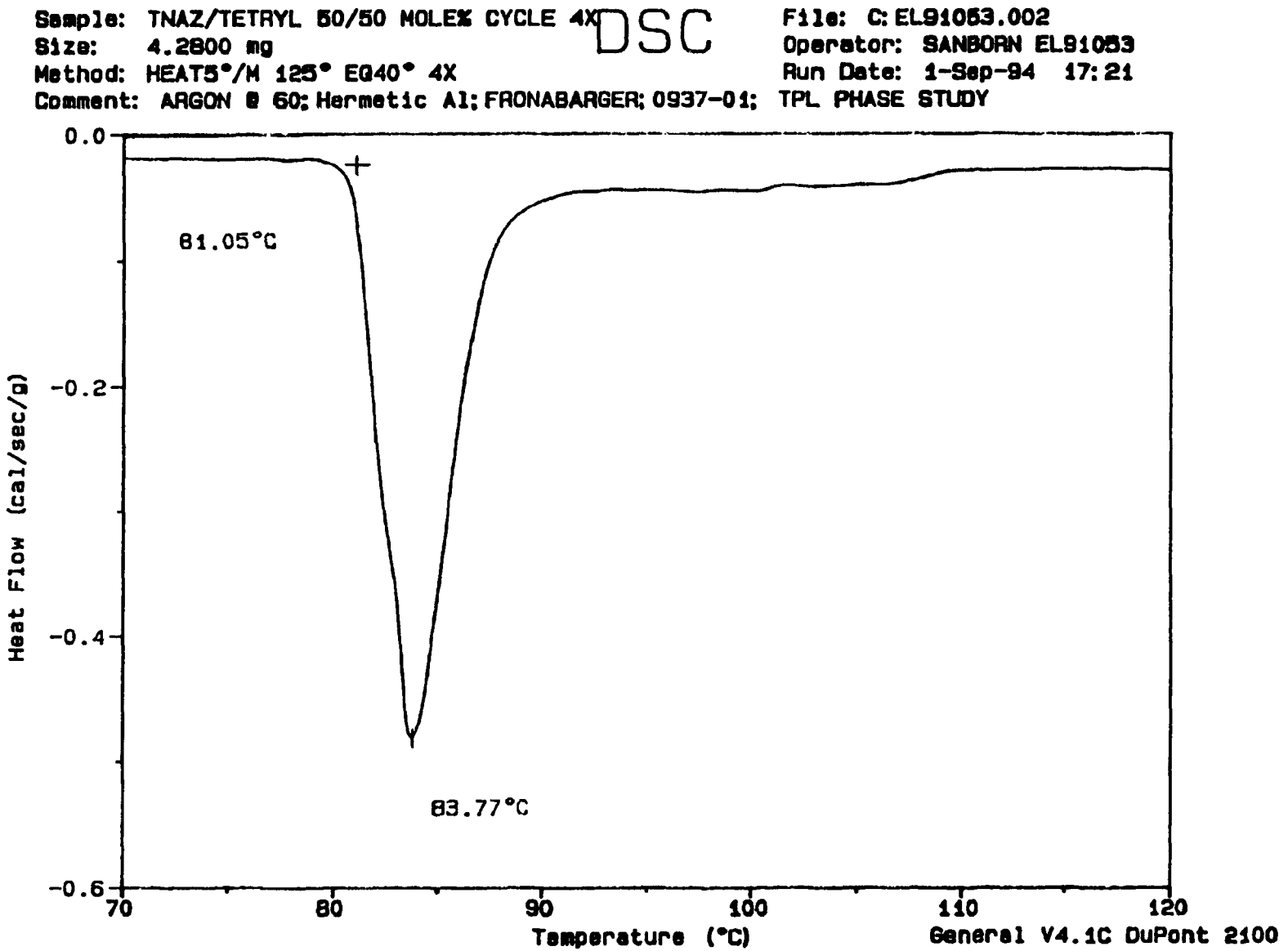

Figure 39. DSC thermogram of 50 mol%/50 mol% TNAZ/tetryl, first cycle through 40–125 °C (5 °C/min)

CONCLUSIONS AND RECOMMENDATIONS

TECHNICAL CONCLUSIONS

An important point made in the Discussion section above is that the new correlation described by equations (15)–(16) allows us to predict with reliability and convenience the likely extent of any eutectic formation between explosive ingredients. With such a convenient correlation at hand for predicting eutectic behavior in explosives, formulations may be tailored to desired thermophysical properties based mainly on their components' melting points. For example, if the significant formation of a eutectic is considered desirable, then we can say that the ingredients should have the properties indicated in Figure 40 by the shaded region of melting point temperature differences of the ingredients (at least 10% content of the minor ingredient). If not, then they should have properties outside of the shaded region.

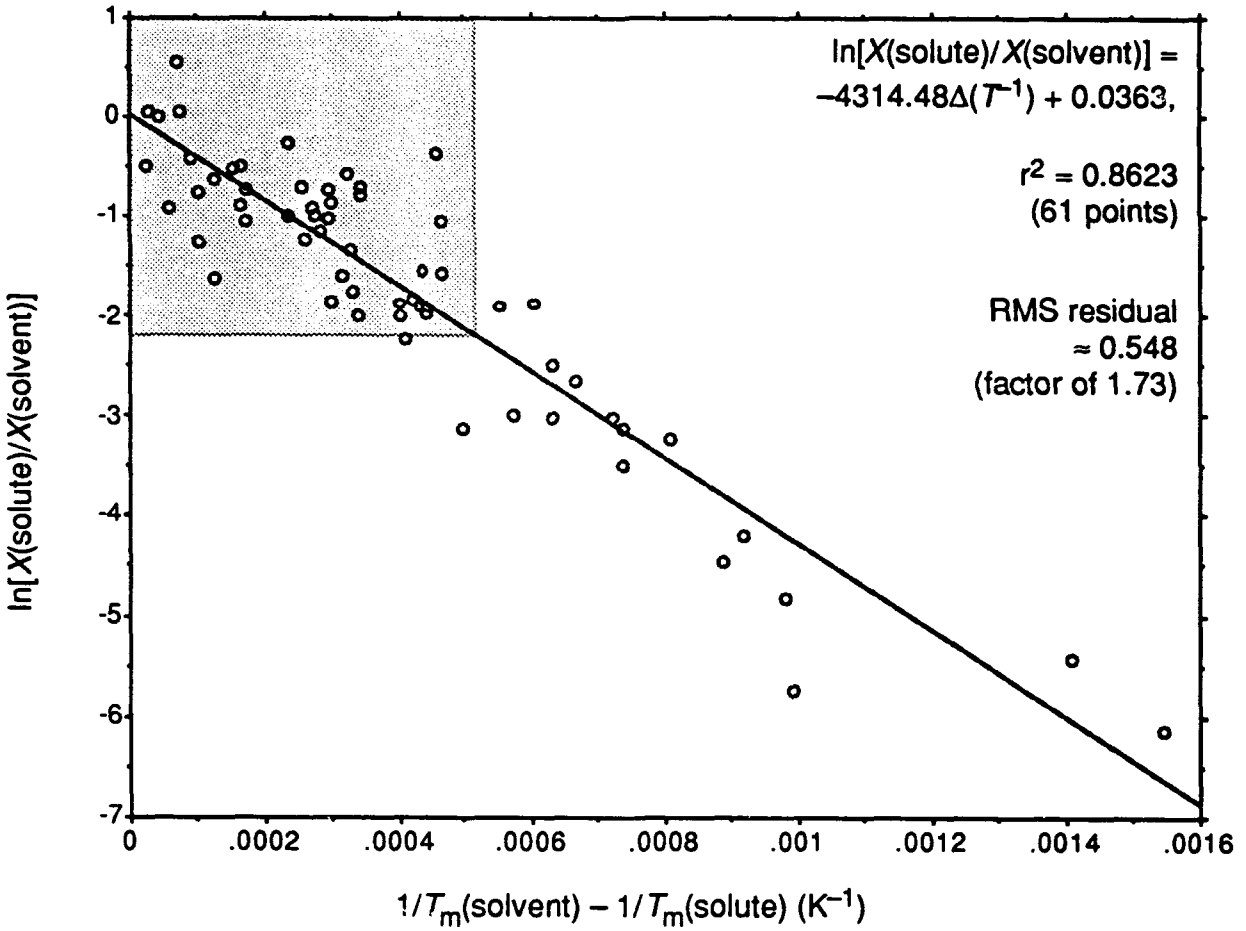

Figure 40. Desirable eutectic regions. Systems of ≥10 mol% minor component are shaded.

An example of a well-behaved significant eutectic involving TNAZ has been discovered at Los Alamos National Laboratory. The binary system of TNAZ with 3,3-dinitro-1-nitrosoazetidine (NO-DNAZ) has ingredients with melting points <3 °C different and shows a melting depression to a eutectic temperature of ~83 °C at 57 mol% TNAZ (Figure 41).[27] In addition, this is an example of a classic binary eutectic with partial solubility in the solid phases.[28] The eutectic temperature and composition predicted according to equations (16) and (10) are 79.3 °C at 51 mol% TNAZ.

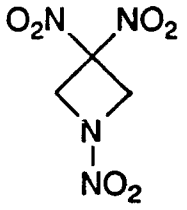

TNAZ
m.p. 99.3 °C

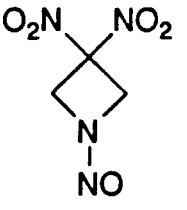

NO-DNAZ
m.p. 101.7 °C

Another TNAZ system with a significant eutectic formation is that with trinitrotoluene, which received some preliminary study early on in the investigations of new TNAZ formulations at ARDEC; its "solubility in TNT melt" was claimed to be 46 wt%.[2b] Further unpublished data on the TNAZ–TNT system had been obtained by Harris (ARDEC),[29] showing the binary eutectic to melt at (59 ± 2) °C (DSC heating rate 10 °C/min) at ~33.4 wt% (37 mol%) TNAZ. The composition predicted according to equation (16) is 35 mol% TNAZ. This formulation may thus be viewed as a potential low-melting, high-performance Composition B analogue with TNAZ replacing RDX as the nitramine constituent.

---

[27] Analysis by Howard Cady (Los Alamos National Laboratory), data provided by Michael Hiskey (LANL). Preliminary presentation by: Hiskey, M.A.; Coburn, M.D. "Synthesis and Utility of 3,3-Dinitroazetidine: A New Route to TNAZ" *Twelfth Annual Working Group Institute on Synthesis of High Energy Density Materials [Proc.]*, Kiamesha Lake, NY, June 1993, pp. 98-125.

[28] Reisman, A. "Phase Equilibria"; Academic Press: New York, 1970; p. 390.

[29] Original data by Joel Harris (ARDEC) provided by Daniel Stec III (Geo-Centers, Inc., Lake Hopatcong, NJ).

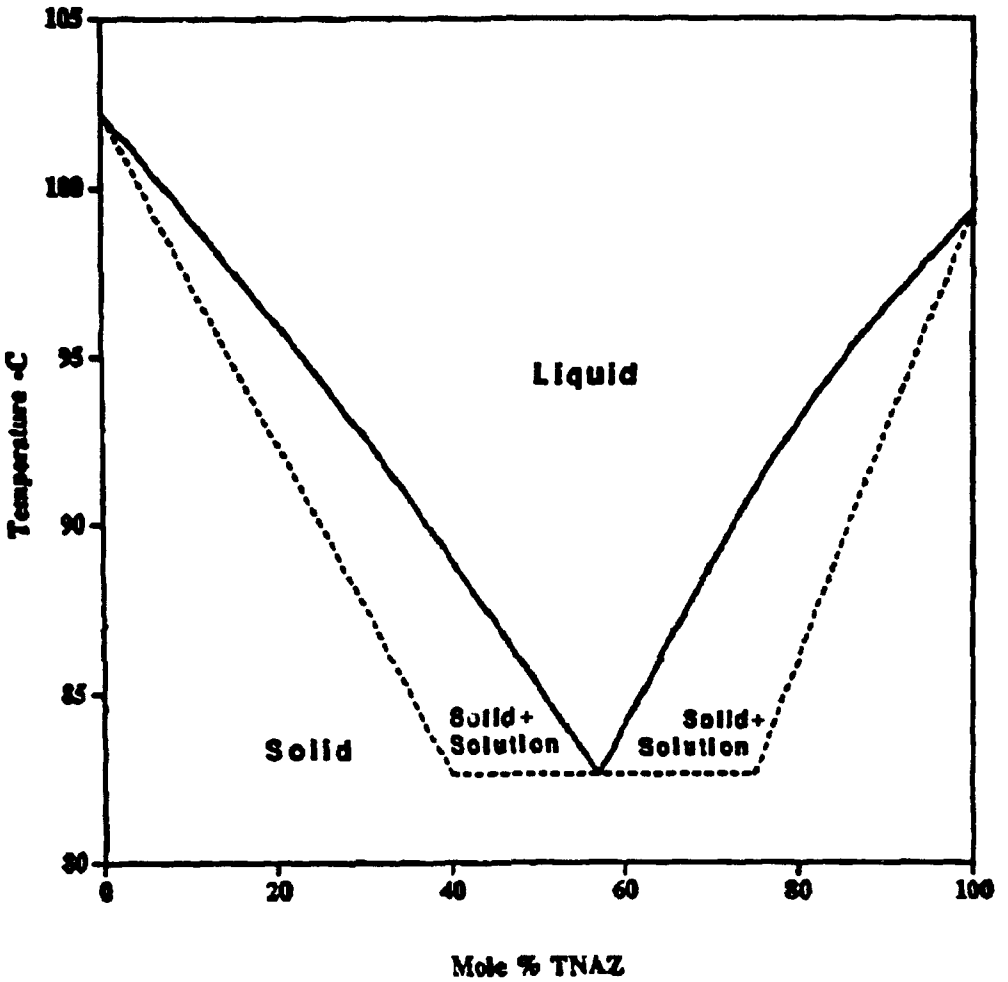

Figure 41. TNAZ–NO-DNAZ phase diagram (from reference 27)

SUMMARY OF CONCLUSIONS

Conclusions arising from the Phase I program may be summarized as follows.

• The best predictor of the extent of eutectic formation between explosive ingredients is the difference between their reciprocal melting temperatures ($r^2 > 0.86$ among 61 examples), as shown graphically in Figure 34. Though the basis for predicting eutectic behavior from thermodynamic relationships such as van't Hoff's equation has come to be recognized in recent years,[23,24] the correlation to melting point differences as the major contributor to this behavior seems to have been unrecognized in the energetic materials community. The quantification of this correlation, derived herein on the basis of thermodynamic theory with simple approximations, seems to be absent from the general chemical literature. Residual variations in the extents of eutectic formation should correlate to minor differences in structural forces, such as different

activity coefficients or enthalpies of fusion.

• "Eutectics" between TNAZ and HMX and between TNAZ and 2,4-DNI have been measured experimentally as essentially only melting point depressions due to <5% of the higher-melting ingredient as a minor constituent. The observation of this result from the TNAZ–HMX system led to the discovery of the correlation described above, which was confirmed by measurements of the new systems TNAZ–2,4-DNI and TNAZ–tetryl. The binary systems with HMX and with 2,4-DNI are predicted to contain 2.13 mol% and 2.33 mol%, respectively.

• The TNAZ–tetryl binary system was determined to have a eutectic temperature of 81.05 °C (DSC onset). The predicted composition based on known enthalpies of fusion is 65/35 TNAZ/tetryl, but only one composition (50/50) was measured experimentally.

• NTO, an ingredient initially of interest for study in this program, is now estimated to exhibit an insignificant eutectic with TNAZ, similarly to HMX and 2,4-DNI. The predicted composition is 2.49 mol% NTO.

• The elucidation of phase behavior in the initial TNAZ compositions (extended to general observations about explosive formulations) consumed the Phase I resources available. Only in the final, preliminary study of *TNAZ–tetryl* was there behavior that may appreciably change properties of the formulations from those expected of a simple physical mixture of ingredients. Thus, there was no benefit to be derived from performance calculations (based on new composition properties), as originally proposed for Task 4 of the Phase I program, nor from scale-up and stability testing, as originally proposed for Task 5 of the Phase I program.

RECOMMENDATIONS

The following technical issues and recommendations for future work become apparent as a direct result of findings in this Phase I program.

Consistent with the intention of this program, "TNAZ Formulations with Enhanced Energetic Output," the development of such improved formulations should take advantage of TNAZ's superior energetics and performance while retaining similarities to conventional ingredients which have already undergone extensive formulation development. Thus, TNAZ exhibits chemical (including thermochemical) characteristics expected for nitramines like RDX and HMX, thermophysical properties (e.g., melting point, volatility) closer to those of TNT, but performance comparable to or better than HMX. These properties suggest that TNAZ may be used as either a nitramine equivalent by replacing RDX, e.g., in Composition C-4 improvements;[5] or as a TNT replacement offering greatly superior energetic output. Initial studies in the current program suggest greater prospects for the latter option.

★ The current findings about thermophysical behavior of the **TNAZ–HMX** system suggest that this formulation should behave physically similarly to the known *Octols* but with significantly superior energetic output. Further development of such variations should be pursued as

described below. Formulations based on the **TNAZ–2,4-DNI** system studied herein should be of value as high-performance but lower-sensitivity explosives. Many formulations can now be reliably predicted to exhibit thermophysical properties similar to those of binary systems between TNAZ and similarly high-melting ingredients; these formulations might be treated as essentially physical mixtures for purposes of property and performance predictions, as there would be no significant phase interactions. Such systems would include **TNAZ–NTO, TNAZ–CL-20,** and **TNAZ–TATB.**

★ Other binary formulations involving TNAZ deserve some fundamental characterization similar to the thermal analyses conducted in this Phase I program. In contrast to the approach taken in the current study, however, the new understanding of the thermodynamic basis for eutectic formation allows much more efficient studies of this phenomenon to be carried out. Reasonably close predictions can be made on the basis of ingredient melting points (with or without literature on or an initial measurement of enthalpy of fusion), so formulations can be studied more carefully in a narrower composition range. Numerous co-ingredients are of potential interest for binary, and eventual full, formulations. The ingredients may be of an energetic or non-energetic nature; both types are important in current explosive formulations. Examples of particular ingredients in these classes are as follows:

Explosives

- **RDX** (m.p. 205 °C): With a lower melting point than HMX, RDX should be expected to have somewhat greater interaction with TNAZ. Similarly, TNAZ should have greater interaction with RDX than does TNT. The TNAZ–RDX system could form the basis for a class of improved Cyclotols and for a Composition B improvement, in both of which TNAZ replaces TNT.
- **DNNC** (m.p. 153 °C): DNNC has two key structural features in common with TNAZ, the *gem*-dinitro group and the nitramino group. Its melting point is sufficiently lower than the commoner nitramines RDX and HMX that there should be appreciable phase interactions.

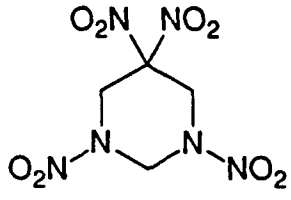

DNNC

- **PETN,** pentaerythritol tetranitrate (m.p. 142 °C): Similarly, an improved class of Pentolite analogues may be developed by replacing TNT with TNAZ. The interaction between these two ingredients is expected to be greater than that of the TNT–PETN system.
- **Tetryl** (m.p. 129 °C): Initial characterizations of this system were conducted in this Phase I program, as described above. Detailed characterization of the observed eutectic could allow

development of a series of tetrytols analogous to the TNT–tetryl system.

- **TNB**, trinitrobenzene (m.p. 121 °C): The explosive ingredients that melt closer to TNAZ will undergo more extensive eutectic formation.
- **BTNEC**, bis(2,2,2-trinitroethyl) carbonate (m.p. 115 °C)[30]
- **BTNEN**, bis(2,2,2-trinitroethyl)nitramine (m.p. 94 °C)[30]
- **TNETB**, 2,2,2-trinitroethyl 4,4,4-trinitrobutyrate (m.p. 93 °C)[30]
- **1,4-DNI**, 1,4-dinitroimidazole (m.p. 92 °C)[31]
- **DNPF**, bis(2,2-dinitropropyl) fumarate (m.p. 89 °C)[30]
- **DINA**, bis(2-nitroxyethyl)nitramine (m.p. 54 °C)[30]

Polymers

- **Estane**, poly(ester–amide) lacquer/coating/binder for LX-14, other formulations
- **CEF**, tris(2-chloroethyl) phosphate, plasticizer for PBX-9404
- **Exon 461**, poly(chlorotrifluoroethylene–vinyl chloride), lacquer/coating/binder for PBX-9407
- **Kel-F 800**, poly(chlorotrifluoroethylene–vinylidene fluoride), lacquer/coating/binder for PBX-9502
- **Viton**, fluoroelastomer binder for PBXN-5,6
- **Nylon**, polyamide binder for PBXN-2,3
- **Polyethylene**, binder for PBX-0280
- **DNPA**, poly(2,2-dinitropropyl acrylate), binder for X-0217[32]

★ Fuller fundamental characterization of new phase forms (especially eutectics) in new formulations of potential interest. This characterization would include the following determinations:

- Density of true eutectics. Differences in density between eutectics and simple physical mixtures would affect performance. This characterization might be most easily conducted by gas pycnometry.
- Thermal expansion behavior of solids (e.g., by thermomechanical analysis) and density changes through the solid-to-liquid transition.
- Fundamental studies of the thermal stability (e.g., decomposition kinetics) of eutectics.
- Precise enthalpy of fusion of exact eutectics (thermodynamics of mixing, manifested as lower-melting eutectics, affects heat of explosion or combustion). Heat of explosion may be measured as a corollary to this.

---

[30] Hall, T.N.; Holden, J.R., Silver Spring (MD), October 1988 "Navy Explosives Handbook: Explosion Effects and Properties. Part III. Properties of Explosives and Explosive Compositions" *NSWC MP 88-116.*

[31] Damavarapu, R.; Iyer, S. "Nitroimidazoles: New Class of Explosives"; *Eleventh Annual Working Group Institute on Synthesis of High Energy Density Materials [Proc.]*, Kiamesha Lake, NY, June 1992, pp. 505-517.

[32] Gibbs, T.R.; Popolato, A., Eds. "LASL Explosive Property Data"; University of California Press: Berkeley, 1980.

★ Computational studies should be carried out on new formulations of interest prior to formulation scale-up. These studies could now accurately account for the modifications in physical (density) and thermophysical (heats of reaction) properties determined from the fundamental characterizations.

★ With the correlations at hand determined in this Phase I program, and additional new data from initial follow-on studies, explosive formulations could be conveniently developed to achieve a variety of tailorable properties. These could include a range of melting points (from <100 °C for steam-castable formulations to ~200 °C) with tailorable performance and sensitivity characteristics depending on the ingredients chosen.

★ The potential for novel *liquid explosives* should be apparent from discussions of thermophysical behavior of explosive mixtures presented in this report. These might be simply derived from binary eutectics with known liquid ingredients. Compositions with TNAZ and the following ingredients should be considered:

- **BDNPA/BDNPF**, bis(dinitropropyl) acetal/formal
- **FEFO**, bis(2-fluoro-2,2-dinitroethyl)formal
- **nitromethane**

★ As a natural extension of the studies of binary eutectics/formulations conducted in the current program, the potential advantages of tailorability in properties of *ternary eutectics/ formulations* should be considered and pursued. (This might be the most convenient means to achieve the liquid explosive systems suggested above. The ternary eutectic among nitrotoluene–dinitrotoluene–trinitrotoluene is liquid at room temperature.[7])

★ A homopolymer of TNAZ ("poly-TNAZ") has been reported to have been recently made at Los Alamos National Laboratory.[33] Should this material prove to be practical for scale-up, formulations between TNAZ and its homopolymer would be of great interest.

★ Ultimately, attractive new formulations need to be brought into development for use in weapons systems. The most valuable of the compositions characterized in the initial stages of a follow-on program would undergo further development with this ultimate goal in mind. The general scientific approaches recommended above would allow diversity in the nature of applications for which new formulations are developed. Either cast-loadable or press-loadable formulations may be conveniently developed within the framework of the program suggested here. Advanced development would include the following tasks:

- Scaled-up preparation of samples (new formulations) for testing
- Preliminary quantitative safety tests
- Small- to large-scale performance tests
- Further scale-up and optimization of processing procedures for new formulations

---

[33] Mitchell, M.A. "Studies on the Synthesis of PolyTNAZ" *Twelfth Annual Working Group Institute on Synthesis of High Energy Density Materials [Proc.]*, Kiamesha Lake, NY, June 1993, pp. 283-305.

EXPERIMENTAL SECTION

Materials. The TNAZ used in these studies was provided by ARDEC and used as is. The HMX sample was pure production-grade material on hand at Pacific Scientific. The 2,4-DNI was provided by ARDEC and was oven-dried, which removed 0.12–0.13% moisture & volatiles, and ground to a finer particle size before thermal analysis. Tetryl was on hand at Pacific Scientific; this sample was recrystallized from acetone–2-propanol and then dried at 80 °C.

Mixing/blending. Most mixtures were prepared by blending in a dry state (Arizona) precisely weighed quantities (to 0.1 mg) of ingredients totalling ~1 gram. Blending was performed with a thin spatula in a 7-cm^3 vial for at least five minutes. Static problems required that the mix of 5% TNAZ/95% HMX be blended as a paste (with water plus 2-propanol) and then thoroughly dried. Tetryl was carefully ground in a mortar before blending; the TNAZ–tetryl sample weighed 0.7 g.

Thermal analysis. Differential scanning calorimetry was conducted with a DuPont/TA Instruments Model 910 DSC, Thermal Analyst 2100 controller, DuPont Cell Base II, and TA Instruments DSC cell. The cell was purged with argon during the analyses. Samples were contained in hermetically sealed aluminum pans.

Data analysis. Thermal analysis trends were analyzed by UltraFit version 2.11 for the Macintosh (Biosoft, Ferguson, MO). Eutectic predictions based on transcendental equation (10) were calculated using Theorist version 1.51 for the Macintosh (Prescience Corp., San Francisco, CA).

ACKNOWLEDGEMENTS

The authors thank Drs. Jack Alster, Sury Iyer, Rao Surapaneni, and Mr. Brian Travers for instigation of the Phase I contract and technical interaction during its conduct. We thank Dr. Daniel Stec III (Geo-Centers, Inc.) and Dr. Michael Hiskey (Los Alamos National Laboratory) for providing unpublished data cited herein.

APPENDIX A.

Typographical corrections to
"Table. Binary Eutectic Mixtures"
in
Fedoroff, B.T.; Sheffield, O.E. "Encyclopedia of Explosives and Related Items";
Picatinny Arsenal: Dover, NJ, 1974; Vol. 6, pp. E 343-E 346

original typo	correction

structure (Refs 7 & 8). In the same year Quilico & Fusco (Ref 9) studied the mechanism of formation of eulite

The structure of *Dislite*, $C_8H_8N_4O_8$, obtd by several investigators as a minor companion of eulite on nitration of citraconic acid was not established until 1946 (Ref 10). As Dislite was mentioned but not described in this Encycl, Vol 5, p D1506-L, we are describing it after the refs

Refs: 1) Beil 2, 770 & 27, [1118] 2) S. Baup, *Jahresberichte für Chemie* 1851, 405; AnnChimPhys 33, 192(1851); Ann 81, 102 (1852) 3) H. Bassett, ChemNews 24, 631 (1871) & ChemZtr 43, 157(1872) 4) A. Angeli, Ber 24, 1303(1891) 5) A. Quilico, Gazz 65, 1203–13(1935) & CA 30, 5219–21 (1936) 6) A. Quilico & R. Fusco, Gazz 66, 278–99(1936) & CA 31, 1805(1937) 7) A. Quilico et al, Gazz 76, 30–43(1946) & CA 41, 382(1947) 8) A. Quilico & M. Freri, Gazz 76, 87–107(1946) & CA 41, 383(1947) 9) A. Quilico & R. Fusco, Gazz 76, 195–99 (1946) & CA 41, 385(1947) 10) R. Fusco & S. Zumin, Gazz 76, 223–38(1946) & CA 41, 2039(1947)

Dislite (Dyslyt, in Ger)

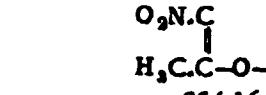

mw 254.16, N 22.05%; long fine ndls (from alc), mp 200.5°; sol in alc; insol in w. It is formed simultaneously with Eulite by reaction of citraconic acid & nitric acid. It forms numerous salts (Refs 1, 2 & 3)

Refs: 1) Beil 2, 770 & [1939]; 27, [869] [Compd called Bis[4-nitro-5-methylisoxazolyl-(3)] and α,α'-Dimethyl-β,β'-dinitro-γ,γ'-diisoxazol] 2) R. Fusco, Gazz 68, 380–86(1938) & CA 32, 9066(1938) 3) R. Fusco & S. Zumin, Gazz 76, 223–38(1946) & CA 41, 2038(1947)

"Eumuco" Shell Forging Press is a vertical type press which combines punching and drawing operations. It was designed and manufd by Eumuco AG, Leverkusen-Schlebush and used during WWII by the following Ger plants: Kronprinz AG; Immigrath, Gutehoffnungshütte AG; and Stenkrade-Kieserling & Albrecht AG, Solingen & Hasenclever AG, Düsseldorf

Refs: 1) BIOS Final Rept 668(1946) 2) PATR 2510(1958), p Ger 45-L

Eutectic Explosive Mixtures

Eutectic is a mixture of two or more substances which has the lowest constant melting point of any mixture of its constituents. Usually the molecular ratios of the components can be expressed in simple whole numbers, such as 1:1, 1:2, 2:3, etc

Following Table lists various eutectic mixtures of explosives. See also BINARY, TERNARY AND QUATERNARY MIXTURES in Vol 2 of Encycl, pp B116 to B120

Note 1: Accdg to Ref 2, p 1026, the binary eutectic temp 26.4° for DNT+TNT was lowered to 25.7° by addns of small quantities of TNX; similarly temp 33.8° of MNT+TNT was lowered to 30.55°, and temp 45.1° of DNT+TNT was lowered to 42.3°

Note 2: Accdg to Ref 14, AN forms the following ternary eutectics: 1) AN 66.5, Na nitrate 21.0 & K nitrate 12.5% (fr p 118.5°); and 2) AN 69, Ca nitrate 18 & Na nitrate 1.3% (fr p 107.5°)

Note 3: Eutectic temperature of temary mixture of three TNT isomers (α 43.5, β 20.0 and γ 36.5%) was given as 44.4° by W.H. Gibson et al in JCS 121, p 282(1922)

Refs: 1) N. Efremov, BullAcadSciPetrograd 1915, 1309–36 and 1916, 21–46 2) J. Bell & J. Sawyer, JIEC 11, 1025(1919) 3) J. Bell & C. Herty, JIEC 11, 1124–33(1919) 4) C.A. Taylor & W.H. Rinkenbach, IEC 15, 73, 795 & 1070(1923) 5) N. Efremov & A. Tikhomirova, CA 21, 3802(1927) 6) Ibid, CA 23, 2349(1929) 7) Ibid, CA 23, 3214 (1929) 8) A. Holleman, Rec 49, 112(1930) 8a) Marshall (1932), 233 9) T. Urbański, CA 28, 27(1934) 10) K. Hrynakowski & Z. Kapuściński, CA 28, 6706(1934) 11) T. Urbański, CA 29, 6129(1935) 12) T. Urbański & B. Kwiatkowski, CA 29, 6129 (1935) 13) T. Urbański, CA 30, 5863(1936) 14) T. Urbański & S. Kolodziejczyk, CA 30, 5863(1936) 15) J. Timmermans, "Les Solutions Concentrées", Masson, Paris (1936), p 520 (List of several eutectic mixtures) 16) E. Burlot & P. Tavernier, MP 31, 39(1949) [Included are curves of mp's vs compns of binary mixtures: DNCB (mp 49.5°) + PA(121°) and DNCB+TNT (79.5°). Eutectics for mixtures are: 38° for DNCB 25 & PA 75%; and 34° for DNCB 35 & TNT 65%] 17) G. Desseigne, MP 31, 48–49(1949) (Ethyltetryl forms with 30–38% of Tetryl an eutectic of mp 75.5°)

Table
Binary Eutectic Mixtures

Components and Their Melting Points	Approximate % by Weight Ratios	Eutectic Temp °C	References
p-MNT (50.25°) – DNT (69.54°) Molecular Ratio (1:1)	45:55	26.4°	3, p1127
p-MNT (50.25°) – TNT (80.35°) Molecular Ratio 2:1	55:45	33.8°	3, p1127
DNT (69.54°) – TNT (80.35°) Molecular Ratio 1:1	55:45	45.1°	3, p1127
DNT (71°) – TNT (80.6°)	54:46	45°	8a, p233
TNT (80.6°) – 2,4,5-TNT (101.5°)	61:39	58°	8a, p233
TNT (80.6°) – Tetryl (127.5°)	52:48	65-68°	8a, p233
TNT (80.6°) – Tetryl (127.5°)	67:33	65-68°	8a, p233
TNT (78.8°) – Tetryl (126.8°)	63.4:36.6	58.8°	5, p3803
TNT (80.27°) – Tetryl (128.72°) Molecular Ratio 2:1	61.3:38.7	67.4°	4, p73
DNT (68.8°) – PA (119°)	60:40	51.6°	8a, p233
TNT (80.27°) – PA (121.8°)	69.8:30.2	59.4°	4, p795
TNT (80.6°) – PA (121.7°)	67:33	55.5°	
Tetryl (128.72°) – PA (121.8°) Molecular ratio 1:1	55.6:44.4	70°(about)	4, p1070
p-MNT (51.2°) – TNX (182.0°)	98:2	50.5°	2, p1026
DNT (69.4°) – TNX (182.0°)	94:6	67.7°	2, p1026
TNT (80.5°) – TNX (182.0°)	92:8	74.8°	2, p1026
m-DNB (69.5°) – Tetryl (126.8°)	66.5:33.5	65.5°	5, p3803
DNT (69.4°) – Tetryl (126.8°)	79.5:20.5	59.1°	5, p3803
DNP (111.4°) – Tetryl (126.8°)	43.3:57.7	83.1°	5, p3803
PA (122.4°) – Tetryl (126.8°)	43:57	75-77°	5, p3803
Styphnic Acid (175.5°) – Tetryl (126.8°)	74.5:25.5	83°	5, p3803
TNCr (101.2°) – Tetryl (126.8°)	63.5:36.5	78°	5, p3803
TNX (180.2°) – m-DNB (89.5°)	17.8:82.2	76.4°	6, p2349
TNX (180.2°) – PA (122°)	21.7:78.3	105.8°	6, p2349
TNX (180.2°) – TNCr (101.2°)	17.2:82.8	84.6°	6, p2349
TNX (180.2°) – Styphnic Acid (175.5°)	37.5:62.5	141.3°	6, p2349
TNX (180.2°) – Tetryl (126.8°)	23.5:76.5	110.8°	6, p2349
TNX (180.2°) – Picryl Chloride (83°)	13.0:87.0	73.2°	6, p2349
TNX (180.2°) – TNB (121°)	16.4:83.6	104.6°	6, p2349

(Continued)

(Continuation)

Table
Binary Eutectic Mixtures

Components and Their Melting Points	Approximate % by Weight Ratios	Eutectic Temp °C	References
Tetryl (126.8°) – Picramide (184.2°)	86.1:13.9	110.8°	7, p3214
Tetryl (126.8°) – DNAn (176°)	80.7:19.3	98.8°	7, p3214
Tetryl (126.8°) – Picryl Chloride (81.2°)	39.4:60.6	57.8°	7, p3214
Tetryl (126.8°) – TNAns (63.8°)	29.5:70.5	22.8°	7, p3214
MHeN (112.5°) – p-MNT (50.2°)	12.5:87.5	49.2°	9, p27
MHeN (112.5°) – m-DNB (89.5°)	52.5:47.5	65.5°	9, p27
MHeN (112.5°) – DNAns (94.5°)	55:45	77.6°	9, p27
MHeN (112.5°) – TNB (121.5°) 123.4°	55:45	78.7°	9, p27
MHeN (112.5°) – TNT (80.2°)	42.5:57.5	62.8°	9, p27
MHeN (112.5°) – PETN (140°)	20:80 80:20	101.3°	9, p27
MHeN (112.5°) – ErN (61°)	18.5:81.5	57.6°	9, p27
ErN (61°) – m-DNB (89.5°)	70:30	42.4°	9, p27
ErN (61°) – p-MNT (54.5°)	47:53	32.4°	9, p27
ErN (61°) – PETN (140°)	95:5	59.5°	9, p27
PETN (140°) – p-MNT (54.5°)	10:90	50.2°	9, p27
PETN (140°) – m-DNB (89.5°)	20:80	82.4°	9, p27
PETN (140°) – DNAns (94.5°)	20:80	94.7°	9, p27
PETN (140°) – TNB (121.5°) 123.4°	30:70	101.1°	9, p27
PETN (140°) – TNT (80.3°)	13:87	76.1°	9, p27
ErN (61°) – DNT (69.4°)	61:39	40.1°	13, p2834
ErN (61°) – TNB (121.5°)	67:33	45.8°	13, p2834
ErN (61°) – TNAns (68.4°)	16:84 *	58.6°	13, p2834
ErN (61°) –TNAns (68.4°)	76:24 *	52°	13, p2384 2834
AN (210°, decomp) – $Ca(NO_3)_2$ (561°)	71:29	111°	14, p5863
HNDPhA (238°) – TNT (80.6°)	12:88	78.7°	7a, p233
Picryl Sulfide (230.5°) – TNT (80.6°)	13.5:86.5	78.3°	8a 7a, p233

Abbreviations: AN – Ammonium Nitrate; DNAn – Dinitroaniline; DNAns – Dinitroanisole; DNB – Dinitrobenzene; DNCB – Dinitrochlorobenzene; DNCr – Dinitrocresole; DNPh – Dinitrophenol; DNT – 2,4,-Dinitrotoluene; ErN – Erythritol Tetranitrate; HNDPhA – Hexanitrodiphenylamine; MHeN – Mannitol Hexanitrate; MNPh – Mononitrophenol; MNT – Mononitrotoluene; PA – Picric Acid; PETN – Pentaerythritol Tetranitrate; TNAn – Trinitroaniline; TNAns – Trinitroanisole; TNB – Trinitrobenzene; TNCr – Trinitrocresole; TNPh – Trinitrophenol; TNT – 2,4,6-Trinitrotoluene; TNX – Trinitro-m-xylene

* These should properly be considered eutectics of the 1:2 addition compound between ErN and TNAns: 42:58 (ErN·2TNAns)–TNAns, and 61:39 ErN–(Ern·2TNAns)

	Major comp. (B)	mp(B) °C	Minor comp. (A)	mp(A) °C	MW(B)	MW(A)	Wt% A	Eutectic (°C)	1/mp(B) - 1/mp(A)	ln[X(A)/X(B)]	mp(A)/mp(B)
1	MHN	112.50	TNB	123.40	452.16	213.11	45.000	78.70	.000071275	.551557	1.028264
2	ErTN	61.00	DNT	69.40	302.11	182.14	39.000	40.10	.000073386	.058703	1.025138
3	PA	122.40	Tetryl	126.80	229.11	287.15	57.000	76.00	.000027813	.056049	1.011124
4	PA	121.80	Tetryl	128.72	229.11	287.15	55.600	70.00	.000043599	-.000859	1.017521
5	ErTN	61.00	DNB	89.50	302.11	168.11	30.000	42.40	.000235188	-.261125	1.085291
6	ErTN	61.00	TNB	121.50	302.11	213.11	33.000	45.80	.000458777	-.359202	1.181056
7	DNT	69.54	TNT	80.35	182.14	227.13	45.000	45.10	.000089235	-.421418	1.031545
8	MNT	51.25	DNT	69.54	137.14	182.14	45.000	26.44	.000164525	-.484444	1.056381
9	SA	175.50	TNX	180.20	245.11	241.16	37.500	141.30	.000023108	-.494579	1.010476
10	TNT	80.50	TNAZ	100.59	227.13	192.09	33.400	59.00	.000151998	-.522580	1.056808
11	PkCl	81.20	Tetryl	126.80	247.56	287.15	39.400	57.80	.000321756	-.578881	1.128686
12	DNAnisole	94.50	MHN	112.50	198.14	452.16	55.000	77.60	.000126953	-.624392	1.048960
13	TNT	80.27	Tetryl	128.72	227.13	287.15	38.700	67.40	.000341128	-.694422	1.137089
14	MNT	51.25	TNT	80.35	137.14	227.13	45.000	33.80	.000253760	-.705191	1.089704
15	TNT	80.60	PA	121.70	227.13	229.11	33.000	55.50	.000294248	-.716865	1.116184
16	TNCr	101.20	Tetryl	126.80	243.13	287.15	36.500	78.00	.000170984	-.720136	1.068385
17	DNPh	111.40	Tetryl	126.80	184.11	287.15	42.300	83.10	.000100130	-.754941	1.040047
18	TNT	78.80	Tetryl	126.80	227.13	287.15	36.600	58.80	.000341000	-.783898	1.136383
19	TNT	80.27	PA	121.80	227.13	229.11	30.200	59.40	.000297529	-.846472	1.117509
20	DNB	89.50	MHN	112.50	168.11	452.16	52.500	65.50	.000164455	-.889334	1.063422
21	MNT	54.50	ErTN	61.00	137.14	302.11	47.000	32.40	.000059369	-.909933	1.019838
22	Tetryl	126.80	SA	175.50	287.15	245.11	25.500	83.00	.000271404	-.913823	1.121765
23	Tetryl	126.80	DNAn	176.00	287.15	183.12	19.300	98.80	.000273885	-.980770	1.123015
24	TNT	80.20	MHN	112.50	227.13	452.16	42.500	62.80	.000237030	-.990794	1.091411
25	Tetryl	126.80	TNX	180.20	287.15	241.16	23.500	110.80	.000294511	-1.005746	1.133517
26	MHN	112.50	PETN	140.00	452.16	316.15	20.000	101.30	.000172596	-1.028475	1.071308
27	TNAnisole	63.80	Tetryl	126.80	243.13	287.15	29.500	22.80	.000467487	-1.037631	1.186971
28	RDX	205.00	HMX	280.00	222.13	296.17	30.000	189.00	.000283566	-1.134969	1.156855
29	DNB	89.50	Tetryl	126.80	168.11	287.15	33.500	65.50	.000257167	-1.221043	1.102854
30	TNB	123.40	PETN	140.00	213.11	316.15	30.000	101.10	.000101322	-1.241706	1.041861
31	PA	122.00	TNX	180.20	229.11	241.16	21.700	105.80	.000324883	-1.334494	1.147286
32	Methyl centralite	122.70	RDX	205.50	240.31	222.13	16.622	112.01	.000437000	-1.534005	1.209170
33	TNCr	101.20	TNX	180.20	243.13	241.16	17.200	84.60	.000465496	-1.563383	1.211032
34	Tetryl	126.80	Picramide	184.20	287.15	228.12	13.900	110.80	.000313803	-1.593488	1.143518
35	Camphor	178.20	RDX	205.50	152.24	222.13	22.495	137.60	.000126366	-1.614854	1.060485
36	TNB	121.00	TNX	180.20	213.11	241.16	16.400	104.60	.000331304	-1.752414	1.150197
37	DNT	69.40	Tetryl	126.80	182.14	287.15	20.500	59.10	.000418969	-1.810561	1.167567
38	DNAnisole	94.50	PETN	140.00	198.14	316.15	20.000	94.70	.000299550	-1.853537	1.123759
39	PkCl	83.00	TNX	180.20	247.56	241.16	13.000	73.20	.000602004	-1.874766	1.272919
40	ErTN	61.00	MHN	112.50	302.11	452.16	18.500	57.60	.000399643	-1.886077	1.154122
41	DNB	89.50	TNX	180.20	168.11	241.16	17.800	76.40	.000551678	-1.890799	1.250103
42	sym-TNB	123.40	RDX	205.50	213.11	222.13	13.475	113.68	.000432541	-1.901052	1.207036
43	PA	121.80	RDX	205.50	229.11	222.13	11.839	112.27	.000442757	-1.976864	1.211926

	Major comp. (B)	mp(B) °C	Minor comp. (A)	mp(A) °C	MW(B)	MW(A)	Wt% A	Eutectic (°C)	1/mp(B) - 1/mp(A)	ln[X(A)/X(B)]	mp(A)/mp(B)
44	Tetryl	128.50	RDX	205.50	287.15	222.13	9.487	118.10	.000400521	-1.998783	1.191709
45	DNB	89.50	PETN	140.00	168.11	316.15	20.000	82.40	.000337051	-2.017893	1.139253
46	TNT	80.30	PETN	140.00	227.13	316.15	13.000	76.10	.000408826	-2.231653	1.168906
47	TNT	80.50	TNX	182.00	227.13	241.16	8.000	74.50	.000630577	-2.502285	1.287007
48	m-DNB	89.90	RDX	205.50	168.11	222.13	8.498	85.65	.000665232	-2.655213	1.318413
49	ErTN	61.00	PETN	140.00	302.11	316.15	5.000	59.50	.000572240	-2.989865	1.236421
50	DNT	69.40	TNX	182.00	182.14	241.16	6.000	67.70	.000722204	-3.032220	1.328711
51	MNT	54.50	PETN	140.00	137.14	316.15	10.000	50.20	.000631609	-3.032439	1.260949
52	TNT	80.50	RDX	205.50	227.13	222.13	4.130	79.00	.000738445	-3.122456	1.353457
53	MNT	50.20	MHN	112.50	137.14	452.16	12.500	49.20	.000499599	-3.138944	1.192670
54	Ethyl centralite	71.40	RDX	205.50	268.36	222.13	3.168	70.41	.000809762	-3.230810	1.387592
55	TNT	80.50	RDX	205.50	227.13	222.13	2.879	78.60	.000738445	-3.496219	1 353457
56	Nitronaphthalene	59.30	RDX	205.50	173.17	222.13	1.885	55.40	.000918762	-4.201310	1.439765
57	MNT	51.20	TNX	182.00	137.14	241.16	2.000	50.50	.000686011	-4.456279	1.403268
58	p-Nitroanisole	52.70	RDX	205.50	153.14	222.13	1.131	50.89	.000979687	-4.842336	1.468927
59	NG (stable)	12.90	RDX	205.50	227.09	222.13	.423	12.30	.001406683	-5.438803	1.673309
60	p-Nitrotoluene	51.20	RDX	205.50	137.14	222.13	.513	50.40	.000993880	-5.750453	1.475721
61	NG (labile)	2.00	RDX	205.50	227.09	222.13	.212	1.20	.001545172	-6.131377	1.739597